Characterization of CD133-positive cells in stem cell regions of the developing and adult murine central nervous system

vorgelegt von
Diplom-Ingenieurin
Cosima Viola Pfenninger
aus Erlangen

Von der Fakultät III – Prozesswissenschaften
der Technischen Universität Berlin
zur Erlangung des akademischen Grades
Doktorin der Naturwissenschaften
– Dr. rer. nat. –

genehmigte Dissertation

Promotionsausschuss:
Vorsitzender: Prof. Dr. Peter Neubauer
Berichter: Prof. Dr. Roland Lauster
Berichter: Prof. Dr. Ulrike Nuber

Tag der wissenschaftlichen Aussprache: 11.12. 2009

Berlin 2010

D 83

Abbreviations

For gene and protein names, the guidelines of the International Committee on Standardized Genetic Nomenclature for Mice were followed (http://www.informatics.jax.org/mgihome/nomen/gene.shtml).

7-AAD	7-aminoactinomycin D
bFGF	Basic fibroblast growth factor
bp	Base pair
BSA	Bovine serum albumin
CC	Central canal
CNS	Central nervous system
DAPI	4´,6-diamidino-2-phenylindole
D-MEM	Dulbecco´s modified Eagle´s medium
DMSO	Dimethyl sulfoxide
dNTP	Deoxynucleotide triphosphates
DPBS	Dulbecco´s phosphate buffered saline
E	Embryonic day
EDTA	Ethylenediaminetetraacetic acid
EGF	Epidermal growth factor
FACS	Fluorescence activated cell sorting
FCS	Fetal calf serum
FSC	Forward scatter
GFP	Green fluorescent protein
HEPES	4-(2-hydroxyethyl)-1-piperazineethanesulfonic acid
Ig	Immunoglobulin
LVW	Lateral ventricle wall
MACS	Magnetic activated cell sorting
NOD-SCID	Nonobese diabetic/ severe combined immunodeficient
NSP	Neurosphere
NT4	Neurotrophin-4
P	Postnatal day
PCR	Polymerase chain reaction
RA	Retinoic acid
RGC	Radial glial cell
RMS	Rostral migratory stream
RT	Room temperature
SSC	Side scatter
SVZ	Subventricular zone

1. Introduction

1.1 Definition of stem and progenitor cells

Stem cells are defined by their ability to self-renew long-term and to generate the primary cell types of the tissue or organ they are derived from. Self-renewal enables a cell to generate (a) daughter cell(s) with features identical to the parent cell. There are two modi of self-renewal, symmetric division, which results in two identical stem cells or asymmetric division, which generates a stem cell and a further differentiated cell (Potten and Loeffler, 1990). The concept of ´long-term self-renewal` is not well defined and depends on the cell type and setting. Long-term self-renewal is sometimes associated with infinite or life-long self-renewal, however it can also refer to a self-renewal capability longer than the one from further differentiated progenitor cells (Mikkers and Frisen, 2005). Progenitor cells are further committed cells derived from stem cells. They can give rise to differentiated progeny and can have a certain self-renewing potential, which is however more restricted compared to the properties of a stem cell (Potten and Loeffler, 1990; Mikkers and Frisen, 2005).

1.2 *In vitro* neural stem/progenitor cell assay

Neural stem/progenitor cells are commonly identified by their functional properties, which can be investigated *in vitro* by means of a neurosphere assay and subsequent differentiation of the derived neurospheres (NSPs) (Reynolds and Weiss, 1992). This assay allows to identify self-renewing neural stem/progenitor cells by their formation of free-floating spheres (NSPs) in culture medium supplemented with growth factors (Fig.1). A NSP is a cell cluster, ideally derived from one initial stem/progenitor cell, which divides to give rise to more stem/progenitor cells and further differentiated cells. *In vitro* self-renewal is determined by primary NSP formation and the number of passages these NSPs can be kept in culture. For passaging, spheres are dissociated into single cells and re-plated into culture medium. Subsequently the majority of cells dies, except for self-renewing stem/progenitor cells, which form new NSPs. Withdrawal of growth factors induces neural stem/progenitor cells to differentiate into neurons, astrocytes and oligodendrocytes (Reynolds and Weiss, 1992), which provides a measure of their multipotency. This assay has certain limitations which need to be considered. It was demonstrated that NSPs are motile in culture and, even when cultivated at a low density (clonal conditions), they can fuse with each other, thereby questioning the clonality of individual NSPs (Singec et al., 2006). Furthermore, not every

primary NSP is *de facto* derived from an isolated stem cell, since it was shown that progenitor cells are also able to form multipotent NSPs *in vitro* (Doetsch et al., 2002). Long-term cultivation can distinguish between NSPs derived from stem or progenitor cells, as the latter has more limited self-renewal properties. It was suggested that cell passaging for more than five times is required in order to distinguish neural stem cell-derived NSPs from progenitor cell-derived NSPs (Reynolds and Rietze, 2005).

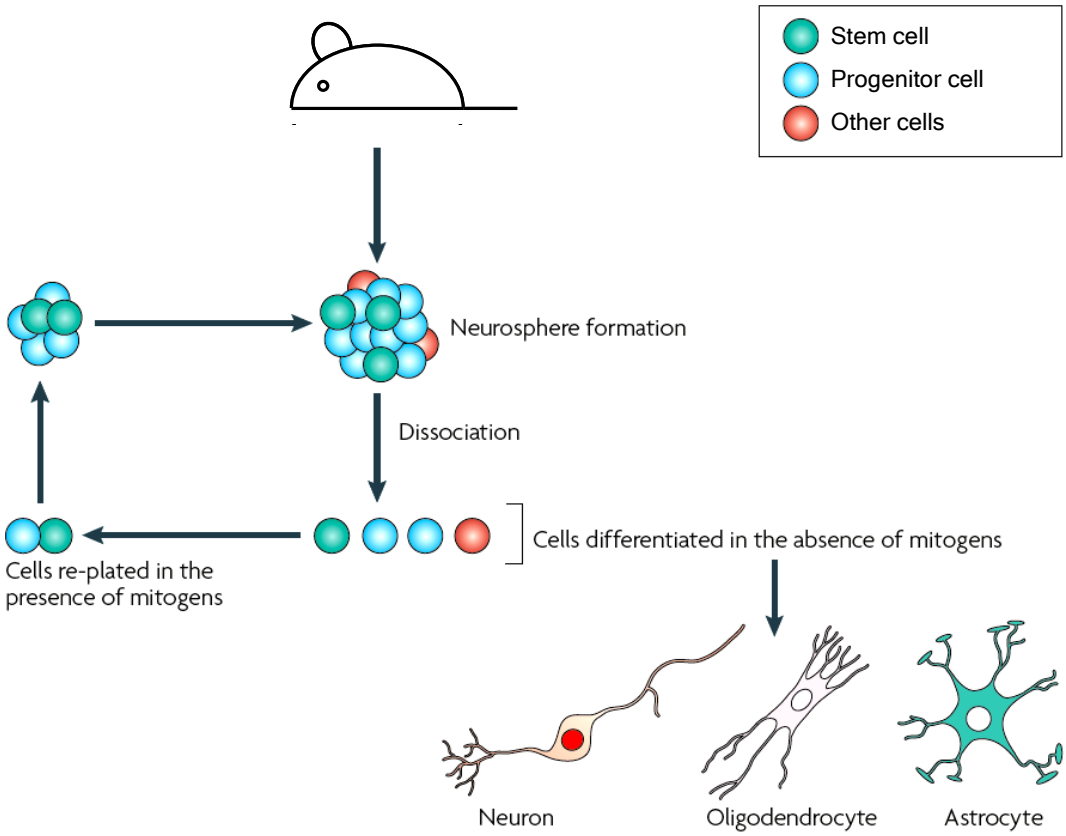

Figure 1: Schematic of the neurosphere assay. Tissue from the respective CNS region is isolated, dissociated into a single-cell suspension and cultivated in the presence of growth factors (mitogens). This results in the formation of free-floating NSPs, which consist of neural stem cells and further differentiated cells (progenitor cells and other cells). For passaging, NSPs can be dissociated and re-plated in the presence of mitogens to generate new NSPs. Withdrawal of mitogens induces NSP-cells to differentiate into cells from the neural lineage (neurons, oligodendrocytes, astrocytes). Figure modified from Chojnacki et al. (2009).

1.3 Stem and progenitor cells in the murine central nervous system

1.3.1 Neural stem and progenitor cells in the developing forebrain

The first stem cells are neuroepithelial cells, which compose the wall of the neural tube. The neuroepithelium consists of one layer of polarized cells which contact the ventricular (apical) and pial (basal) surfaces (Fig.2). Initially neuroepithelial cells divide symmetrically to increase their cell number, but at later stages they also give rise to differentiated progeny. The

neuroepithelium appears stratified, since the cell nuclei migrate between the apical and basal surface during the cell cycle (Merkle and Alvarez-Buylla, 2006).

The same phenomenon, which is termed interkinetic nuclear migration, can be observed in radial glial cells (RGC), which start to replace neuroepithelial cells at the onset of neurogenesis. Neurogenesis starts around embryonic day 9-10 (E9-10) and the majority of RGC develops between E10 to E12 (Gotz and Huttner, 2005; Kriegstein and Alvarez-Buylla, 2009). As their predecessors, RGC have contact to the ventral and pial surfaces (Fig.2). Their cell body remains in the ventricular zone, which is the most apical cell layer next to the ventricle, and their long radial processes extend to the pial membrane. RGC and neuroepithelial cells possess a primary cilium, which extends into the ventricular lumen. Primary cilia have a 9+0 microtubule-based cytoskeleton (axoneme), which differs from motile cilia with a 9+2 axoneme (Spassky et al., 2005). RGC and neuroepithelial cells share the expression of Nestin, however only RGC synthesize proteins characteristic for ´glial` cells, such as the Glutamate/aspartate transporter (GLAST), Brain lipid binding protein (BLBP), S100 and Vimentin, proteins which are also present in certain astrocytes in the adult brain. These proteins show a locally distinct, gradual appearance during RGC development (Mori et al., 2005). RGC are heterogeneous in terms of progeny they give rise to. In most cases, RGC divide asymmetrically to self-renew and generate a further differentiated cell. However, dependent on location and time, they give rise to different subtypes of neuronal or glial cells. This regional diversity might in part be initiated through morphogen gradients, which divide the proliferative regions in the forebrain into distinct zones, thereby establishing different transcription factor expression patterns in RGC. The existence of uni- and multipotent cells indicates further functional differences between RGC. Single multipotent RGC were found to follow a predetermined developmental sequence from the generation of neuronal cells first and then glial cells, which seems to be a cell autonomous process (Mori et al., 2005; Kriegstein and Alvarez-Buylla, 2009).

Neurons can be generated either directly by RGC or indirectly by intermediate progenitor cells (IPC). IPC are derived from RGC and are located in the region above the ventricular zone, the subventricular zone (SVZ). They have no contact with the apical or basal surface (Fig.2). IPC divide symmetrically to produce two neurons or two new IPC, thereby forming a secondary proliferative layer and amplifying the number of generated neurons. IPC for oligodendrocytes and potentially astrocytes exist as well.

Neurogenesis is followed by gliogenesis at the early postnatal stage, where most RGC disconnect from the ventricle, migrate to the cortical plate and transform into astrocytes (Mori et al., 2005; Kriegstein and Alvarez-Buylla, 2009).

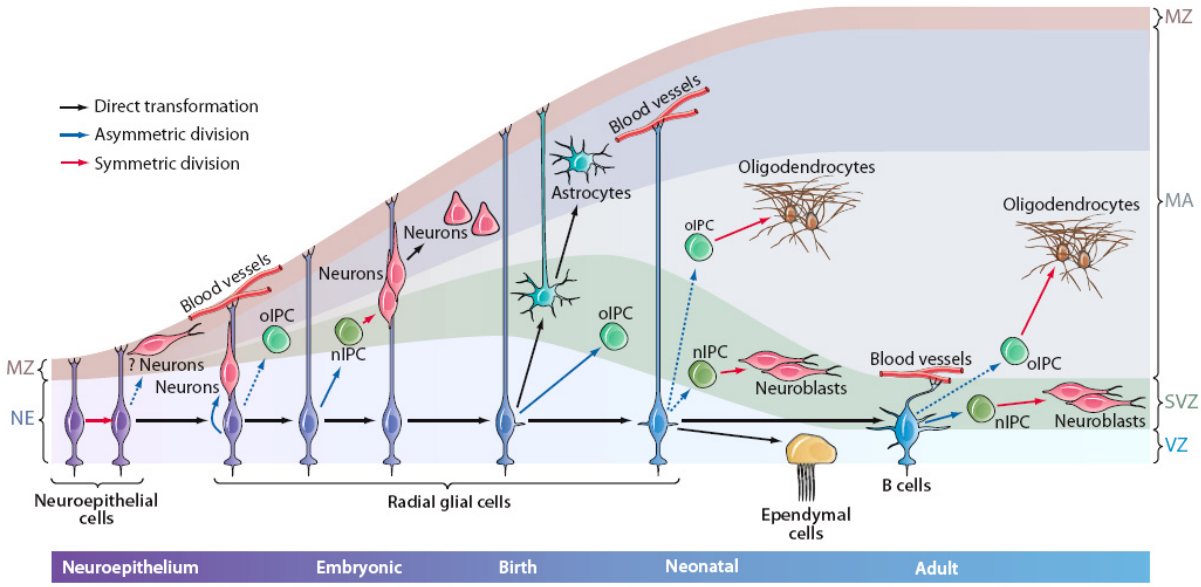

Figure 2: Overview of neural stem cells and their progeny during development and in the adult murine brain. The ventricle lumen (apical surface) is located at the bottom, the pial (basal) surface at the top part of the figure. Solid arrows are supported by experimental evidence, dashed arrows indicate hypothetical connections. MA, mantle; MZ, marginal zone; NE, neuroepithelium; nIPC, neurogenic intermediate progenitor cell; oIPC, oligodendrocytic intermediate progenitor cell; SVZ, subventricular zone; VZ, ventricular zone. Figure taken from Kriegstein and Alvarez-Buylla (2009).

1.3.2 Origin of neurogenic astrocytes and ependymal cells

RGC disappear within the first two weeks after birth. Fate-mapping experiments of permanently labeled neonatal striatal RGC provided evidence that RGC not only transform into terminally differentiated glial cells, but also into neurogenic astrocytes (B cells; Fig.2) in the lateral ventricle wall (LVW), a neurogenic region in the adult brain (see 1.3.3) (Merkle et al., 2004). Furthermore, using the same technique, it could be shown that striatal RGC also give rise to LVW ependymal cells, which constitute the uppermost cell layer lining the ventricles (Merkle et al., 2004; Spassky et al., 2005) (Fig.2). Besides the subpopulation of postnatally generated ependymal cells described in the latter experiments, most ependymal cells are born between E14 and E16 during development. Their final maturation occurs in the first postnatal week along a ventral to dorsal gradient. Immunostainings showed that the transition from RGC to ependymal cells occurs via an intermediate stage, where the cells co-express the radial glia protein GLAST and a protein of mature LVW ependymal cells, S100 (Spassky et al., 2005). Based on these findings, it is now accepted that neurogenic astrocytes

and embryonic/postnatally born ependymal cells are, at least in part, derived from RGC (Kriegstein and Alvarez-Buylla, 2009).

1.3.3 Neurogenesis in the adult forebrain

1.3.3.1 Composition of the neurogenic region in the adult lateral ventricle wall

The largest neurogenic zone in the adult rodent brain is located along the wall of the lateral ventricles (LVW) (Alvarez-Buylla and Garcia-Verdugo, 2002). Ultrastructural and antigenic characterization of the LVW *in situ* revealed the presence of four major cell types: Ependymal cells (type E cells), neuronal precursors (neuroblasts; type A cells), two types of B cells (type B1 and type B2) and the most actively dividing LVW cells, type C cells. Both type B cells show ultrastructural characteristics of astrocytes and are positive for glial fibrillar acidic protein (GFAP), a common protein of astrocytes. Type B1 cells are located close to ependymal cells, whereas type B2 cells reside next to the striatal parenchyma (Doetsch et al., 1997). Using whole mounts of the adult lateral ventricle to study the LVW cytoarchitecture, revealed that type B1 cells contact the ventricle via an apical processes and their cell body is either in close proximity to or intercalated between ependymal cells (Fig.3A). Type B1 cells carry a primary cilium (9+0 axoneme) at their apical surface and have long basal processes which terminate on blood vessels. Twenty-nine percent of GFAP-positive type B1 cells were found to synthesize the surface protein CD133 at their primary cilium and apical surface. However, the staining for CD133 appeared weak in comparison to the intense CD133 staining of ependymal cells (Mirzadeh et al., 2008). Another recent study found three distinct type B cells in the LVW: Ventricle-contacting apical type B cells, penetrating or beneath the ependymal layer, tangential type B cells next to the ventricular layer with long basal processes running parallel to the surface and type B cells with characteristics of mature astrocytes, located near the striatal parenchyma (Shen et al., 2008). It is currently not known, whether ventricle-contacting apical type B cells described in the latter study and type B1 cells are the same population. To avoid confusion, in the following all LVW astrocytes will be referred to as type B cells and type B cell subpopulations will be described by their location in the LVW (e.g. ventricle-contacting type B cells).

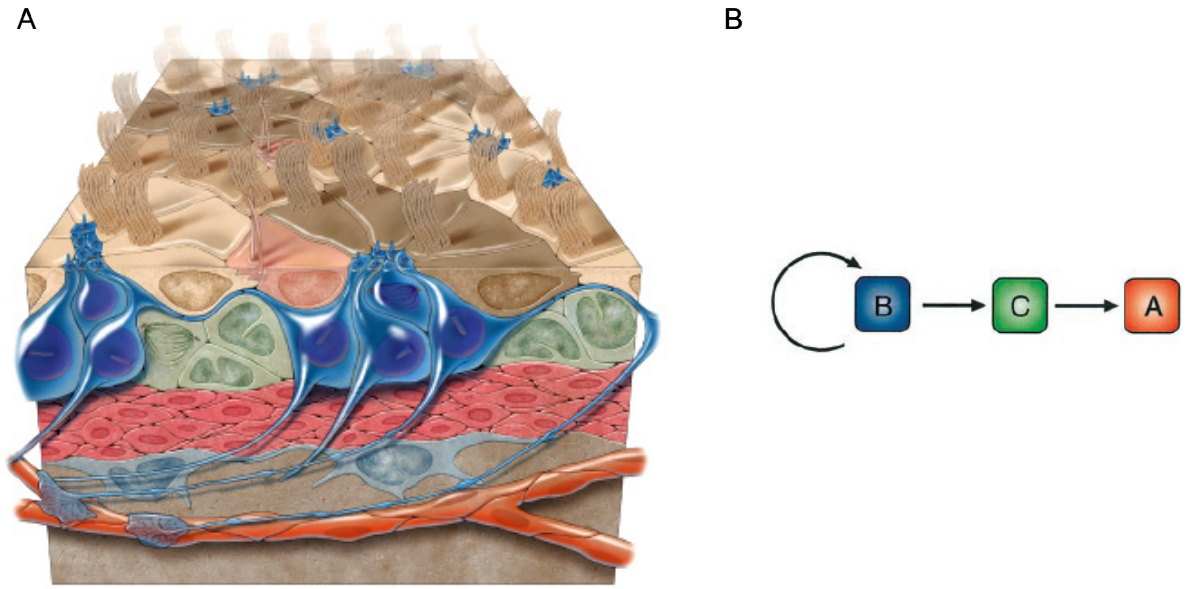

Figure 3: Model of the LVW neurogenic region and LVW cell linage. (A) Multiciliated type E1 (light and dark brown) and biciliated type E2 (peach) ependymal cells surround ventricle contacting type B1 astrocytes (blue). The long basal processes of type B1 cells terminate on blood vessels (orange). Chains of tangentially migrating neuroblasts (red) in the SVZ and clusters of type C cells (green) are illustrated. Figure taken from Mirzadeh et al. (2008). (B) Self-renewing type B cells give rise to transit-amplifying type C cells, which in turn generate type A cells. Figure taken from Alvarez-Buylla and Garcia-Verdugo (2002).

New neurons are constantly born in the LVW and migrate along each other in a chain–like manner from the LVW, along a defined route, the rostral migratory stream (RMS), to the olfactory bulb where they fully mature into periglomerular and granule interneurons (Fig.4). Type B cells form tubular networks around migrating neuroblasts. In the olfactory bulb, neuroblasts separate from each other and migrate radially to their final destination (Alvarez-Buylla and Garcia-Verdugo, 2002).

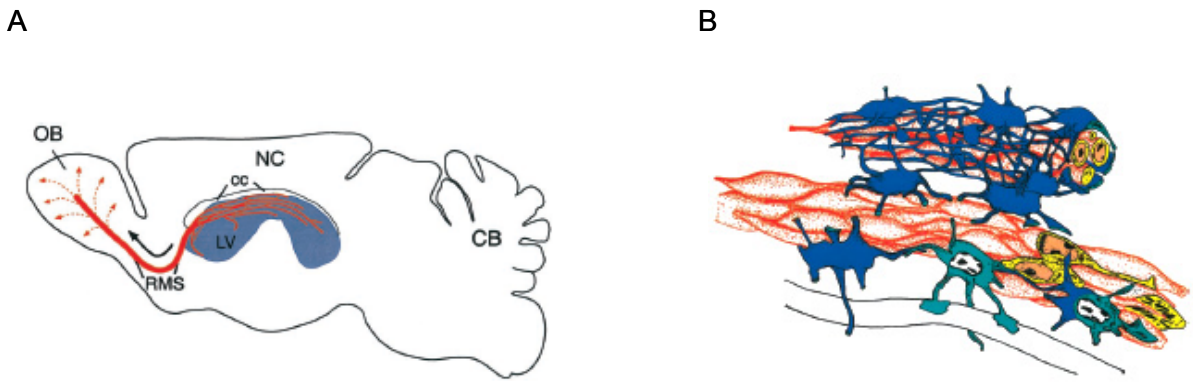

Figure 4: Schematic of the LVW-RMS-OB region in the adult rodent brain. (A) Sagittal view of the brain with the olfactory bulb (OB) to the left and the cerebellum (CB) to the right. Chains of new-born neurons (red lines) migrate along the lateral ventricles (LV, blue) via the rostral migratory stream (RMS) to the OB. Within the OB, neuroblasts move radially as single cells to their destination (dotted lines). NC, neocortex; cc, corpus callosum. (B) Two chains of neuroblasts (red) in the LVW-RMS region, ensheated by type B cells (blue), which frequently have contact to blood vessels (white tube, bottom). To better illustrate the structure, only a few type B cells are shown along the bottom neuroblast chain. Intracellular characteristics of type B cells (light blue) and neuroblasts (yellow) are illustrated. A dividing neuroblast is shown in the bottom chain to the right (yellow). Figure taken from Alvarez-Buylla and Garcia-Verdugo (2002).

1.3.3.2 Identity of neural stem cells in the adult lateral ventricle wall

Early experiments by Brent A. Reynolds and Samuel Weiss showed that isolated cells from the adult mouse LVW region can self-renew and give rise to progeny in culture, indicating the existence of neural stem cells in this area (Reynolds and Weiss, 1992). However, the identity of the stem cells remained unknown. In 1999, Jonas Frisen and colleagues suggested that ependymal cells are the LVW neural stem cells, since they gave rise to neurospheres *in vitro* and new neurons *in vivo* (Johansson et al., 1999). In the same year, these findings were challenged by the group of Alvarez-Buylla, who provided evidence that cells with an astrocytic phenotype function as neural stem cells in the ventricular wall (Doetsch et al., 1999b; Doetsch et al., 1999a). In these studies, proliferating cells were ablated with the anti-mitotic drug cytosine-β-D-arabinofuranoside (Ara-C) leaving type B cells and ependymal cells as only remnants in the LVW. Within five days, type C cells, followed by type A cells re-appeared (Doetsch et al., 1999a). Labeling with [^{3}H]thymidine, a marker for DNA synthesis, identified type B cells and not ependymal cells as proliferating cells shortly after Ara-C treatment, suggesting that these cells gave rise to type C and type A cells. Further experiments with retrovirally labeled GFAP-positive LVW cells in the intact brain, confirmed that type B cells can generate olfactory bulb neurons. The following lineage was suggested (Fig.3B): Type B cells are LVW stem cells, which can self-renew and give rise to type C cells. Type C cells divide repeatedly followed by the generation of type A cells (Doetsch et al., 1999b). These findings were supported by subsequent studies (Chojnacki et al., 2009) and led to the current, commonly accepted view that neural stem cells of the adult LVW are represented by type B cells (the term ´type B cell` is based on ultrastructural and immunocytochemical criteria and includes all LVW astrocytes). Morphologically different subpopulations of type B cells were identified (see 1.3.3.1), but their functional properties are not fully elucidated yet (Chojnacki et al., 2009). It was shown though, that one subpopulation, ventricle-contacting type B cells (type B1 cells), are neurogenic *in vivo* and *in vitro* (Mirzadeh et al., 2008).

Besides that, the functional properties of ependymal cells in the adult LVW remained unsolved. Can these cells act as stem/progenitor cells or are they terminally differentiated cells? A study by the group of Yi Sun proposed that a subpopulation of LVW ependymal cells has neural stem cell properties (Coskun et al., 2008). In this study, CD133 was found to be expressed exclusively by a subpopulation of adult LVW ependymal cells, which could be subdivided into CD24-positive and CD24-negative cells. Isolated CD133-positive, but not

CD24-positive cells, displayed neural stem/progenitor cell features in culture. Lineage-tracing experiments, which allowed to follow the progeny of permanently marked *Prom1*-expressing LVW cells, identified labeled cells in the olfactory bulb after two to four weeks. Based on these experiments, the authors concluded that $CD133^{+}/CD24^{-}$ ependymal cells function as neural stem cells in the LVW. However, it was suggested elsewhere that the CD133-positive cells investigated in the latter study are *de facto* ventricle-contacting type B cells and not ependymal cells (Mirzadeh et al., 2008). Studies using proliferation markers or BrdU and [^{3}H]thymidine incorporation to investigate the proliferative capacity of adult LVW ependymal cell *in situ*, did not reveal any dividing cells, which led to the conclusion that adult LVW ependymal cells are postmitotic (Spassky et al., 2005; Mirzadeh et al., 2008). These findings are supported by a recent study, where the properties of adult LVW ependymal cells were investigated by genetic fate mapping experiments (Carlen et al., 2009). Lentiviral expression of Cre recombinase under the *Foxj1* promoter, which was found to specifically label ependymal cells and their progeny in transgenic reporter mice, or ependymal-specific adenoviral transduction revealed that LVW ependymal cells do not divide or give rise to progeny under physiological conditions. Canonical Notch signaling was found to be required to keep ependymal cells in this state. However, upon stroke or inhibition of Notch signaling these cells could be activated to enter the cell cycle and differentiate into neuronal cells or astrocytes. The generation of progeny resulted in the loss of the ependymal cells, indicating that these cells are not able to self-renew (Carlen et al., 2009). These findings show that even though LVW ependymal cells can give rise to differentiated cells under non-physiological conditions, they do not fulfill the defining criteria of stem cells.

1.3.4 Neural stem and progenitor cells in the adult spinal cord

In contrast to the adult forebrain, where neurogenic activity is maintained throughout life, the adult spinal cord is considered a non-neurogenic region (Obermair et al., 2008). However, *in vitro* experiments provided evidence for the existence of neural stem/progenitor cells in this region (Weiss et al., 1996). Their location and function *in situ* has been investigated in a variety of studies. Neural stem or progenitor cells were suggested to reside in the area around the central canal, in the parenchyma of the spinal cord, or in both regions (Barnabe-Heider and Frisen, 2008; Obermair et al., 2008).

Under homeostatic conditions, cells of the ependymal layer around the central canal divide only rarely in order to self-renew and do not give rise to further differentiated progeny

(Johansson et al., 1999; Meletis et al., 2008; Hamilton et al., 2009). *In vitro* however, they can proliferate extensively and give rise to astrocytes, oligodendrocytes and neuronal cells (Martens et al., 2002; Sabourin et al., 2009). Similarily, changing the environmental conditions through injury, activates lumen-contacting cells to increase their proliferative rate and generate astrocytes (Johansson et al., 1999; Mothe and Tator, 2005). The use of indirect labeling techniques or the inability to trace the progeny of labeled cells in the above described studies did not allow to determine the precise identity of the lumen-contacting neural stem/progenitor cells. Findings of a recent study, which specifically labeled adult spinal cord ependymal cells and their progeny (using tamoxifen-inducible expression of Cre recombinase under the control of the *Foxj1* or *Nestin* regulatory sequences in transgenic reporter mouse lines) provide evidence that ependymal cells are the above described stem/progenitor cells in the central canal region. *In vitro* experiments in this study revealed that ependymal cells represent the vast majority of stem/progenitor cells in the spinal cord. Under physiological conditions *in vivo* ependymal cells did not give rise to progeny, but upon injury, they started to proliferate extensively and gave rise to oligodendrocytes and astrocytes, which migrated towards the lesion site and contributed to glial scar formation. The response to injury did not deplete the ependymal layer, indicating that these cells self-renew *in vivo* (Meletis et al., 2008).

Progenitor cells in the parenchyma constitute the majority of proliferating cells in the adult spinal cord under non-pathological conditions (Barnabe-Heider and Frisen, 2008; Obermair et al., 2008). Their functional properties are not fully understood yet. Findings from different studies suggest that parenchymal progenitor cells are either glial-restricted precursors (Horner et al., 2000; Yoo and Wrathall, 2007), that they do not form NSPs in culture (Martens et al., 2002), or that they possess a broader differentiation potential and self-renew in culture (Yamamoto et al., 2001).

1.4 Ependymal cells of the adult LVW and spinal cord

Ependymal cells form a continuous layer of cells, the ´ependyma`, along the cerebrospinal fluid-filled ventricular system and the spinal cord in the adult CNS. Ependymal cells are typically polarized with an apical and basal surface and the majority has motile cilia (9+2 axoneme) at the apical membrane (Bruni, 1998; Gabrion et al., 1998; Meletis et al., 2008). Coordinated beating of motile cilia in the LVW ependyma was shown to induce gradients of chemorepulsive factors, which are important for the directed migration of new-born neurons

in the LVW (Sawamoto et al., 2006). The ependyma is thought to function as a barrier between the cerebrospinal fluid and the CNS tissue, regulating the molecular transport between both systems, but also protecting the CNS from potentially harmful substances (Bruni, 1998). The ependymal barrier is established by means of tight and adherens junctions (Lippoldt et al., 2000; Alvarez and Teale, 2007; Mirzadeh et al., 2008). However, low levels of tight junction proteins suggest a certain permissiveness of the ependymal layer (Alvarez and Teale, 2007).

LVW ependymal cells are, at least in part, derived from radial glial cells and are born mainly around E14 to E16. Their maturation occurs postnatally (Spassky et al., 2005) (see 1.3.2). The ependymal layer along the adult lateral ventricles contains two types of ependymal cells, multiciliated type E1 cells and biciliated type E2 cells (Fig.3). Both cell types are positive for CD133, CD24 and S100, but negative for GFAP (Mirzadeh et al., 2008). In addition, tanycytes, a special ependymal subtype, were reported earlier to be part of the LVW ependyma (Doetsch et al., 1997). Tanycytes express GFAP and have long radially directed basal processes (Bruni, 1998). Due to phenotypic similarities, it was suggested that tanycytes might correspond to GFAP-positive ventricle-contacting type B cells (Chojnacki et al., 2009).

Ependymal cells of the adult spinal cord were suggested to be derived from NKX6-1 homeodomain transcription factor-positive ventral neuroepithelial cells (Fu et al., 2003). In the adult spinal cord, ependymal cells are divided into three distinct cell types according to morphological criteria: Cuboidal ependymal cells, tanycytes and a less frequent population of radial ependymal cells with long dorsoventral-oriented basal processes (Fig.5) (Meletis et al., 2008). All cells have one to three motile cilia (9+2 axoneme) and microvilli at their apical membrane (Sturrock, 1981; Meletis et al., 2008). Spinal cord ependymal cells synthesize CD133, S100 and proteins associated with immature cells, such as Nestin, Vimentin, Musashi-1, Platelet-derived growth factor receptor alpha (PDGFR-α) and SRY-box containing gene 2 (SOX2), but are negative for proteins associated with parenchymal progenitors, namely Oligodendrocyte transcription factor 2 (OLIG2) and the proteoglycan NG2 (Barnabe-Heider and Frisen, 2008; Meletis et al., 2008; Hamilton et al., 2009; Sabourin et al., 2009). Controversial data exists in case of GFAP. In two studies a subpopulation of mostly dorsally-located ependymal cells was reported to express GFAP (Hamilton et al., 2009; Sabourin et al., 2009), whereas the group of Jonas Frisen described all ependymal cells as GFAP-negative (Meletis et al., 2008). Furthermore, the existence of ependymal

subpopulations with distinct functional properties were proposed due to antigenic differences between ependymal cells (Hamilton et al., 2009; Sabourin et al., 2009).

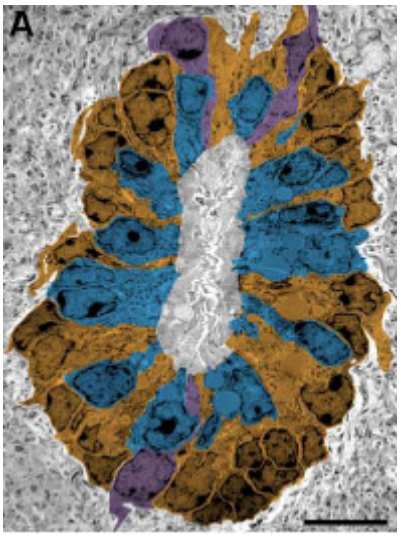

Figure 5: Immunoelectron microscopy of the adult spinal cord central canal. As illustrated by pseudo-coloring, ependymal cells can be divided into cuboidal ependymal cells (blue), tanycytes (brown) and radial ependymal cells (purple). Figure taken from Meletis et al. (2008).

1.5 The transmembrane protein CD133

The pentaspan membrane protein CD133 (Prominin-1) was first identified by Huttner and colleagues in embryonic and adult mouse epithelial cells (Weigmann et al., 1997). CD133 was found to be enriched at subdomains of the cell surface, such as microvilli of neuroepithelial cells and in cell protrusions, like filopodia, lamellipodia and microspikes in non-epithelial cells. Due to its specific location on the cell surface, this protein was termed ´Prominin`, from the Latin word *´prominere`*, which means to stand out, to be prominent. In the same year, the homolog of mouse CD133 was detected in human CD34-positive hematopoietic stem cells, by using an antibody against the surface antigen AC133 (Yin et al., 1997). In the mouse, CD133 is encoded by the *Prom1* gene on chromosome 5 (location 5 B3). Several splice variants are identified so far (in the mouse variant s1-s8) and their expression seems to be tissue-specific and developmentally regulated (Fargeas et al., 2007). CD133 has five putative transmembrane domains with two extracellular loops which contain more than 250 amino acids each, an extracellular N-terminal and a cytoplasmic C-terminal domain (Fig.6). Eight potential N-gycosylation sites are located at the extracellular loops (Fargeas et al., 2003).

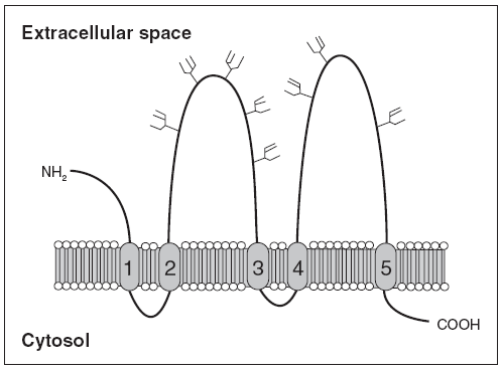

Figure 6: Predicted protein structure of CD133. Five transmembrane domains (1-5) divide two smaller cytosolic and two larger glycosylated extracellular loops. Forks represent potential glycosylation sites. Figure taken from Fargeas et al. (2003).

1.5.1 Function of CD133

Little is known about the physiological role of CD133, however the interaction with plasma membrane cholesterol and the involvement in the formation and organization of photoreceptor plasma membranes outgrowths, provide some clues about its function (Corbeil et al., 2001). CD133 is located at plasma membrane evaginations at the base of the outer segment of murine photoreceptor cells and mutations in the *Prom1* gene were shown to cause retinal degeneration due to impaired photoreceptor disk morphogenesis (Maw et al., 2000; Yang et al., 2008; Zacchigna et al., 2009).

Aside from that, neuroepithelial and radial glial cells were shown to release CD133-containing particles from cellular structures, such as microvilli, primary cilia and midbodies into the neural tube fluid (Marzesco et al., 2005; Dubreuil et al., 2007). Midbodies are remnants of the spindle midzone formed during the final stage of cell division, which connect the two dividing cells (Otegui et al., 2005). CD133-positive particles were found in the ventricular fluid at the onset and early phase of neurogenesis, a time when symmetrically dividing neuroepithelial cells are replaced by asymmetrically dividing radial glial cells. Two mechanistical explanations were suggested: The release of CD133-bearing particles as a means of intercellular signaling with the surrounding tissue or the disposal of CD133-containing membrane parts via the midbody in order to switch from symmetrical to asymmetrical divisions (Marzesco et al., 2005; Dubreuil et al., 2007). The apical cell membrane was suggested to have a defining role in the daughter cell´s fate to retain the proliferative stem cell potential of the parent cell or to become a further differentiated cell. According to this concept, the apical membrane of a cell needs to be reduced to switch from symmetrical to asymmetrical divisions (Kosodo et al., 2004).

1.5.2 CD133 distribution in the central nervous system

Similarly to its expression in primary progenitor cells of the mouse CNS, Uchida *et al.* found CD133-positive cells in the fetal human forebrain, which showed neural stem/progenitor cell characteristics *in vitro* and *in vivo* (Uchida et al., 2000). In the mouse, CD133-positive neural stem/progenitor cells were also detected in the postnatal cerebellum (Lee et al., 2005). As described in previous chapters, CD133 is expressed by several cell types in the adult murine CNS: CD133 is located at the outer segment of rod and cone photoreceptor cells (Zacchigna et al., 2009), synthesized by ependymal cells along the lateral ventricles and the central canal of the spinal cord and is found on a subpopulation of ventricle-contacting LVW type B cells (Coskun et al., 2008; Meletis et al., 2008; Mirzadeh et al., 2008; Sabourin et al., 2009). Moreover, the CD133 splice variant s3 was detected in myelin-forming oligodendrocytes, another glial cell type in the adult CNS. Interestingly, cultivated astrocytes derived from embryonic primary glial cell cultures expressed another CD133 splice variant (s1), suggesting the possibility to distinguish CD133 expression in glial cells by the presence of different splice variants (Corbeil et al., 2009).

1.5.3 CD133 as a tumor stem cell marker in the CNS?

The tumor stem cell hypothesis proposes that only a subset of cells within the tumor, termed tumor stem cells, possesses the ability to constitute and sustain the tumor, whereas the remaining tumor cells lack those features (Clarke et al., 2006). According to this model, the tumor stem cell fraction is the driving force of the tumor and represents the primary therapeutic target. Currently, the best functional assay to identify tumor stem cells is based on tumor initiation and serial transplantation in animal models (Clarke et al., 2006). The first evidence of a tumor stem cell fraction in brain tumors was provided by Singh *et al*., using the surface marker CD133 to enrich tumor stem cells from human glioblastoma and medulloblastoma. As few as 100 CD133-positive tumor cells were enough to give rise to new tumors after intracranial transplantation into NOD-SCID mice, whereas one thousand times more CD133-negative cells did not form any tumors. Tumors derived from CD133-positive tumor cells could be serially transplanted and the xenograft tumors resembled the original patient´s tumor (Singh et al., 2004).

A tumor stem cell can, but does not necessarily have to be the cell, which received the first oncogenic hits (cell of origin). Different tumor cells derived from the cell of origin can acquire additional mutations, which might provide them with tumor stem cell properties

(Clarke et al., 2006). Region-specific radial glial cells were proposed as cells of origin for ependymomas from the supratentorial, posterior fossa and spinal cord region. This was based on the identification of a $CD133^{+}/RC2^{+}/BLBP^{+}$ tumor stem cell population in ependymomas, a phenotype that characterizes RGC as well, and a microarray-based ´gene expression signature` of supratentorial and spinal cord ependymomas, which resembled the gene expression pattern of radial glial cells from the corresponding region (Taylor et al., 2005).

CD133 has been used in a variety of CNS neoplasms to enrich tumor stem cells (Cheng et al., 2009), however, there is emerging evidence that cells with the ability to initiate xenograft tumors can be found among CD133-negative tumor cells as well (Beier et al., 2007; Ogden et al., 2008; Wang et al., 2008). Thus, stem cell properties do not seem to be exclusive to CD133-positive cells within the tumor. In this context, it is also important to note that the above described studies used xenotransplantation assays (human cells transplanted into immunocompromised rodents) to identify tumor stem cells, which was suggested to select rather for cells that adapt best in a foreign host than for tumor stem cells (Clarke et al., 2006; Sakariassen et al., 2007).

2. Aims of the thesis

The surface protein CD133 is present on early murine and human neural stem cells during development and was used to enrich human tumor stem cells from glioblastomas, medulloblastomas and ependymomas (Weigmann et al., 1997; Uchida et al., 2000; Singh et al., 2004; Taylor et al., 2005). Whether this protein is a general marker for neural stem cells and tumor stem cells in the central nervous system (CNS), as well as its functional importance for these populations remains to be determined. Furthermore, it is not known, if the presence of CD133 on CNS tumor stem cells and certain neural stem cells indicates a lineage relationship between both. One step to solve these questions is the identification and characterization of CD133-presenting cells in the CNS.

The objectives of the first part of this thesis were (1) to investigate the cellular localization of CD133 in stem cell regions of the developing and adult murine CNS, namely the neurogenic region around the lateral ventricles as well as in the stem cell niche of the adult spinal cord, and (2) to study the stem/progenitor cell properties (self-renewal and multipotency) of the identified CD133-presenting cells *in vitro*.

Ependymal cells from the adult murine lateral ventricle wall (LVW) and the spinal cord central canal share certain phenotypic similarities, such as the presence of CD133 (Coskun et al., 2008; Meletis et al., 2008; Mirzadeh et al., 2008; Sabourin et al., 2009). However, both populations seem to have different functional properties. Accumulating evidence suggests that adult LVW ependymal cells are quiescent under physiological conditions *in vivo* (Spassky et al., 2005; Carlen et al., 2009), whereas ependymal cells from the adult spinal cord possess certain stem cell properties, as they can self-renew *in vivo* and *in vitro* and give rise to progeny upon activation by injury or in culture (Meletis et al., 2008). However, ependymal cells of both regions have not been directly compared under the same culture conditions. Moreover, little is known about the molecular basis underlying these functional differences.

Conflicting results regarding the functional properties of adult LVW ependymal cells were published in earlier studies (Chojnacki et al., 2009). This was caused partly due to the lack of defining surface markers and non-stringent cell isolation conditions. In stem cell niches, different cell types are tightly connected to each other and surface markers are often not exclusive for one population (Mirzadeh et al., 2008; Hamilton et al., 2009). Thus, it becomes more and more evident that a set of surface markers, together with more stringent

tissue dissociation procedures, is necessary for the specific isolation of distinct cell types within CNS stem cell niches.

The aims of the second part of this thesis were (1) to establish a protocol to purify CD133-positive ependymal cells from the adult murine LVW and spinal cord by flow cytometry, (2) to investigate their self-renewal and differentiation capacity under similar culture conditions and (3) to compare the gene expression profile of both ependymal cell populations.

3. Materials and Methods

3.1 Animals

Embryonic day 9.5 (E9.5) brain, E14.5 forebrain, postnatal day 4 (P4) and adult LVW and adult spinal cord tissue was obtained from C57Bl/6 wild-type mice (Taconic Europe, Ry, Denmark; Charles River, Sulzfeld, Germany) Additionally, transgenic C57Bl/6 mice, expressing green fluorescent protein (GFP) under a chicken Beta-actin promoter (Okabe et al., 1997) (Jackson Laboratory, Bar Harbor, ME, USA), were used as source for adult LVW tissue. All animal procedures were performed with consent from the ethical committee at Lund University.

3.2 Cell isolation and cultivation

3.2.1 Cell culture media

D-MEM/B27 medium		
D-MEM/F-12 (1:1) with GlutaMax		Invitrogen, Carlsbad, CA, USA
B27 supplement (minus vitamin A)	1x	Invitrogen
HEPES	10 mM	Invitrogen
Insulin	20 µg/ml	Sigma-Aldrich, St. Louis, MO, USA
Penicillin /Streptomycin	100 U/ml / 100 µg/ml	Invitrogen
Partricin	0.5 µg/ml	Biochrom AG, Berlin, Germany
Human recombinant EGF (EGF)	20 ng/ml	PAN Biotech, Aidenbach, Germany
Human recombinant FGFbasic (bFGF)	20 ng/ml	PAN Biotech

D-MEM/N2 medium		
D-MEM/F-12 (1:1) with GlutaMax		Invitrogen
N2 supplement	1x	Invitrogen
Penicillin /Streptomycin	100 U/ml / 100 µg/ml	Invitrogen
Partricin	0.5 µg/ml	Biochrom
EGF	20 ng/ml	PAN Biotech
bFGF	20 ng/ml	PAN Biotech

NB/B27 medium		
Neurobasal medium		Invitrogen
B27 supplement (minus vitamin A)	1x	Invitrogen
L-glutamine	2 mM	Invitrogen
Penicillin /Streptomycin	100 U/ml / 100 µg/ml	Invitrogen
Partricin	0.5 µg/ml	Biochrom
EGF	20 ng/ml	PAN Biotech
bFGF	20 ng/ml	PAN Biotech

NB/N2 medium		
Neurobasal medium		Invitrogen
N2 supplement	1x	Invitrogen
L-glutamine	2 mM	Invitrogen
Penicillin /Streptomycin	100 U/ml / 100 µg/ml	Invitrogen
Partricin	0.5 µg/ml	Biochrom
EGF	20 ng/ml	PAN Biotech
bFGF	20 ng/ml	PAN Biotech

NBA/B27 medium		
Neurobasal A medium		Invitrogen
B27 supplement (minus vitamin A)	1x	Invitrogen
L-glutamine	2 mM	Invitrogen
Penicillin /Streptomycin	100 U/ml / 100 µg/ml	Invitrogen
Partricin	0.5 µg/ml	Biochrom
EGF	20 ng/ml	PAN Biotech
bFGF	20 ng/ml	PAN Biotech

NBA/N2 medium		
Neurobasal A medium		Invitrogen
N2 supplement	1x	Invitrogen
L-glutamine	2 mM	Invitrogen
Penicillin /Streptomycin	100 U/ml / 100 µg/ml	Invitrogen
Partricin	0.5 µg/ml	Biochrom
EGF	20 ng/ml	PAN Biotech
bFGF	20 ng/ml	PAN Biotech

Attachment medium		
Neurobasal A medium		Invitrogen
B27 supplement (minus vitamin A)	1x	Invitrogen
L-glutamine	2mM	Invitrogen
Penicillin /Streptomycin	100U/ml / 100µg/ml	Invitrogen
Partricin	0.5µg/ml	Biochrom
FCS	1%	Biochrom
bFGF	20ng/ml	PAN Biotech

RA-medium		
Neurobasal A medium		Invitrogen
B27 supplement (minus vitamin A)	1x	Invitrogen
L-glutamine	2 mM	Invitrogen
Penicillin /Streptomycin	100 U/ml / 100 µg/ml	Invitrogen
Partricin	0.5 µg/ml	Biochrom
Retinoic acid	1 µM	Sigma-Aldrich

3.2.2 Isolation of embryonic and postnatal tissue

Eight to 12 E9.5 embryos, 5-10 E14.5 embryos and 5-15 P4 mice were used per experiment. The animals were sacrificed and whole embryos or brains were isolated. Subsequently, brains (E9.5), anterior part of the forebrains (E14.5) and P4 LVW tissues were dissected (Fig.7). For magnetic activated cell sorting (MACS), E9.5, E14.5 and P4 tissue was digested with 1 ml TrypLE Express (TLE; Invitrogen, Carlsbad, CA) for 10 min at 37°C, triturated with a 1000µl pipette and diluted 1:10 with D-MEM/F-12. The cell solution was filtrated with a cell strainer (40 µm; BD Biosciences, San Jose, CA) and the cell number was determined with a CASY cell counter according to the manufacturer´s instructions (Innovatis AG, Reutlingen, Germany). For fluorescence activated cell sorting (FACS), E14.5 and P4 tissue was digested with trypsin/EDTA (0.05%, Invitrogen) for 20 min at 37°C and triturated afterwards. Digestion was stopped 1:10 with D-MEM/F-12, containing 10% FCS (Biochrom AG, Berlin, Germany). After filtration, the trypsin/EDTA solution was removed by centrifugation (300 x g, 5 min, RT) with an Eppendorf 5810R centrifuge (Eppendorf, Hamburg, Germany) and the cell pellet was washed three times with D-MEM/F-12. The cell number was determined using a counting chamber (Carl-Roth, Karlsruhe, Germany). Trypan blue (0.4%; Sigma-Aldrich) was added to the cells to distinguish live and dead cells. In some experiments (4.2.2.3), cells were washed once with D-MEM/F-12 after filtration and erythrocytes were lysed with 0.5-1.0 ml ammonium chloride (0.8% NH_4Cl with 0.1 mM EDTA; Stemcell Technologies, Vancouver, Canada) for 2 min at room temperature (RT). Lysis was stopped with 14 ml Dulbecco's phosphate buffered saline (DPBS; Lonza, Basel, Switzerland) and the cells were washed once with DPBS.

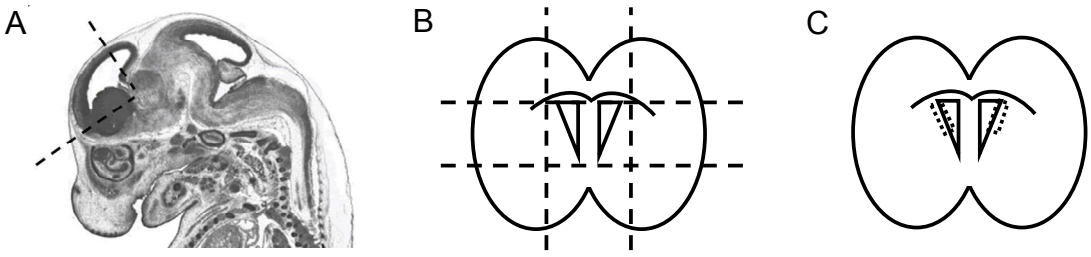

Figure 7: Tissue dissection from the E14.5, P4 and adult forebrain. (A) Dotted lines indicate the dissected area from the E14.5 anterior forebrain (A), P4 (B) and the adult (C) LVW region. In (A), the scull and meninges were removed before the tissue around the anterior lateral ventricles was isolated. For the frontal tissue sections shown in (B) and (C), the brain was cut coronally between the rhinal fissure and the hippocampus. In (B), the rectangular centrepiece, containing the lateral ventricles, was used for dissociation. From the adult brain, the anterior, dorsal part of the LVW was isolated (C). Figure (A) taken from http://www.genepaint.org/.

3.2.3 Isolation of adult LVW tissue

Seven to 20 adult animals were used per experiment. Animals were sacrificed and whole brains were isolated. LVW tissue was dissected out of frontal sections according to Fig.7C and digested with trypsin/EDTA (0.05%; 1 ml per LVW tissue from 2-3 mice) for 20-25 min at 37°C. The cells were triturated with a 1000µl pipette and the digestion stopped 1:10 with D-MEM/F-12, containing 10% FCS. After filtration with a cell strainer (40 µm), cells were centrifuged (300-330 x g, 5 min, RT), washed once with D-MEM/F-12 and, except for experiments described in section 4.1, erythrocytes were lysed with 0.2-0.6 ml ammonium chloride for 2 min at room temperature (RT). Lysis was stopped with 14 ml PBS and cells were washed once with PBS. The cell number was determined using a counting chamber. In case of low cell numbers, the last washing step was omitted.

3.2.4 Isolation of adult spinal cord tissue

Ten to 11 adult animals (4-5 weeks old) were used per experiment. The animals were sacrificed and spinal cord tissue (cervical and thoracic region) was isolated. For this, the animals were decapitated and the dorsal skin removed to expose the vertebral column. A cross cut in the lumbar region created a caudal opening of the column. A needle (18 gauge) of a PBS-filled syringe (20 ml), was inserted into the central canal of this caudal opening. By quickly compressing the plunger, the spinal cord was flushed out of the sourrounding vertebral column (Shihabuddin, 2002) (Fig.8). Minced spinal cord tissue was digested with trypsin/EDTA (0.05%; 1 ml per spinal cord) for 25 min at 37°C and triturated afterwards. The digestion was stopped 1:10 with D-MEM/F-12, containing 10% FCS. After filtration through a cell strainer (40 µm), the cells were centrifuged (330 x g, 5 min, RT) and washed once with D-MEM/F-12. To remove myelin debris, cells were suspended in 0.5-0.6 M sucrose/PBS (1 ml per spinal cord) and centrifuged with 850 x g (low deceleration) for 10 min at RT. The myelin-containing supernatant was removed and the remaining cell pellet was washed once with PBS. Erythrocytes were lysed with 0.5-1.0 ml ammonium chloride for 2 min at RT, which was stopped with 14 ml PBS afterwards. The cell number was determined using a counting chamber.

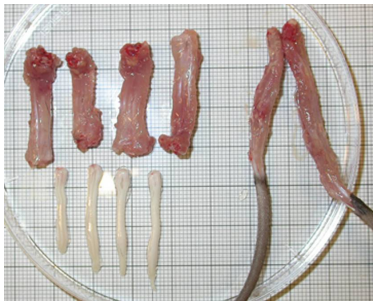

Figure 8: Isolation of spinal cord tissue. The cervical and thoracic parts of the spinal cord were isolated according to the technique described above. Examples of isolated spinal cords (left, bottom) and respective vertebral columns (left, top) are shown. To the right, intact vertebral columns with tails are shown.

3.2.5 Cultivation of FACS- and MACS-isolated cells

Experiments described in section 4.1: After sorting, E9.5, E14.5, P4 and adult LVW cells were plated out in suspension cell flasks (Nunc /Thermo Fisher Scientific, Roskilde, Denmark) or 12-well plates (TPP, Techno Plastic Products, Trasadingen, Switzerland) with $2x10^4$-$1x10^5$ cells/ml (FACS) or $2{,}5x10^4$-$3x10^5$ cells/ml (MACS) in D-MEM/B27 medium. Cells were cultivated at 37°C in 5% CO_2 in a HEPA class 100 incubator (Thermo Fisher Scientific, Waltham, MA, USA). The neurosphere (NSP) number was determined 4-7 days after plating. Pictures of cultured cells were taken with an Olympus IX70 (Olympus, Hamburg, Germany) and a Nikon Coolpix 4500 digital camera (Nikon, Tokyo, Japan).

In some experiments, sorted cells were attached to glass slides (Menzel, Braunschweig, Germany) by a Cytospin 3 SHANDON centrifuge (Labex instrument, Helsingborg, Sweden). 100 µl of cells in 1% BSA/PBS were centrifuged with 450 rpm for 1 min onto a glass slide. Attached cells were air-dried for 10 min at RT, followed by fixation with 4% formaldehyde in PBS for 10 min at RT. The cells were washed once with PBS, covered with 50% glycerol/PBS and stored at -20°C until use.

Experiments described in section 4.2: After sorting, E14.5, adult LVW and adult spinal cord cells were plated out in ultra-low attachment 24-well plates (Corning Life Sciences, Amsterdam, The Netherlands) and were kept at 37°C in 5% CO_2. In case of adult LVW and spinal cord cells, 1-6 cells/mm^2 (FACS) or 5-26 cells/mm^2 (MACS) were plated out in NBA/B27 medium. Of E14.5 cells, 2-3 cells/mm^2 were cultivated in D-MEM/B27 medium. The NSP number was determined six to ten days after plating.

For further cultivation, NSPs (5-10 days old) were centrifuged at 150 x g for 5 min at RT, dissociated using Accutase (incubation for 10 min at 37°C; PAA, Pasching, Austria) or TLE, as described in 3.2.2. Up to $1x10^5$ cells/ml were re-plated in the respective medium and culture dish.

For differentiation, NSPs were centrifuged at 150 x g for 5 min at RT to remove the growth-supporting medium and re-suspended in new medium without EGF and bFGF, but with NT4 (20 ng/ml; R&D Systems, Minneapolis, MN, USA) or without EGF, but FCS (1%) and bFGF (20 ng/ml, PAN Biotech). NSPs were plated onto coverslips (Menzel), coated with poly-L-lysine (PLL; 0.01% solution; Sigma-Aldrich), and cultivated for 3-4 days at 37°C in 5% CO_2. Coverslips were coated by incubation with PLL for 10 min at RT, followed by three washing steps with PBS.

3.2.6 Cultivation of adult LVW and spinal cord cells under different culture conditions

Adult LVW cells were isolated according to 3.2.3. $5x10^3$ cells per 24-well (TPP) were cultivated in D-MEM/B27, D-MEM/N2, NB/B27, NB/N2, NBA/B27 and NBA/N2 medium at 37°C in 5% CO_2. The NSP number was determined five days after plating.

CD133-positive and CD133-negative cells (10 cells/well) were sorted directly into 96-well plates (TPP), containing D-MEM/B27, NBA/B27 or NB/B27 medium (200 µl/well) and were cultivated at 37°C in 5% CO_2. The NSP number was determined up to 22 days after plating. For passaging of a single NSP, old medium was carefully removed with a pipette and 30 µl TLE were added into the well. After incubation for 10 min at 37°C and trituration, 300 µl of fresh medium were added and dissociated cells were distributed into 2-4 new 96-wells. After one or two passages, the number of NSPs was large enough to passage them according to 3.2.5.

Adult spinal cord cells were isolated according to 3.2.4 without the myelin removal step. $3x10^4$ cells per 6-well (TPP) were cultivated in D-MEM/B27, D-MEM/N2, NB/B27, NB/N2, NBA/B27 and NBA/N2 medium at 37°C in 5% CO_2. All media, except D-MEM/B27 contained Heparin (2 µg/ml; Lund University pharmacy). Since Heparin addition showed no effect in terms of primary NSP number other experiments (not shown in this thesis), this supplement was omitted in further experiments. The NSP number was determined eight days after plating.

3.2.7 Co-culture of CD133-positive and CD133-negative adult LVW cells

For the co-cultivation of adult GFP-expressing and wildtype LVW cells, lateral ventricular tissue was dissected according to Fig.7B and digested with TLE as described in section 3.2.2. Before the isolation of CD133-positive and CD133-negative cells according to 3.4.2, dead and apoptotic cells were removed through incubation with Dead Cell Removal MicroBeads (Miltenyi Biotec, Bergisch Gladbach, Germany) according to the manufacturer's instructions. $1.5x10^4$ MACS-isolated cells ($7.5x10^3$ CD133-positive and $7.5x10^3$ CD133-negative cells) were cultivated per 12-well (TPP) in D-MEM/B27 medium at 37°C in 5% CO_2. The NSP number was determined seven days after plating and documented with a Zeiss Axiovert 200M microscope using AvioVision 4.5 software (Carl Zeiss, Oberkochen, Germany).

3.2.8 Cultivation of adult spinal cord ependymal cells with retinoic acid

$CD133^+/CD24^+/CD45^-/CD34^-$ sorted spinal cord cells were plated onto PLL-coated chamber slides (1-2 cells/mm^2; 8-well Lab-Tek Chamber Slide, Nunc/Thermo Fisher Scientific, Roskilde, Denmark) in attachment medium. After 60 h, the attachment medium was replaced by retinoic acid (RA)-medium. RA was dissolved in DMSO according to the manufacturer´s instructions. As control, DMSO without RA was added. The cells were cultivated in RA-medium for 6 days in total and the medium was changed once after 3 days. Initial cell numbers were determined after sorting with a counting chamber and identical cell numbers were plated out for subsequent RA- and DMSO-supplemented cultures. After nine days in culture (attachment periode and RA/DMSO cultivation), cells were fixed with 4% formaldehyde in PBS for 10 min at RT. DAPI-positive cell nuclei of fixed cells were counted to determine final cell numbers. The relative cell number was calculated by dividing the final cell number after fixation by the number of plated cells.

3.3 Statistical analysis and illustration of data

The arithmetic mean and frequencies were determined with Microsoft Excel. The illustration of data and calculation of standard devation, standard error and *p*-values was performed with GraphPad Prism 4.03.

3.4 Fluorescence and magnetic activated cell sorting

3.4.1 Fluorescence activated cell sorting

Cells were resuspended in 1% BSA/PBS (1-2x10^6 cells/100 µl) in 96-U-well plates (Carl Roth; 100 µl cell suspension per well) and incubated either with an anti-Prominin I antibody conjugated to phycoerythrin (PE) (in the following referred to as CD133-PE) or with an antibody-mix, containing CD133-PE, CD24-Fluorescein isothiocyanate (FITC), CD34-Alexa Fluor 647 and CD45-PE-Cyanine 5 (Cy5) (Table 1) for 30 min on ice in the dark. Isotype matched control antibodies were used as negative controls (Table 1). After incubation, cells were centrifuged (300-330 x g, 5 min, 4°C) to remove excess antibody with the supernatant and the cell pellet was washed twice with 1% BSA/PBS. The cells were then resuspended in the final sorting volume of 1% BSA/PBS and filtered through a cell strainer (50 µm) into sterile FACS tubes (both from BD Biosciences). 7-amino-actinomycin D (7-AAD, Sigma-Aldrich) in a final concentration of 1 µg/ml was added to exclude dead cells. Cell doublets were eliminated during the sorting procedure by FSC- or SSC-Width versus Height gating. A FACSDiva flow cytometer (BD Biosciences) was used for cell sorting. For cell culture and

cytospins, cells were sorted into 1.5 ml tubes (Eppendorf), containing 500 µl of culture medium. For microarray experiments, cells were sorted into 350 µl RLT buffer (Qiagen, Hilden, Germany), containing 1% β-Mercaptoethanol (SERVA Electrophoresis, Heidelberg, Germany); for rtPCR, cells were sorted into 100 µl rtPCR lysis buffer. In case of experiments described in section 3.2.6 and CD133-positive and CD133-negative LVW cells were pre-sorted into 1% BSA/PBS. Subsequently, CD133-positive and CD133-negative cells were sorted individually into culture medium-filled 96-well plates (TPP). During the whole staining and sorting procedure, cells were kept on ice and in the dark. FACS data was processed with the FACSDiva software v5.0.3 or analysed with FlowJo v6.3.3 (Tree Star, San Carlos, CA, USA).

Table 1: Antibodies used for cell sorting

Antibody	Dilution	Supplier
CD133-PE, clone 13A4	1:100	eBioscience, San Diego, CA, USA
CD24-FITC, clone M1/69	1:500	BD Biosciences
CD34-AlexaFluor 647, clone RAM34	1:40	eBioscience
CD45-PE-Cy5, clone 30-F11	1:150	BD Biosciences
Rat IgG1-PE isotype control	1:100	eBioscience
Rat IgG2a-AlexaFluor 647 isotype control	1:40	eBioscience
Rat IgG2b-FITC isotype control	1:500	eBioscience
Rat IgG2b-PE-Cy5 isotype control	1:150	BD Bioscience

3.4.2 Magnetic activated cell sorting

Cells were resuspended in 0.5% BSA/PBS with 2 mM EDTA (MACS buffer) and incubated with CD133-PE (1:100, clone 13A4) for 30 min on ice in the dark. Cells were centrifuged (250 x g, 5 min, 4°C) to remove excess antibody with the supernatant and the cell pellet was washed once with MACS buffer. Cells were incubated with anti-PE magnetic microbeads (Miltenyi Biotec) and applied to a cell separation column (Miltenyi Biotec) according to the manufacturer's instructions. To increase the purity, CD133-positive and CD133-negative sorted cells were passed separately over new columns in some experiments. The cell numbers were determined with a CASY cell counter or with a counting chamber. To investigate the purity of the sort, aliquots of magnetically sorted cells were anaysed with a FACSCalibur flow cytometer (BD Biosciences). Unsorted cells incubated with rat IgG1-PE (1:100, eBioscience) were used to set the background fluorescence. FACS data was analysed with FlowJo software v6.3.3.

3.5 Immunostaining

Cells, grown on coverslips were fixed with 4% formaldehyde/PBS for 10 min at RT and either used directly or covered with 50% glycerol/PBS and stored at -20°C until use. Mouse brain and spinal cord tissue was fixed 2-16 h in 4% formaldehyde/PBS, followed by incubation in sucrose (25% in PBS) for cryoprotection. Cryostat (HM 560 Microm, Waldorf, Germany) tissue sections (10-12 µm) were placed on glass slides (Superfrost plus; Menzel) and stored at -80°C until use. Tissue cryosections and cells on coverslips were treated 5 min with 0.1% Triton-X-100 in PBS, and in case of stainings with 3220 and Ephrin-B1 antibodies with 0.5% Triton-X-100 in PBS, washed with PBS three times (5 min each) and blocked with 5-10% donkey serum (Jackson ImmunoResearch, West Grove, PA; USA) in PBS for 30 min at RT. Primary antibodies (Table 2) were diluted in PBS and applied for 16 h at 4°C or 1 h at RT. Appropriate isotype control antibodies or PBS were used as negative control. After three washing steps in PBS (15 min each), secondary antibodies coupled to Alexa Fluor 488, Alexa Fluor 647 (Invitrogen), Cy3, Cy5, FITC or Streptavidin-Cy3 (all from Jackson ImmunoResearch) were applied for 30 min at RT in the dark. Secondary antibodies were diluted in PBS with 5% donkey serum. Specimen were washed three times in PBS (15 min each), rinsed briefly in water, dehydrated in 100% ethanol, and air-dried. Sections and coverslips were embedded in mounting medium (VectaShield, Vector Laboratories, Burlingame, CA, USA), containing 1 µg/ml 4´,6´-diamidino-2-phenylindole (DAPI; SERVA Electrophoresis) nuclear stain. Immunofluorescence was documented with a Zeiss Axiovert 200M microscope using AvioVision 4.5/4.6 software (Carl Zeiss, Oberkochen, Germany).

Table 2: Primary antibodies for immunostainings

Antibody	Dilution	Supplier
3220 (recognizes FEN-1)	1:200	Kind gift from E. Warbrick*
Catenin beta-1	1:1000	Sigma-Aldrich
CD24-FITC, clone M1/69	1:500	BD Bioscience
CD34-FITC, clone RAM34	1:100	eBioscience
CD133, clone 13A4	1:100	eBioscience
CD133-Biotin, clone 13A4	1:100	eBioscience
Ephrin-B1	1:100	R&D Systems
Glial fibrillary acidic protein (GFAP)	1:400-1:800	Dako, Glostrup, Denmark
GFAP, clone G-A-5	1:500	Millipore, Billerica, MA, USA
GLAST	1:300	Abcam, Cambridge, United Kingdom
Nestin	1:200	BD Biosciences
Nestin	1:500	Neuromics, Edina, MN, USA
Ki-67	1:100	Novocastra, Newcastle upon Tyne, UK
O4, clone 81	1:100-1:200	Millipore
S100	1:200	Dako

SOX2	1:100	Santa Cruz Biotechnology, CA, USA
Tubulin beta-III, clone TU-20	1:100	Millipore
Tubulin beta-IV, clone ONS.1A6	1:100	Abcam

* University of Dundee, Scotland, United Kingdom

3.6 RNA isolation and amplification

$CD133^+/CD24^+/CD45^-/CD34^-$ adult spinal cord, $CD133^+/CD24^+/CD45^-/CD34^-$ LVW ependymal cells and $CD133^+/CD24^-/CD45^-/CD34^-$ radial glial cells were sorted directly into RLT lysis buffer (Qiagen), containing 1% β-Mercaptoethanol, snap-frozen in dry ice and stored at -80°C until use. Spinal cord–derived NSP cells were harvested at passage 2 and 3, washed once with PBS and the cell pellet was stored at -80°C until use. Total RNA from three samples of $CD133^+/CD24^+/CD45^-/CD34^-$ LVW ependymal cells, $CD133^+/CD24^+/CD45^-/CD34^-$ spinal cord ependymal cells, $CD133^+/CD24^-/CD45^-/CD34^-$ radial glial cells and from spinal cord derived NSPs, was isolated using the RNeasy Micro Kit (Qiagen) according to the manufacturer´s instructions. The obtained RNA was used for subsequent RNA amplification and biotin-labeling with the TargetAmp 2-Round Biotin-aRNA Amplification Kit (Epicentre Biotechnologies, Madison, WI, USA). Amplification and labeling procedures were performed as recommended by the manufacturer. Before the second *in vitro* transcription round, the cDNA quality was determined by a control PCR with primers for the housekeeping gene B2m (Table 3). The RNeasy Micro Kit (Qiagen) was employed for RNA purification during the amplification procedure, according to the manufacturer´s instructions (RNA cleanup and concentration). During RNA isolation and purification, two times 14 µl RNase-free water were used for RNA elution. The final biotin-labeled cRNA amount was measured with a Spectrophotometer (Nanodrop ND-1000; Thermo Fisher Scientific) and the cRNA quality was verified by agarose gel electrophoresis.

Table 3: Control PCR

Reaction mix (50µl total volume)		Supplier	Thermal profile		
			Temperature	Time	Cycle number
Primer (fw)	0.4 µM	Operon/ IDT*	94°C	1 min	1x
Primer (rv)	0.4 µM	Operon/ IDT	94°C	45 s	40x
dNTPs	200 µM	Fermentas	53°C	1 min	
Reaction buffer	1x	Applied Biosystems	72°C	1 min	
Taq Poymerase	2 U	Applied Biosystems			
H_2O			Primer		
cDNA	1 µl		B2m forward: TCGAGACATGTGATCAAGCA		
			B2m reverse: TGGGGGTGAGAATTGCTAAG		

*Eurofins MWG Operon; Ebersberg, Germany / Integrated DNA Technology (IDT), Coralville, IA, USA

3.7 Gene expression microarray and data analysis

(The hybridization was performed by SCIBLU Genomics at Lund University, Sweden, and the microarray data was analysed by Dr. Christine Steinhoff, Max Planck Institute for Molecular Genetics, Berlin, Germany)

Biotin-labeled cRNA (1.5 µg/sample) was hybridized onto MouseWG-6 v1.1 gene expression microarrays (Illumina, San Diego, CA, USA). Three independent biological replicates of $CD133^+/CD24^+/CD45^-/CD34^-$ LVW ependymal cells, $CD133^+/CD24^+/CD45^-/CD34^-$ spinal cord ependymal cells, $CD133^+/CD24^-/CD45^-/CD34^-$ radial glial cells, and spinal cord ependymal cell-derived NSPs were analysed. Hybridization was performed by the Lund University microarray facility (http://www.lth.se/sciblu/genomics_services) following the standard protocol for whole genome gene expression direct hybridization assays (Illumina). The gene expression raw data was background-corrected and summarized using BeadStudio software (Illumina) and further processed applying the Lumi package (Du et al., 2008) developed within the Bioconductor project in the R statistical programming environment (Gentleman et al., 2004). Data was normalized using quantile normalization and variance stabilization (function vst). The resulting log2 intensities ranged from 6.46 to 14.51 and were used for further analysis. Differentially expressed genes were determined applying the limma Bioconductor package and using the functions lmFit and eBayes with default settings. The resulting *p*-values were adjusted for multiple testing according to Benjamini-Hochberg (Hochberg and Benjamini, 1990). Gene expression differences with adjusted p values below 0.05 were considered relevant. TM4 (Saeed et al., 2003) was used for calculation and display of biclustering of absolute, normalized, logarithmic expression values. Average linkage and euclidean distance and otherwise default settings were chosen. All calculations were performed in the R statistical programming environment (Gentleman et al., 2004) version 2.8.0.

3.8 Multiplex reverse transcriptase PCR (rtPCR)

Table 4 : rtPCR primers (5'-3')

Gene	Forward primer (outer)	Reverse primer (outer)
Cd24a	CTTCTGGCACTGCTCCTACC	AACCTGTGCCCAATTTCAAG
Dlx2	ACACCGCCGCGTACACCTCCTA	CTCGCCGCTTTTCCACATCTTCTT
Fen1	ACTGTCCAGAGAACGCTGTG	ATGCGGATGGTACGGTAGAA
Foxg1	GCAAGGGCAACTACTGGATG	CGTGGGGGAAAAAGTAACTG
Foxj1	GATCACTCTGTCGGCCATCT	GGTAGCAGGGCAGTTGATGT
Hey1	TGGATCACCTGAAAATGCTG	ATCTCTGTCCCCCAAGGTCT
Id2	CTCCAAGCTCAAGGAACTGG	TTCAACGTGTTCTCCTGGTG
Nf2	GGGGAAGGACCTGTTTGATT	CGCATACCAAGCCGTAATTC

Prom1	TCCTGGGACTGCTGTTCATT	GCCTTGTTCTTGGTGTTGGT
Rtel1	AAGGGGAACTCTTTGCCAGT	ACATCACGGGGAGTCAAGTC
Rxrg	GCCTGGGATTGGAAATATGA	CACGTTCATGTCACCGTAGG
	Forward primer (inner)	**Reverse primer (inner)**
Cd24a	CTTCTGGCACTGCTCCTACC	AGGAGACCAGCTGTGGACTG
Dlx2	AACCACGCACCATCTACTCC	CCGCTTTTCCACATCTTCTT
Fen1	GCCTTGCCAAACTAATTGCT	GTCTCACCCTCCTCGTTCTG
Foxg1	GAGCGACGACGTGTTCATC	CGACATGGGCCAGTAGAGG
Foxj1	GCTGCTTCAGGAGTTTGAGG	TAGCTCCAGACCCTCCAGTG
Hey1	TGGATCACCTGAAAATGCTG	TGGGATGCGTAGTTGTTGAG
Id2	GTCCTTGCAGGCATCTGAAT	CTCCTGGTGAAATGGCTGAT
Nf2	CCTGAAAATGCTGAGGAGGA	GAGGGGTCATAGTCGCCATA
Prom1	GGTGGGCTGCTTCTTTTGTA	GTCCTGGTCTGCTGGTTAGC
Rtel1	GCACTCCCAGCTAACTCAGG	GCGACTTGCTACCTTCTTGC
Rxrg	GACAGATCCTCAGGGAAGCA	CCTCACTCTCTGCTCGCTCT

2 µl drops, containing single $CD133^+/CD24^+/CD45^-/CD34^-$ sorted LVW ependymal cells in 1% BSA/PBS, were placed onto coverslips (PeCON, Erbach, Germany) and evaluated by light microscopy for their ependymal morphology (long motile cilia). The cells with approved morphology were documented and transferred into 96-wells or 0.2 mL PCR reaction tubes (Applied Biosystems, Foster City, CA, USA), containing 2 µl of 2x rtPCR lysis buffer (Table 5). Cells in lysis buffer were centrifuged with 3,000 rpm for 1 min at 4°C and frozen at -80°C until use. 370-500 $CD133^+/CD24^+/CD45^-/CD34^-$ spinal cord ependymal cells were sorted directly into 100 µl rtPCR lysis buffer, vortexed for 1 min and frozen at -80°C until use.

RNA of the cell lysate was reverse transcribed with multiple gene-specific outer reverse (rv) primers according to Table 6. In the first round PCR, 40 µl PCR mix, containing multiple gene-specific outer forward (fw) primers, was added to the reverse transcriptase reaction product (cDNA). The PCR conditions are described in Table 7. Two microliter aliquots of the first-round PCR product were used in a second gene-specific nested PCR (individual PCR reactions for every gene) using gene-specific inner primer pairs (Table 8). Second-round PCR products were evaluated by agarose gel electrophoresis and visualized with a GelLogic 100 gel documentation system (Kodak, Raytest Höllviken, Sweden).

Table 5: rtPCR lysis buffer

Lysis buffer mix		**Supplier**
NP-40 Alternative	0.4%	Calbiochem/ Merck, Darmstadt, Germany
dNTPs	65 µmol/l	Fermentas
Dithiothreitol	2.4 mmol/l	Invitrogen
RNAsin	0.5 U/µl	Promega, Madison, WI

Table 6: Reverse transcription (RT)

Reaction mix (10 µl total volume)		Supplier	Thermal profile		
			Temperature	Time	Cycle number
Primers (outer rv)	1.25 µM (each)	Operon/ IDT	37°C	60 min	1
MMLV buffer	1x	Promega			
M-MLV-RT	50 U	Promega			
H_2O					
Cell lysate	4 µl				

Table 7: First-round PCR

Reaction mix (50 µl total volume)		Supplier	Thermal profile		
			Temperature	Time	Cycle number
Primers (outer fw)	0.25 µM (each)	Operon/ IDT	94°C	5 min	1x
dNTPs	200 µM	Fermentas	94°C	1 min	35x
Reaction buffer	1x	Applied Biosystems	58°C	1 min	
Taq Poymerase	1.25U	Applied Biosystems	72°C	2 min	
H_2O			72°C	7 min	1x
cDNA template	10 µl				

Table 8: Second-round PCR

Reaction mix (25 µl total volume)		Supplier	Thermal profile		
			Temperature	Time	Cycle number
Primer (inner fw)	0.25 µM	Operon/ IDT	94°C	5 min	1x
Primer (inner rv)	0.25 µM	Operon/ IDT	94°C	30 s	35x
dNTPs	200 µM	Fermentas	58°C	1 min	
Reaction buffer	1x	Applied Biosystems	72°C	1 min	
Taq Poymerase	0.625 U	Applied Biosystems	72°C	7 min	1x
H2O					
cDNA template	2 µl				

3.9 Web resources

Word wide web addresses of tools and databases used in this work are listed below:

Literature research

http://www.ncbi.nlm.nih.gov/pubmed/

Gene/gene expression/ gene sequence information

http://www.ncbi.nlm.nih.gov/unigene

http://www.ensembl.org/Mus_musculus/Info/Index

http://blast.ncbi.nlm.nih.gov/Blast.cgi

http://www.genecards.org/

Primer design

http://frodo.wi.mit.edu/primer3/

Protein information

http://www.uniprot.org/

Brain atlas

http://www.genepaint.org/

4. Results

4.1 Identification and functional characterization of CD133-positive cells in stem cell regions of the murine central nervous system

4.1.1 Localization of CD133 in stem cell regions of the developing forebrain and in the adult central nervous system

The earliest neural stem/progenitor cells in the developing mouse brain, neuroepithelial cells, carry the transmembrane protein CD133 at their apical surface (Weigmann et al., 1997). To investigate which other cells in neural stem cell niches of the developing and adult murine central nervous system (CNS) are immunoreactive to CD133, the lateral ventricle wall (LVW) region in the embyonic, postnatal and adult brain and the central canal in the adult spinal cord was investigated.

4.1.1.1 Localization of CD133 in the LVW region during development

At the onset of neurogenesis, neuroepithelial cells are replaced by radial glial cells (RGC). The cell body of RGC is located in the ventricular zone, whereas their long basal processes extend to the pial surface (Mori et al., 2005). In this thesis, a subpopulation of lateral ventricle-contacting cells in the embryonic day 14.5 (E14.5) forebrain was CD133-positive and co-expressed Nestin and GLAST, two proteins which are characteristic for RGC at this develomental stage (Mori et al., 2005) (Fig.9A). Most CD133-positive cells were found in the dorsal, but not in the striatum-lining ventral ventricular zone.

RGC give rise to ependymal cells and it was shown that at least a radial glial subpopulation directly transforms into ependymal cells in the first two postnatal weeks (Spassky et al., 2005). In immunostainings of the postnatal day 4 (P4) LVW shown in Figure 9B, the majority of CD133-positive cells were located in the ventral ventricular zone and some scattered CD133-positive cells were found at the dorsal wall. These cells still expressed the glial cell protein GLAST, but also S100, a protein found on ependymal cells in the adult lateral ventricle wall (Spassky et al., 2005). As ependymal cells mature, they develop long motile cilia and Tubulin beta-IV, a marker for ciliated cells (Renthal et al., 1993), co-localized with CD133 at the apical cell membrane of ventricle-contacting cells (Fig.9B). Thus, CD133-positive cells co-expressed radial glial and ependymal cell proteins, which suggest that they are in an

intermediate state between these two cell types. In the dorsal ventricular zone, most GLAST-positive cells were negative for CD133, S100 and Tubulin beta-IV (Fig.9B), an expression pattern compatible with CD133-negative RGC.

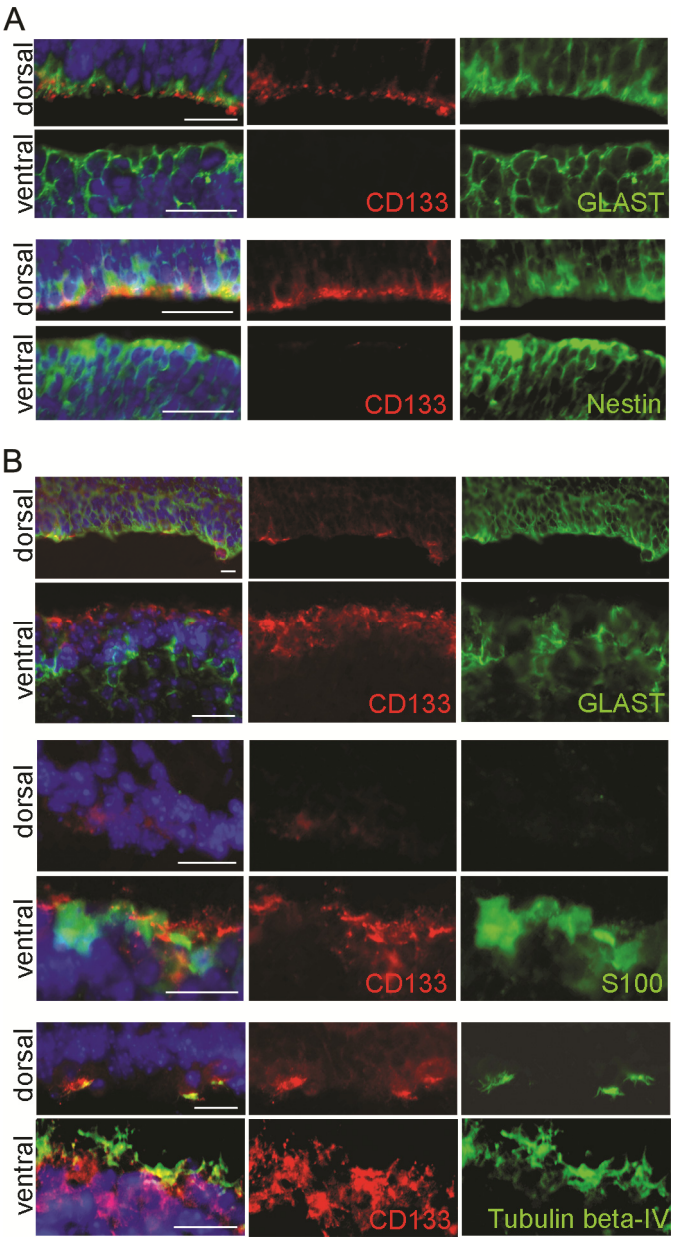

Figure 9: Immunolocalization of CD133 at the embryonic and postnatal lateral ventricle wall. Sagittal sections through the LVW of E14.5 (A) and P4 (B) mouse brain are shown. Images of the dorsal (top images) and ventral ventricular wall (bottom images) are depicted with the ventricular lumen facing downwards (top images) or upwards (bottom images). (A) CD133 is located at the ventricular surface of the dorsal wall. CD133-positive cells are also stained by GLAST and Nestin. CD133 staining is faint to absent at a region of the ventral wall lining the striatum. (B) CD133 is present at the ventral side of the P4 LVW. Very few CD133-positive cells are localized at the dorsal side. CD133-positive cells are also synthesizing S100, GLAST and Tubulin beta-IV. Cell nuclei are visualized with 4´,6-diamidino-2-phenylindole (DAPI, blue). Scale bars: 20 µm.

4.1.1.2 Localization of CD133 in the adult LVW and spinal cord

In the adult LVW, two cell types have contact to the ventricle: Ependymal cells and a subpopulation of type B cells, which are located in close proximity to ependymal cells and contact the ventricle with their apical processes (Mirzadeh et al., 2008; Shen et al., 2008). Immunostainings of the LVW (Fig.10) revealed that CD133 was localized at the apical membrane of ventricle-contacting cells. Most CD133-positive cells expressed Tubulin beta-IV and S100, thereby confirming an ependymal identity of these cells. In addition, the vast majority of CD133-expressing cells could be co-stained with CD24, a surface protein found

on ependymal cells and neuroblasts (Calaora et al., 1996). Neuroblasts, however, are located in the subventricular zone and do not contact the ventricle. The intermediate filament protein GFAP is expressed by type B cells in the LVW (Doetsch et al., 1997). The majority of GFAP-positive cells, located mainly in the SVZ, was negative for CD133. However, of 182 investigated CD133-positive cells at the ventricular surface, 1.6% could be co-stained with GFAP (Fig.10).

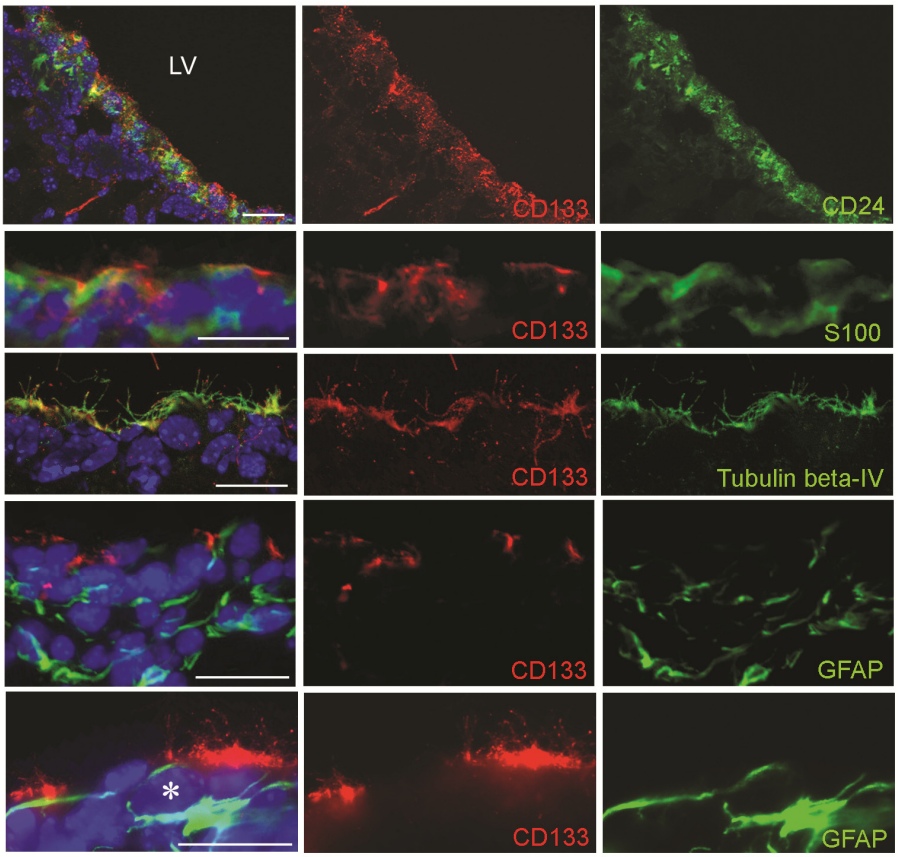

Figure 10: Immunolocalization of CD133 at the adult lateral ventricle (LV) wall. Images from panel two to five are depicted with the ventricular lumen facing upwards. Upper three panels: CD133 co-localizes with CD24, S100 and Tubulin beta-IV at the surface of the adult LVW. Fourth panel: The vast majority of cells synthesizing GFAP do not express CD133. Lowest panel: A single ventricle-contacting cell (asterisk) positive for CD133 and GFAP. Nuclei are stained with DAPI (blue). Scale bars: 20 µm.

Ependymal cells of the adult spinal cord can be morphologically subdivided into three types of ciliated, lumen-contacting cells: cuboidal ependymal cells, tanycytes and radial ependymal cells (Meletis et al., 2008). The sub-ependymal layer, which is smaller compared to the forebrain subventricular zone, consists of astrocytes, neurons and oligodendrocyte progenitors (Hamilton et al., 2009). Figure 11 shows that similar to the LVW region, CD133 was localized at the apical membrane of lumen-contacting cells. Note that here the CD133 signal was weaker compared to the ependymal staining in the LVW, which can be explained by the lower number of cilia (1-3/cell) (Meletis et al., 2008). CD133-positive ependymal cells could

be co-stained with antibodies against CD24 and the majority was also positive for SOX2, a transcription factor expressed by ependymal cells and dividing cells in the adult LVW (Ferri et al., 2004). GFAP-positive cells were located in close proximity to the ependymal layer, but lumen-contacting CD133-expressing cells were negative for GFAP. However, a co-expression of CD133 and GFAP proteins in a small subpopulation of ependymal cells can not be excluded, since the CD133 staining was faint in some areas and for example radial ependymal cells contact the ventricle with a small part of their apical cell surface only, which makes the detection of a CD133/GFAP co-staining difficult. Outside the ependymal layer, CD133 was present on a subfraction of CD34-positive cells in blood vessel-like structures (Fig.11).

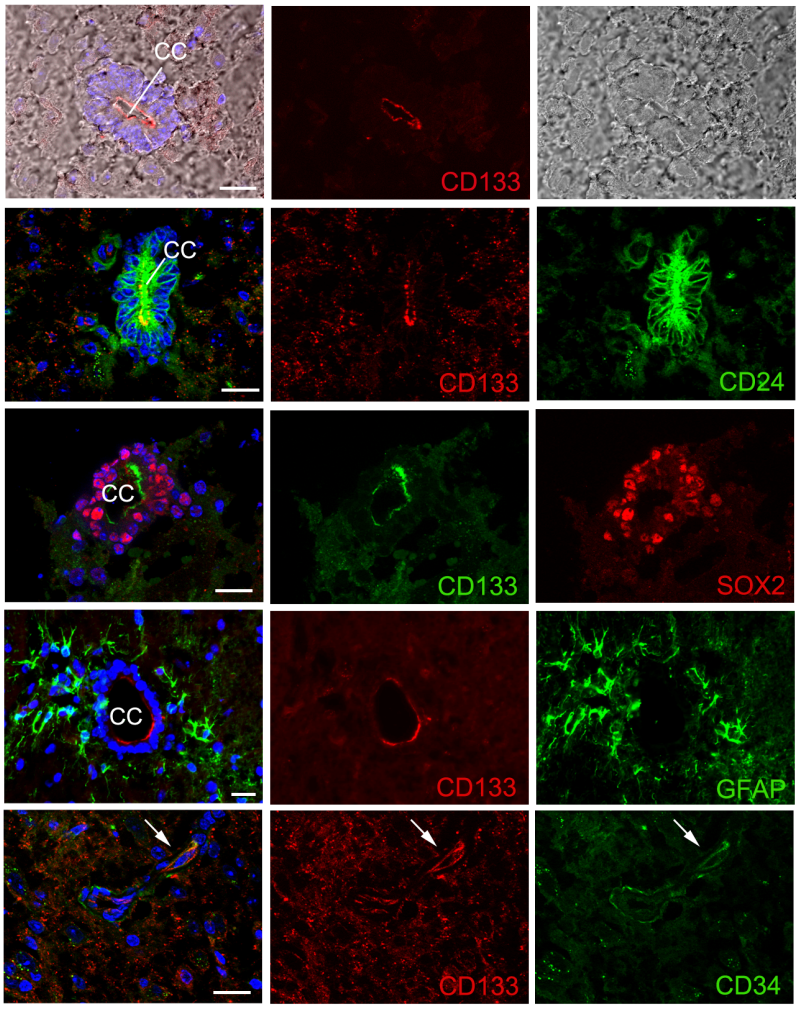

Figure 11: Immunolocalization of CD133 in the adult spinal cord. Upper three panels: Cells lining the central canal (CC) are CD133 positive. CD133-positive cells can be co-stained with CD24 and in part with SOX2 antibodies. Fourth panel: GFAP-positive cells are located outside the ependymal layer. Lowest panel: Co-expression of CD133 and CD34 at vessel-like structures (arrow) in the spinal cord parenchyma. Cell nuclei are visualized with DAPI (blue). Scale bars: 20 µm.

Taken together, the phenotypic characterization of CD133-positive cells in the developing and adult CNS showed that this protein was expressed by a subpopulation of radial glial cells, an intermediate radial glial/ependymal cell type in the postnatal LVW and the majority of ependymal cells in the adult spinal cord and LVW. In addition, a small number of $CD133^{+}/GFAP^{+}$ cells was found in the adult LVW.

4.1.2 Establishment of flow cytometry-based cell isolation from the adult LVW with CD133 antibodies

To isolate antibody-labeled cells from the adult LVW by fluorescence activated cell sorting (FACS), certain characteristics of the adult brain have to be considered. First, single cell solutions devoid of cellular and extracellular debris are desirable for FACS. However, the adult brain contains a high amount of extracellular matrix molecules in comparison to embryonic and postnatal brain tissue, which can cause tissue dissociation difficulties, unspecific antibody binding and sorting impurities. Second, surface markers can get cleaved or changed during the cell dissociation procedure (Panchision et al., 2007). After initial tests with mechanical dissociation, TLE, trypsin/EDTA and papain to optimize tissue dissociation versus cell survival, trypsin/EDTA digestion was used for further experiments. To avoid surface antigen degradation, a low trypsin/EDTA concentration (0.05%) was chosen. These cell preparations still contained some debris, which was excluded during the sorting procedure by size versus granularity gating (gate P1, Fig.12A). An initial experiment with ubiquitous GFP-expressing cells allowed the distinction between cells and debris (not shown). All CD133-positive cells, and as control CD133-negative cells were selected for sorting, however intermediate CD133-low/negative cells were excluded to obtain sorted populations with high purity (Fig.12B).

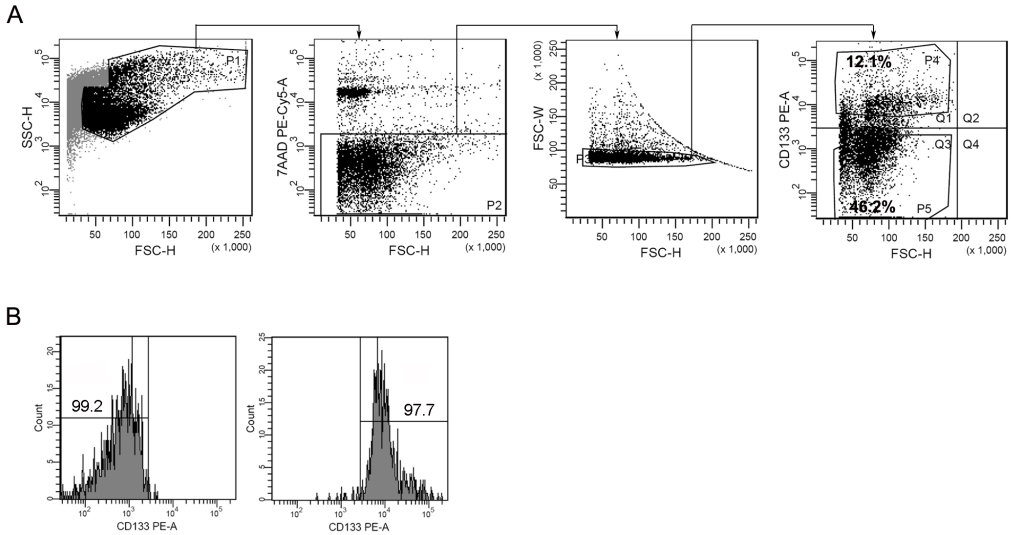

Figure 12: Isolation of CD133-positive and CD133-negative adult LVW cells by flow cytometry. (A) Representative dot plots illustrate the sorting strategy to isolate CD133-positive cells from whole LVW preparations. Forward and Side Scatter (FSC-H and SSC-H) were used to separate cells (gate P1) from debris (light grey). 7-AAD served to distinguish dead from live cells (P2). FSC-Width (FSC-W) versus FSC-Height (FSC-H) was used to select single cells (P3) and exclude cell doublets. CD133-positive (P4) and CD133-negative (P5) cells were sorted. Gates (Q1-Q4) were set according to an isotype control. Arrows display the gating sequence. Percentages of gated cells with respect to P1 are indicated within the gated regions. (B) Re-analysis of CD133-negative (left image) and CD133-positive (right image) fractions indicates the purity of the sorted populations. The x-axis shows CD133-PE intensity and the y-axis the number of event counts.

4.1.3 Functional characterization of CD133-positive cells in stem cell regions of the developing and adult brain

Neural stem and progenitor cells are commonly indentified based on functional criteria, such as self-renewal and multipotency. The *in vitro* stem/progenitor cell properties of CD133-positive and as control CD133-negative cells of the developing brain and adult lateral ventricle wall were investigated through their isolation by FACS or magnetic activated cell sorting (MACS) and subsequent determination of the primary neurosphere (NSP) frequency, NSP passage number and differentiation potential.

4.1.3.1 Functional properties of CD133-positive cells from the developing brain in vitro

CD133-positive and CD133-negative cells from the developing E9.5 brain, E14.5 forebrain and P4 lateral ventricle region were investigated. At E9.5, shortly before the onset of neurogenesis, most neuroepithelial cells have not yet transformed into radial glial cells (Gotz and Huttner, 2005). This time point was included as internal control, since neuroepithelial cells are CD133-positive (Weigmann et al., 1997) and were shown earlier to form multipotent NSPs *in vitro* (Tropepe et al., 1999). The number of primary NSPs per total number of plated cells was determined and indicated as NSP frequency. In line with previous published results, CD133-positive (CD133-pos) MACS-isolated cells from E9.5 brain, gave rise to primary NSPs (average NSP frequency 1/3,268), whereas CD133-negative (CD133-neg) cells did not form NSPs (Fig.13). The obtained NSPs differentiated into astrocytes and neuronal cells (Fig.14A). At E14.5, primary NSPs were formed by CD133-positive and CD133-negative MACS-isolated cells (average NSP frequency CD133-pos: 1/323, CD133-neg: 1/809; Fig.13). Similar results were obtained with MACS-isolated CD133-positive and CD133-negative cells from P4 tissue (average NSP frequency CD133-pos: 1/962 CD133-neg: 1/1,818). The results obtained with MACS-isolated E14.5 and P4 cells were confirmed using FACS as an alternative isolation method (Fig.13, one experiment per stage). NSPs from CD133-positive and CD133-negative cells of E14.5 and P4 tissue could be kept in culture for more than eight passages and differentiated into glial and neuronal cells (Fig.14A).

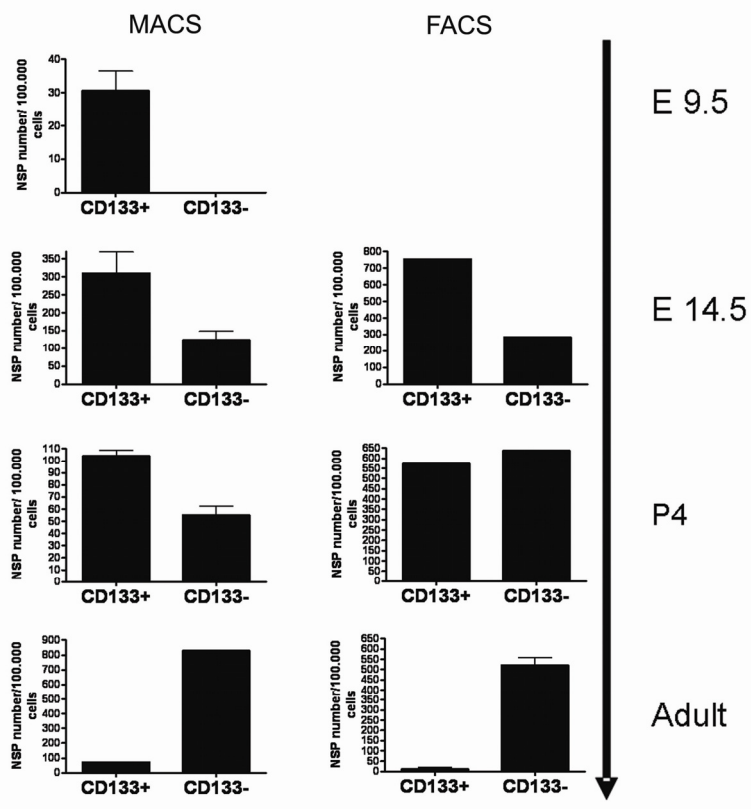

Figure 13: NSP frequency of CD133-positive and CD133-negative populations at different stages of brain development. Columns illustrate primary NSP numbers per 100,000 plated cells. NSP frequencies of MACS-isolated cell populations are shown on the left side, results of FACS-isolated cells are depicted to the right. CD133-positive and CD133-negative cells were isolated from E9.5 brain, E14.5 forebrain, P4 and adult LVW. Three independent experiments were performed in case of MACS-isolated cells from E9.5 brain, E14.5 forebrain, P4 LVW and in case of FACS-isolated cells from the adult LVW. Note that the neurosphere number of TLE-digested cell populations (MACS isolated cells from E9.5, E14.5 and P4) is generally lower as compared to trypsin/EDTA-treated cells. Error bars indicate the standard deviation. The other results represent single experiments.

4.1.3.2 Functional properties of CD133-positive cells from the adult LVW in vitro

In the adult LVW, the majority of NSPs was formed by CD133-negative cells (average NSP frequency 1/121), whereas the NSP frequency of CD133-positive MACS-isolated cells was only 1 in 1,389 cells on average (Fig.13). Since adult brain preparations contained a high amount of debris, which lowered the purity of MACS isolated fractions, FACS was used as the main isolation method (see also 4.1.2). Three independent FACS experiments confirmed the trend observed with LVW MACS-isolated cells, with an even lower average NSP frequency in the CD133-positive fraction (1/8,850) compared to the CD133-negative sorted population (average NSP frequency 1/192; Fig 13). Immediately after sorting, cells with multiple CD133- and Tubulin beta-IV-stained cilia could be observed in the CD133-positive sorted fraction (Fig.14C). Live cell imaging confirmed active beating of these cilia (not shown). CD133-negative derived NSPs could be kept in culture for more than nine passages and gave rise to all three neural lineages (Fig.14A). NSPs derived from CD133-positive cells were smaller in size compared to the ones derived from CD133-negative cells (Fig.14B) and could be kept in culture no more than two passages. Upon differentiation induction they gave rise to astrocytes only (Fig.14A).

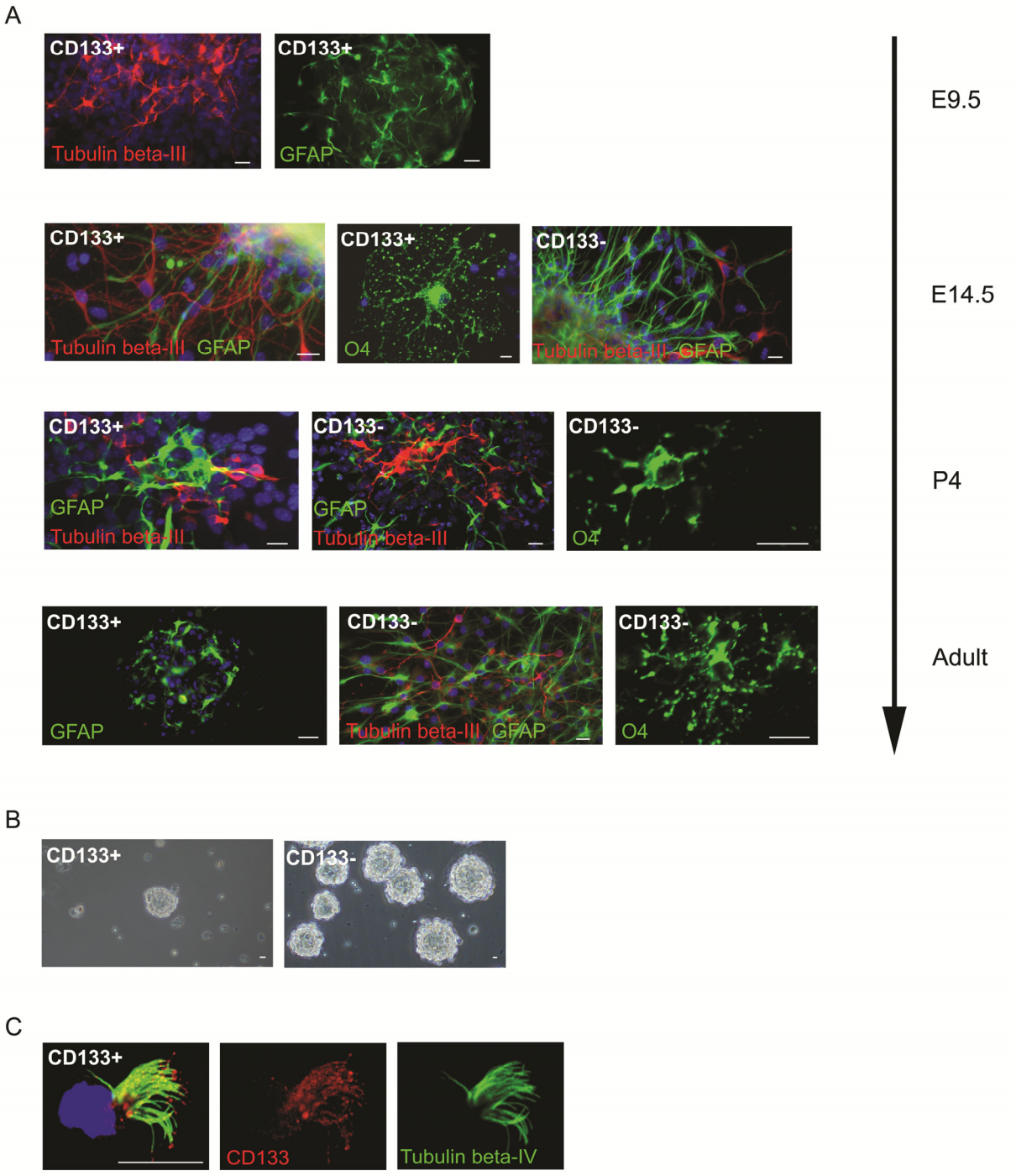

Figure 14: Immunostainings of cultured and directly isolated cells from CD133-positive and CD133-negative populations. (A) NSPs derived from CD133-positive and CD133-negative cells of E9.5 brain, E14.5 forebrain, P4 and adult LVW give rise to Tubulin beta-III-positive neuronal cells, GFAP-positive astrocytes and O4-positive oligodendrocytes. Note that at E14.5, neurosphere cells derived from the CD133-positive fraction give rise to cells of all three neural lineages, whereas CD133-negative derived spheres only differentiate into astrocytes and neuronal cells. At P4, NSPs from CD133-negative, but not from CD133-positive cells differentiate into oligodendrocytes. In the adult LVW, a differentiating sphere from the CD133-positive fraction is shown, which expresses only GFAP, whereas differentiating spheres from the CD133-negative fraction are positive for GFAP, Tubulin beta-III, and O4. (B) Most neurospheres derived from the adult LVW are formed by CD133-negative cells. A low number of smaller neurospheres is found in the CD133-positive fraction. (C) A CD133-positive sorted cell from the adult LVW, showing multiple cilia which are stained with antibodies against CD133 and Tubulin beta-IV. Scale bars: 15 µm. Cell nuclei are stained with DAPI (blue).

4.1.3.3 Influence of extracellular signals on the NSP frequency of CD133-positive adult LVW cells

To test whether CD133-negative cells secrete factors that influence the NSP-forming capacity of CD133-positive cells, both populations were cultivated together in the same culture dish. To distinguish CD133-positive from CD133-negative cells, one population was derived from transgenic mice with ubiquitous GFP-expression under the Beta-actin promoter and the other population from wild-type animals. The cells were isolated by MACS and similar cell numbers of both populations were plated out. First, GFP-expressing CD133-negative cells were cultivated together with CD133-positive wild-type (GFP-negative) cells. The majority of primary NSPs, developed after seven days in culture, expressed GFP (NSP frequency GFP-positive: 1/750; GFP-negative: 1/3750; Fig.15). The reverse experiment with GFP-expression in CD133-positive cells and CD133-negative cells from wild-type mice gave similar results (NSP frequency GFP-negative: 1/936; GFP-positive: 1/3750). In these experiments, cells were isolated from a larger LVW area, which might explain the lower NSP frequency of CD133-negative cells compared to previous experiments.

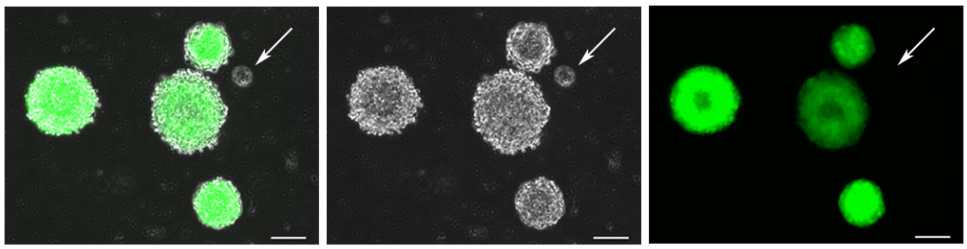

Figure 15: Co-cultivation of CD133-positive and CD133-negative cells from the adult LVW. Primary neurospheres in mixed cultures of GFP-expressing CD133-negative cells and wild-type (GFP-negative) CD133-positive cells are shown. The majority of NSPs are GFP-positive. Arrow indicates a small NSP, derived from wild-type CD133-positive cells. Scale bars: 100 µm.

4.1.3.4 Influence of culture conditions on the NSP-forming potential of CD133-positive adult LVW cells

Uncertainty in data interpretation is caused by the existence of different protocols to cultivate neural stem/progenitor cells (Chaichana et al., 2006). To rule out that culture conditions influence the NSP-forming potential of CD133-positive cells from the adult LVW, different culture media were investigated. First, the NSP development of total adult LVW cells in three different basal media, DMEM/F-12 medium (DMEM), Neurobasal medium (NB) and Neurobasal-A medium (NBA), each combined with two different media supplement cocktails, B27 and N2, was tested in one initial experiment (Fig.16A). Since LVW cells developed low numbers of NSPs or no NSPs in N2-containing media, media supplemented with B27 were chosen for the following experiments. CD133-positive and CD133-negative FACS-sorted

adult LVW cells were cultivated under clonal pre-selected culture conditions (<1cell/mm^2; DMEM/B27, NB/B27, NBA/B27) and NSP formation was observed up to 22 days post cell plating (Fig.16B). Under all three culture conditions, the vast majority of NSPs was derived from CD133-negative sorted cells. Single NSPs derived from CD133-negative cells (n=10/medium) were cultivated further and some of them could be passaged more than eight times (30% of NSPs in NB/B27 medium, 20% in NBA/B27 medium and 0% in DMEM/B27 medium). CD133-positive derived NSPs could not be passaged more than twice. This indicates that the medium composition has an influence on the number and survival of primary NSPs, but does not change the overall NSP-forming potential of CD133-positive and CD133-negative cells.

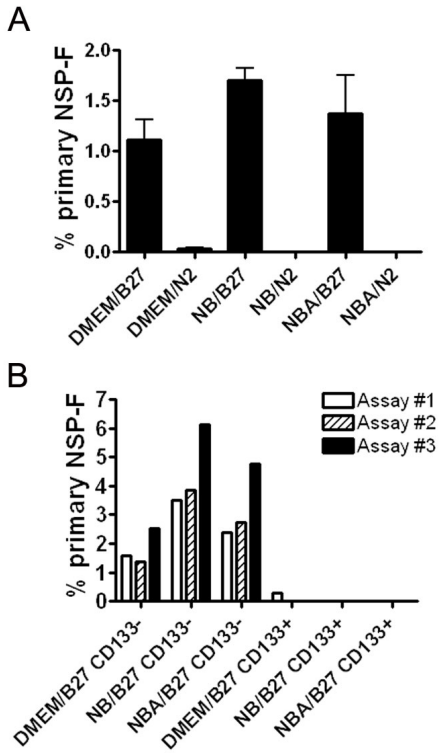

Figure 16: NSP frequency of adult LVW cells under different culture conditions. (A) Primary NSP frequencies (NSP-F) of total LVW cells in DMEM/F-12 (DMEM), Neurobasal (NB) and Neurobasal-A (NBA) medium supplemented with B27 or N2. The primary NSP frequency indicates the percentage of primary NSPs related to the number of plated cells. Bars indicate standard error of three technical replicates. (B) Primary NSP-F of CD133-negative and CD133-positive sorted LVW cells cultivated in NBA/B27 medium, NB/B27 medium and DMEM/B27 medium. Results from three independent experiments (Assay#1-#3) are shown

In summary, CD133-positive cells in the developing brain, neuroepithelial cells, a subpopulation of radial glial cells and intermediate radial glial/ependymal cells, were able to self-renew long-term and gave rise to neural progeny in culture. In the adult LVW, CD133 was present on ependymal cells and a subpopulation of GFAP-positive cells which lacked stem/progenitor cell properties *in vitro*. Self-renewing and multipotent cells in culture were found among CD133-negative E14.5 forebrain, P4 and adult LVW cells.

4.2 Comparison of CD133-positive ependymal cells from the adult murine LVW and spinal cord

4.2.1 Functional properties of adult LVW and spinal cord ependymal cells

Experiments performed in this thesis and elsewhere (Spassky et al., 2005; Carlen et al., 2009) suggest that adult LVW ependymal cells lack stem/progenitor cell properties, whereas ependymal cells from the adult spinal cord were shown to self-renew, proliferate and give rise to progeny *in vitro* and *in vivo* upon injury (Meletis et al., 2008). A direct comparison of both ependymal cell populations under similar culture conditions has not been performed. Thus, adult LVW and spinal cord ependymal cells were isolated and cultivated under identical conditions to directly compare their NSP-forming capacity and differentiation potential *in vitro*.

4.2.1.1 Preparation of adult spinal cord cells for flow cytometry and optimization of culture conditions

Myelin debris, created during dissociation of spinal cord tissue, can cause unspecific antibody binding and impair cell sorting. Thus, after digestion of adult spinal cord tissue with trypsin/EDTA, myelin debris was removed by centrifugation with a Sucrose/PBS solution. Remaining debris was excluded during the sorting procedure, as described in Figure 18A. Different culture media, as described in section 4.1.3.4, were tested in one initial experiment to find optimal culture conditions for NSP-forming cells from the adult spinal cord (Fig.17). The highest number of primary NSPs developed in B27-supplemented Neurobasal-A medium, which was therefore selected as culture medium for the following experiments. In this initial experiment, the myelin-removal step was omitted and total spinal cord cells were cultivated, leading to lower NSP frequencies compared to later experiments.

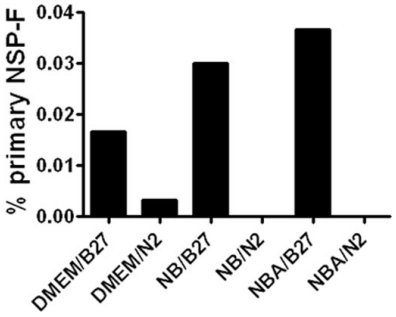

Figure 17: NSP frequency of adult spinal cord cells under different culture conditions. Primary NSP frequencies (NSP-F) of total spinal cord cells in DMEM/F-12 (DMEM), Neurobasal (NB) and Neurobasal-A (NBA) medium supplemented with B27 or N2. The primary NSP frequency indicates the percentage of primary NSPs related to the number of plated cells.

4.2.1.2 Ependymal cell isolation by a combination of surface markers

CD133 recognizes ependymal cells of the adult LVW and spinal cord, however this protein is also present on other cells, namely hematopoietic progenitor cells (Corbeil et al., 2000), endothelial progenitor cells (Balasubramaniam et al., 2007; Nolan et al., 2007; Rosell et al., 2009), oligodendrocytes (Corbeil et al., 2009), ventricle-contacting type B cells (Mirzadeh et al., 2008) and potentially endothelial cells (Fig.11). Thus, to exclude other cells that share the expression of CD133 with ependymal cells, a combination of antibodies against CD24, CD34, CD45 and CD133 was used for the ependymal cell isolation. CD24 showed a general co-staining with CD133 on most LVW and spinal cord ependymal cells (Fig.10, Fig.11), whereas CD45 and CD34 antibodies, well-known markers for hematopoietic progenitor cells, endothelial progenitor cells and endothelial cells, were absent from both ependymal cell populations (data not shown). The combination of CD133 and CD24 antibodies, together with the exclusion of CD34- and CD45-positive cells ($CD133^+/CD24^+/CD45^-/CD34^-$), targets ependymal cells only and allowed the isolation of LVW and spinal cord ependymal cells with high purity.

4.2.1.3 Functional properties of $CD133^+/CD24^+/CD45^-/CD34^-$ LVW and spinal cord ependymal cells in vitro

To investigate whether $CD133^+/CD24^+/CD45^-/CD34^-$ ependymal cells from the adult LVW and spinal cord display differences in terms of NSP-formation and differentiation, both populations were isolated and cultivated under identical conditions. Experiments from the spinal cord region will be described first. Flow cytometry analysis of CD133-, CD24-, CD34- and CD45-stained total spinal cord cells revealed the existence of several populations (Fig.18A): $CD133^+/CD24^+/CD45^-/CD34^-$ cells, which represent ependymal cells, $CD133^+/CD24^-/CD45^-$ cells, a population which might contain CD133-positive oligodendrocytes, and the remaining $CD133^+/CD45^-$ cells. In addition, a small population of $CD133^+/CD24^{low}/CD45^-/CD34^+$ cells (not shown) was found which could be endothelial or endothelial progenitor cells. The cell number of the latter population was always much lower compared to the cell number of the other fractions, or this population was completely absent, making further investigations difficult.

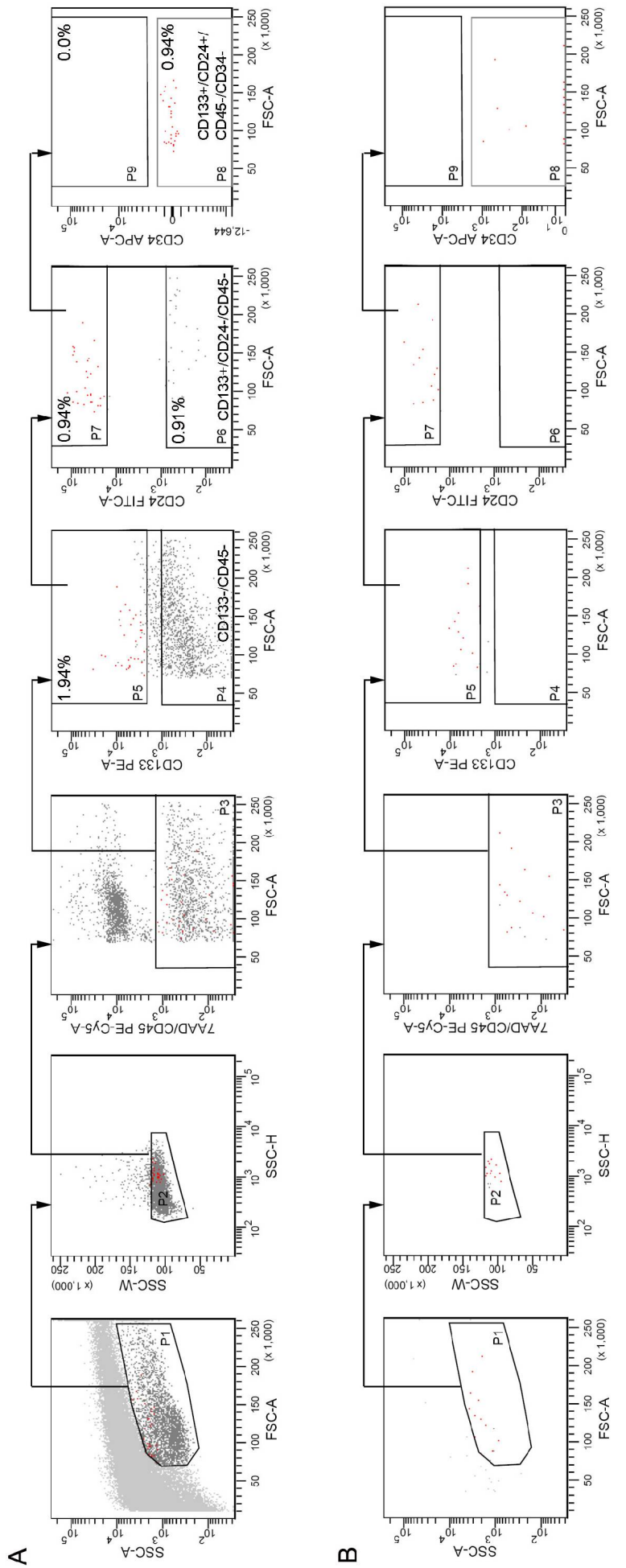

Figure 18: Isolation of adult spinal cord cells by flow cytometry. (A) Representative dot plots illustrate the sorting strategy. Forward and Side Scatter (FSC-A and SSC-A) were used to separate cells (gate P1) from debris (light grey). SSC-Width (SSC-W) versus SSC-Height (SSC-H) served to select single cells (P2). 7-AAD and CD45 were used to eliminate dead and white blood cells, respectively. The sorted $CD133^+/CD24^+/CD45^-/CD34^-$ ependymal cell population is depicted in red. As control, cells from gate P4 ($CD133^-/CD45^-$) and P6 ($CD133^+/CD24^-/CD45^-$) were isolated. Isotype matched control antibodies were used as negative controls. Arrows display the gating sequence. Percentages of gated cells with respect to P1 are indicated within the gated regions. (B) Re-analysis of the sorted $CD133^+/CD24^+/CD45^-/CD34^-$ spinal cord ependymal cell population (P8) shown in (A).

$CD133^+/CD24^+/CD45^-/CD34^-$ ependymal cells and the two control fractions, $CD133^+/CD45^-$ and $CD133^+/CD24^-/CD45^-$ cells were isolated by flow cytometry, and their primary NSP frequency together with the number of passages these NSPs could be kept in culture, was determined. Five independent assays showed that $CD133^+/CD24^+/CD45^-/CD34^-$ spinal cord ependymal cells consistently gave rise to primary NSPs with an average NSP frequency of 3.16% (Fig.19A). $CD133^-/CD45^-$ spinal cord cells had a primary NSP frequency of only 0.14% on average and $CD133^+/CD24^-/CD45^-$ spinal cord cells never gave rise to any NSPs. NSPs derived from $CD133^+/CD24^+/CD45^-/CD34^-$ spinal cord ependymal cells could be passaged more than 10 times and differentiated into glial and neuronal cells (Fig.19C). $CD133^-/CD45^-$ derived NSPs could be kept in culture up to four passages.

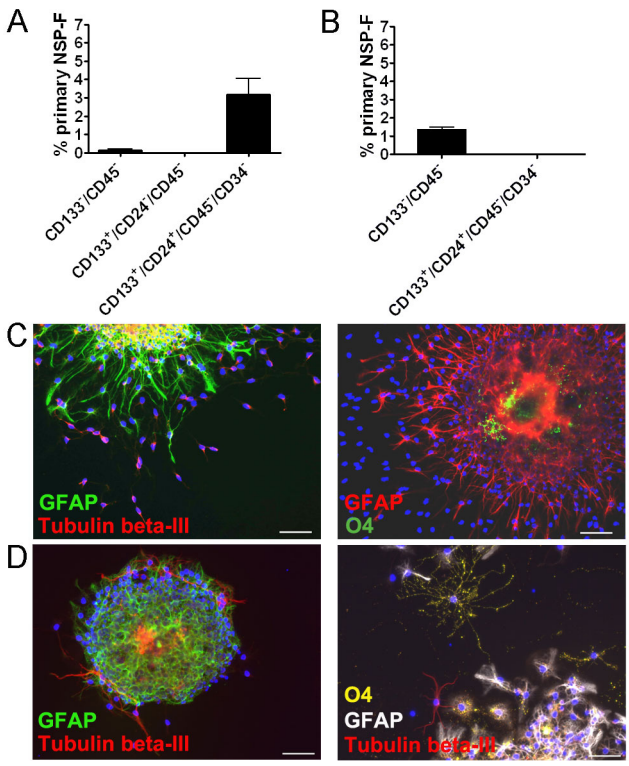

Figure 19: NSP frequencies and differentiation potential of adult spinal cord and LVW cells. Primary NSP frequency (NSP-F) of flow cytometry isolated populations illustrated in Fig.18 and Fig.20 from the (A) spinal cord and (B) LVW. The primary NSP frequency indicates the percentage of primary NSPs related to the number of plated cells. Bars indicate standard errors of five independent experiments. GFAP-positive astrocytes, Tubulin beta-III-positive neuronal cells and O4-positive oligodendrocytes derived from neurosphere cells formed by (C) $CD133^+/CD24^+/CD45^-/CD34^-$ sorted spinal cord ependymal cells and (D) $CD133^-/CD45^-$ sorted LVW cells. Cell nuclei are visualized with DAPI (blue). Scale bars: 50 µm.

The same staining and sorting procedure was applied to cells from the LVW (Fig.20A). Note that here the CD133 signal was higher as compared to experiments with spinal cord cells, which can be explained by the increased number and length of CD133-positive cilia on LVW ependymal cells. $CD133^+/CD24^+/CD45^-/CD34^-$ ependymal cells from the LVW, cultivated under the same culture conditions as spinal cord ependymal cells, never gave rise to primary NSPs (n=5; Fig.19B). Primary NSPs were formed by $CD133^+/CD45^-$ LVW cells with an average NSP frequency of 1.35%. NSPs derived from $CD133^+/CD45^-$ LVW cells could be kept in culture for more than 10 passages and gave rise to all three neural lineages (Fig.19D).

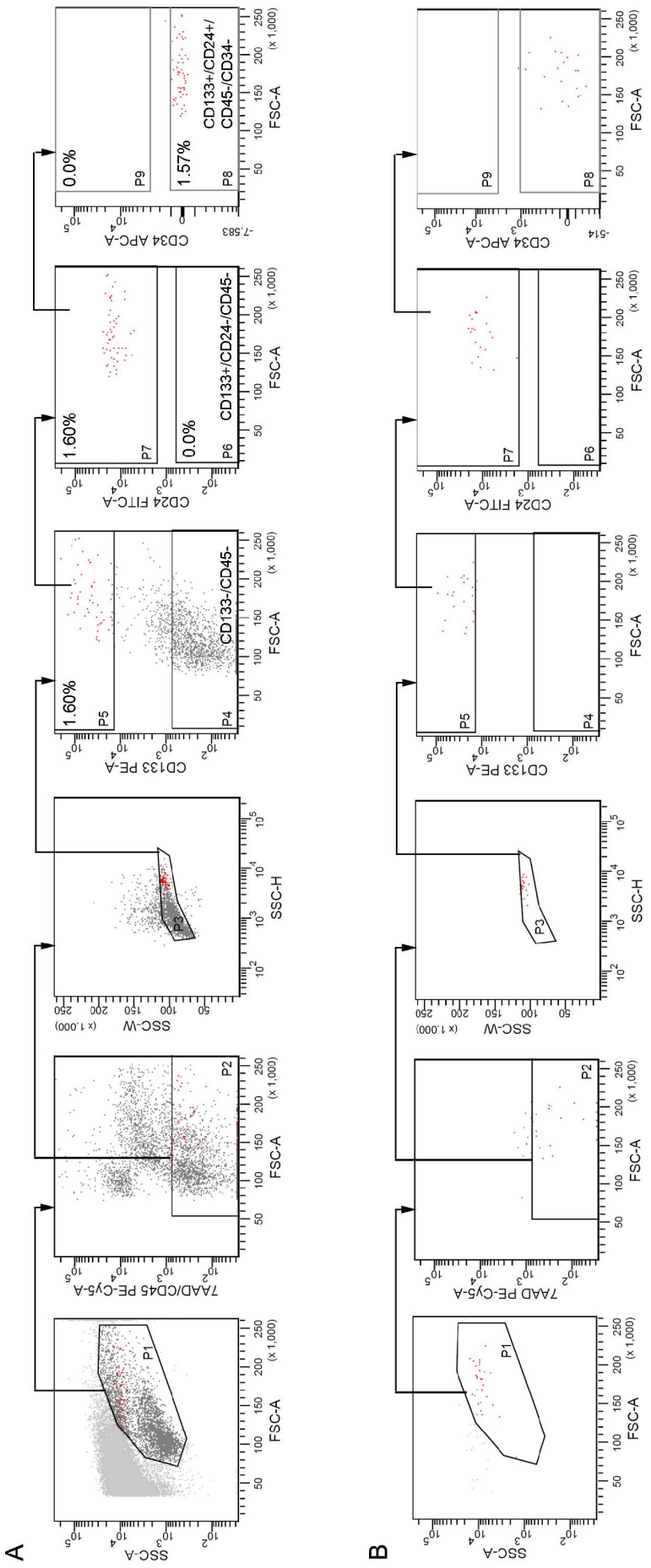

Figure 20: Isolation of adult LVW cells by flow cytometry. (A) Representative dot plots illustrate the sorting strategy. Forward and Side Scatter (FSC-A and SSC-A) were used to separate cells (gate P1) from debris (light grey). 7-AAD and CD45 served to eliminate dead and white blood cells, respectively. SSC-Width (SSC-W) versus SSC-Height (SSC-H) were used to select single cells (P3). The sorted $CD133^+/CD24^+/CD45^-/CD34^-$ ependymal cell population is depicted in red. As control, cells from gate P4 ($CD133^-/CD45^-$) were isolated. No $CD133^+/CD24^-/CD45^-$ cells were found in gate P6. Isotype matched control antibodies were used as negative controls. Arrows display the gating sequence. Percentages of gated cells with respect to P1 are indicated within the gated regions. (B) Re-analysis of the sorted $CD133^+/CD24^+/CD45^-/CD34^-$ LVW ependymal cell population (P8) shown in (A).

4.2.1.4 Functional properties of CD133$^+$/CD24$^-$ adult LVW cells in vitro

CD133$^+$/CD24$^-$ cells were previously suggested to be ependymal cells with neural stem cell properties (Coskun et al., 2008). No CD133$^+$/CD24$^-$/CD45$^-$ cells were found in the LVW experiments described in section 4.2.1.3 (Fig.20A). However, upon inclusion of CD133-low positive cells into the CD133-positive sorting gate (P5), a CD133$^+$/CD24$^-$/CD45$^-$ population was observed (Fig.21A). The CD133 gate was therefore changed to include all CD133 positive cells and CD133$^+$/CD24$^-$/CD45$^-$ cells were isolated to investigate their NSP-forming potential *in vitro*. CD133$^+$/CD24$^+$/CD45$^-$/CD34$^-$ and CD133$^-$/CD45$^-$ cells were sorted as control and all fractions were cultivated under similar culture conditions. In line with previous results (section 4.2.1.3), CD133$^-$/CD45$^-$ cells gave rise to primary NSPs, however NSP-formation from CD133$^+$/CD24$^-$/CD45$^-$ cells was not observed (n=4; Fig.21B), indicating that these cells do not possess stem/progenitor cell properties *in vitro*.

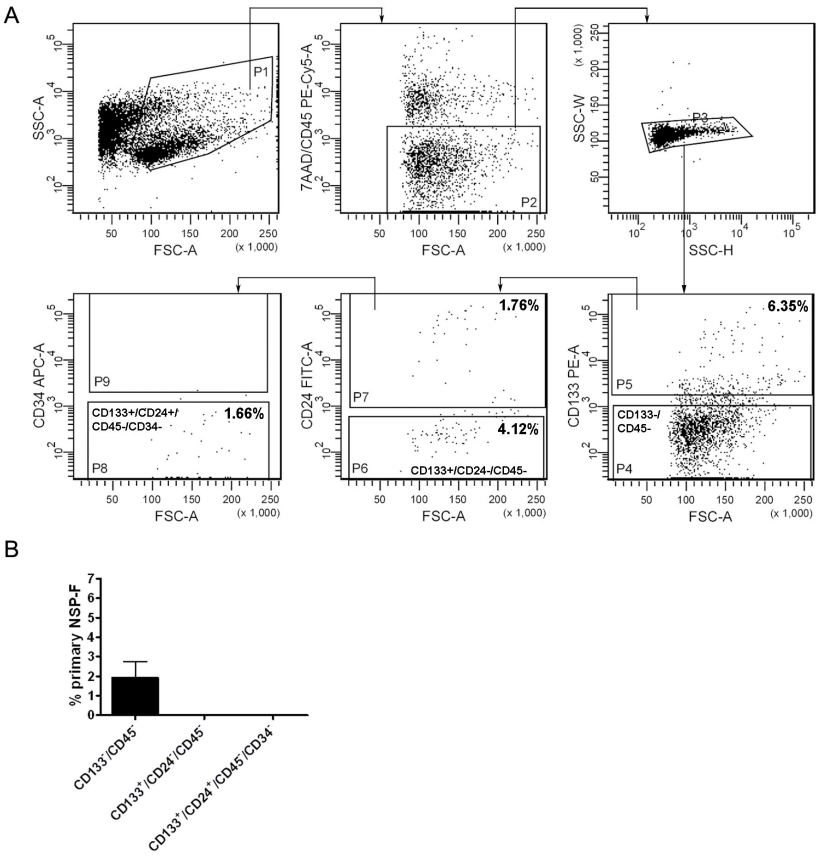

Figure 21:
Isolation and NSP frequency of CD133$^+$/CD24$^+$/CD45$^-$/CD34$^-$ cells, CD133$^+$/CD24$^-$/CD45$^-$ cells and CD133$^-$/CD45$^-$ cells from the adult LVW. (A) Representative dot plots illustrate the sorting strategy. Forward and Side Scatter (FSC-A and SSC-A) were used to separate cells (gate P1) from debris (light grey). 7-AAD and CD45 served to eliminate dead and white blood cells, respectively. SSC-Width (SSC-W) versus SSC-Height (SSC-H) was used to select single cells (P3). CD133$^+$/CD24$^-$/CD45$^-$ cells and as controls, cells from gate P4 (CD133$^-$/CD45$^-$) and P8 (CD133$^+$/CD24$^+$/CD45$^-$/CD34$^-$), were sorted. Note that here also CD133-low positive cells are included in gate P5. Isotype matched control antibodies were used as negative controls. Arrows display the gating sequence. Percentages of gated cells with respect to P1 are indicated within the gated regions. (B) Primary NSP frequency (NSP-F) of flow cytometry-isolated populations described in (A). The primary NSP frequency indicates the percentage of primary NSPs related to the number of plated cells. The bar indicates the standard error from four independent experiments.

In conclusion, CD133$^+$/CD24$^+$/CD45$^-$/CD34$^-$ ependymal cells from the spinal cord could self-renew and were multipotent *in vitro*, whereas CD133$^+$/CD24$^+$/CD45$^-$/CD34$^-$ LVW ependymal cells lacked stem/progenitor cell properties in culture.

4.2.2 Gene expression profile of adult LVW and spinal cord ependymal cells

To identify molecular differences between $CD133^+/CD24^+/CD45^-/CD34^-$ LVW and spinal cord ependymal cells, their transcriptional profile was analyzed using microarrays. Due to the low number of $CD133^+/CD24^+/CD45^-/CD34^-$ cells obtained by FACS from both regions, RNA was amplified twice before hybridization onto Illumina MouseWG-6 v1.1 gene expression microarrays. The reproducibility of the method was confirmed by similar gene expression patterns obtained from one sample, which was amplified four times independently (not shown). Three biological replicates of $CD133^+/CD24^+/CD45^-/CD34^-$ LVW and spinal cord ependymal cells were analyzed. Gene expression differences between ependymal cells of both regions with *p*-values below 0.05 were considered relevant. 156 genes were identified as differentially expressed between $CD133^+/CD24^+/CD45^-/CD34^-$ LVW and spinal cord ependymal cells (in the following referred to as LVW and spinal cord ependymal cells), of which 77 were higher and 79 lower expressed in spinal cord ependymal cells compared to ependymal cells from the LVW (Table 9A,B).

Table 9A: Genes higher expressed in CD133+/CD24+/CD45-/CD34- ependymal cells from the spinal cord

SYMBOL	Fold change	PROBE_ID	DEFINITION
Hoxa7	108.01	ILMN_2518986	
Hoxc6	66.73	ILMN_1217328	homeo box C6 (Hoxc6), mRNA.
Hoxa5	59.49	ILMN_2636480	homeo box A5 (Hoxa5), mRNA.
Hoxa7	56.54	ILMN_2621038	homeo box A7 (Hoxa7), mRNA.
Hoxb7	41.13	ILMN_3160837	homeo box B7 (Hoxb7), mRNA.
Nkx6-1	34.30	ILMN_1245585	NK6 transcription factor related, locus 1 (Drosophila) (Nkx6-1), mRNA.
Hoxd4	26.04	ILMN_1219807	homeo box D4 (Hoxd4), mRNA.
Hoxb5	23.63	ILMN_1242977	homeo box B5 (Hoxb5), mRNA.
Slc14a1	20.25	ILMN_1243081	solute carrier family 14 (urea transporter), member 1 (Slc14a1), mRNA.
Hoxc9	19.80	ILMN_2772764	homeo box C9 (Hoxc9), mRNA.
Hoxb2	19.22	ILMN_1234966	homeo box B2 (Hoxb2), mRNA.
Hoxc8	16.37	ILMN_1213675	
A2bp1	15.98	ILMN_2685291	ataxin 2 binding protein 1 (A2bp1), transcript variant 1, mRNA.
Dbc1	15.93	ILMN_2472606	deleted in bladder cancer 1 (human) (Dbc1), mRNA.
AU023871	13.42	ILMN_3161372	expressed sequence AU023871 (AU023871), mRNA.
Lin7a	13.22	ILMN_2500540	lin-7 homolog A (C. elegans) (Lin7a), transcript variant 1, mRNA.
Slc14a1	11.98	ILMN_1235006	solute carrier family 14 (urea transporter), member 1 (Slc14a1), mRNA.
Hoxd8	11.88	ILMN_2693052	homeo box D8 (Hoxd8), mRNA.
2700088M07Rik	10.78	ILMN_2455624	
Ifitm6	9.75	ILMN_1218181	interferon induced transmembrane protein 6 (Ifitm6), mRNA.
Col23a1	7.35	ILMN_2650447	procollagen, type XXIII, alpha 1 (Col23a1), mRNA.
Vtn	6.56	ILMN_1234111	vitronectin (Vtn), mRNA.
6430550H21Rik	6.28	ILMN_2771951	
Gpd1	6.28	ILMN_1216847	glycerol-3-phosphate dehydrogenase 1 (soluble) (Gpd1), mRNA.
Fndc5	6.15	ILMN_1214878	fibronectin type III domain containing 5 (Fndc5), mRNA.
Ovca2	5.96	ILMN_2724815	candidate tumor suppressor OVCA2 (Ovca2), mRNA.
Pcsk2	5.36	ILMN_1244247	proprotein convertase subtilisin/kexin type 2 (Pcsk2), mRNA.
Lrrc52	5.19	ILMN_2526954	leucine rich repeat containing 52 (Lrrc52), mRNA.
Cbln1	5.13	ILMN_1252953	cerebellin 1 precursor protein (Cbln1), mRNA.
B230323A14Rik	5.07	ILMN_2480427	
Hoxd10	5.01	ILMN_2702687	homeo box D10 (Hoxd10), mRNA.
Ret	5.01	ILMN_1236477	ret proto-oncogene (Ret), transcript variant 4, mRNA.

Table 9A … continued

SYMBOL	Fold change	PROBE_ID	DEFINITION
Dgkg	4.25	ILMN_2456435	
Otoa	4.24	ILMN_2735754	otoancorin (Otoa), mRNA.
Rxrg	4.18	ILMN_1232561	retinoid X receptor gamma (Rxrg), mRNA.
Astn1	3.88	ILMN_2697205	astrotactin 1 (Astn1), mRNA.
Nme7	3.67	ILMN_1246498	non-metastatic cells 7, protein expressed in (Nme7), transcript variant 1, mRNA.
Efnb1	3.62	ILMN_1257372	ephrin B1 (Efnb1), mRNA.
Fen1	3.56	ILMN_1259473	flap structure specific endonuclease 1 (Fen1), mRNA.
Bhlhb2	3.47	ILMN_1249378	basic helix-loop-helix domain containing, class B2 (Bhlhb2), mRNA.
Wdr68	3.44	ILMN_2546073	WD repeat domain 68 (Wdr68), mRNA.
Slc14a1	3.33	ILMN_2622909	solute carrier family 14 (urea transporter), member 1 (Slc14a1), mRNA.
Gosr2	3.31	ILMN_2600339	golgi SNAP receptor complex member 2 (Gosr2), mRNA.
9130404D08Rik	3.28	ILMN_2757006	RIKEN cDNA 9130404D08 gene (9130404D08Rik), mRNA.
Rtel1	3.12	ILMN_1250838	regulator of telomere elongation helicase 1 (Rtel1), mRNA.
D0H4S114	2.79	ILMN_2680054	DNA segment, human D4S114 (D0H4S114), mRNA.
Specc1l	2.63	ILMN_2700448	SPECC1-like (Specc1l), mRNA.
Bhmt	2.60	ILMN_2620994	betaine-homocysteine methyltransferase (Bhmt), mRNA.
LOC100048037	2.49	ILMN_1243433	PREDICTED: similar to myosin, light polypeptide 6, alkali, smooth muscle and non-muscle (LOC100048037), misc RNA.
Hoxb13	2.49	ILMN_2723267	homeo box B13 (Hoxb13), mRNA.
Ndst2	2.48	ILMN_2751587	N-deacetylase/N-sulfotransferase (heparan glucosaminyl) 2 (Ndst2), mRNA.
4932443I19Rik	2.41	ILMN_2627818	PREDICTED: RIKEN cDNA 4932443I19 gene, transcript variant 1 (4932443I19Rik).
EG277333	2.40	ILMN_1235086	predicted gene, EG277333 (EG277333) on chromosome 1.
Rab6b	2.40	ILMN_1245451	RAB6B, member RAS oncogene family (Rab6b), mRNA.
LOC100044756	2.35	ILMN_2707808	PREDICTED: similar to PX domain-containing protein kinase-like protein (Modulator of Na,K-ATPase) (MONaKA) (LOC100044756), mRNA.
Sema3e	2.32	ILMN_2720976	sema domain, immunoglobulin domain (Ig), short basic domain, secreted, (semaphorin) 3E (Sema3e), mRNA.
Tmem55b	2.31	ILMN_1216624	transmembrane protein 55b (Tmem55b), mRNA. XM_919952 XM_919965
A130010J15Rik	2.27	ILMN_2601755	RIKEN cDNA A130010J15 gene (A130010J15Rik), mRNA.
Nf2	2.26	ILMN_1244011	neurofibromatosis 2 (Nf2), mRNA.
Rtel1	2.03	ILMN_2641946	regulator of telomere elongation helicase 1 (Rtel1), mRNA.
Slc9a8	1.97	ILMN_2595992	solute carrier family 9 (sodium/hydrogen exchanger), member 8 (Slc9a8), transcript variant 2
C130045I22Rik	1.97	ILMN_2485964	
Tns1	1.96	ILMN_1229315	PREDICTED: tensin 1 (Tns1), mRNA.
Unc119b	1.95	ILMN_1245813	unc-119 homolog B (C. elegans) (Unc119b), mRNA.
Brd2	1.93	ILMN_2751505	bromodomain containing 2 (Brd2), transcript variant 2, mRNA.
Man2b2	1.91	ILMN_1244876	
Pcgf6	1.90	ILMN_2751009	polycomb group ring finger 6 (Pcgf6), mRNA.
Crtc2	1.89	ILMN_2711531	CREB regulated transcription coactivator 2 (Crtc2), mRNA.
Gpr108	1.88	ILMN_2618882	G protein-coupled receptor 108 (Gpr108), mRNA.
A030001A03Rik	1.84	ILMN_1233811	
Stk36	1.80	ILMN_2465146	serine/threonine kinase 36 (fused homolog, Drosophila) (Stk36), mRNA.
Ei24	1.78	ILMN_2775512	
1700012P22Rik	1.75	ILMN_1229341	PREDICTED: RIKEN cDNA 1700012P22 gene (1700012P22Rik), mRNA.
1500015O10Rik	1.73	ILMN_1249000	RIKEN cDNA 1500015O10 gene (1500015O10Rik), mRNA.
3010031K01Rik	1.68	ILMN_2522460	
4732435K05Rik	1.52	ILMN_2557957	
Chkb	1.46	ILMN_2755021	choline kinase beta (Chkb), mRNA.
D430034A07Rik	1.45	ILMN_1232293	
Gnptg	1.44	ILMN_2731999	N-acetylglucosamine-1-phosphotransferase, gamma subunit (Gnptg), mRNA.
Gnptg	1.42	ILMN_2617865	N-acetylglucosamine-1-phosphotransferase, gamma subunit (Gnptg), mRNA.
2410012M04Rik	1.33	ILMN_2448184	
Birc5	1.13	ILMN_2632712	baculoviral IAP repeat-containing 5 (Birc5), transcript variant 1, mRNA.

Table 9B: Genes higher expressed in CD133+/CD24+/CD45-/CD34- ependymal cells from the LVW

SYMBOL	Fold change	PROBE_ID	DEFINITION
Tgm2	48.19	ILMN_2692615	transglutaminase 2, C polypeptide (Tgm2), mRNA.
1700021K14Rik	41.08	ILMN_1224436	PREDICTED: RIKEN cDNA 1700021K14 gene (1700021K14Rik), mRNA.
Cyp4f15	28.80	ILMN_2738192	cytochrome P450, family 4, subfamily f, polypeptide 15 (Cyp4f15), mRNA.
Ces3	28.55	ILMN_2625893	carboxylesterase 3 (Ces3), mRNA.
Hp	20.72	ILMN_2644764	haptoglobin (Hp), mRNA.
Cpe	17.19	ILMN_2758940	carboxypeptidase E (Cpe), mRNA.
6430537F04	15.45	ILMN_2513378	
Pcsk6	14.32	ILMN_2637094	PREDICTED: proprotein convertase subtilisin/kexin type 6, transcript variant 4 (Pcsk6)
Nme7	14.03	ILMN_1214703	non-metastatic cells 7, protein expressed in (Nme7), transcript variant 1, mRNA.
Scin	13.89	ILMN_1259174	scinderin (Scin), mRNA.
Dlx2	13.61	ILMN_2860958	distal-less homeobox 2 (Dlx2), mRNA.
Nkd2	11.61	ILMN_1228631	naked cuticle 2 homolog (Drosophila) (Nkd2), mRNA.
Emb	11.14	ILMN_1218799	embigin (Emb), mRNA.
Ush1c	11.13	ILMN_2501719	Usher syndrome 1C homolog (human) (Ush1c), transcript variant b3, mRNA.
BC055107	10.47	ILMN_2768972	cDNA sequence BC055107 (BC055107), mRNA.
Nme7	10.22	ILMN_1259075	non-metastatic cells 7, protein expressed in (Nme7), transcript variant 1, mRNA.
Car9	9.30	ILMN_1244145	carbonic anhydrase 9 (Car9), mRNA.
Nme7	8.93	ILMN_2510694	non-metastatic cells 7, protein expressed in (Nme7), transcript variant 1, mRNA.
D12Ertd647e	8.32	ILMN_2681232	DNA segment, Chr 12, ERATO Doi 647, expressed (D12Ertd647e), transcript variant 4
Lbp	7.19	ILMN_2771237	lipopolysaccharide binding protein (Lbp), mRNA.
Clmn	7.06	ILMN_1241142	calmin (Clmn), transcript variant 2, mRNA.
Nt5c	6.87	ILMN_1223097	5,3-nucleotidase, cytosolic (Nt5c), mRNA.
Nat8l	6.75	ILMN_2594039	N-acetyltransferase 8-like (Nat8l), mRNA.
Ghrh	6.59	ILMN_1253853	growth hormone releasing hormone (Ghrh), mRNA.
Bmp6	6.02	ILMN_2705217	bone morphogenetic protein 6 (Bmp6), mRNA.
9630007E23Rik	5.97	ILMN_1253602	
Lamb3	5.84	ILMN_2605512	laminin, beta 3 (Lamb3), mRNA.
Lrfn2	5.41	ILMN_1225860	leucine rich repeat and fibronectin type III domain containing 2 (Lrfn2), mRNA.
Apoe	5.21	ILMN_1216042	apolipoprotein E (Apoe), mRNA.
S100a6	5.21	ILMN_2712120	S100 calcium binding protein A6 (calcyclin) (S100a6), mRNA.
Sirpa	5.17	ILMN_2722996	signal-regulatory protein alpha (Sirpa), mRNA.
Osbpl6	4.87	ILMN_1221789	oxysterol binding protein-like 6 (Osbpl6), mRNA.
LOC245892	4.83	ILMN_1230065	
Arhgdig	4.78	ILMN_1240164	Rho GDP dissociation inhibitor (GDI) gamma (Arhgdig), mRNA.
Mmd2	4.68	ILMN_1252636	monocyte to macrophage differentiation-associated 2 (Mmd2), mRNA.
LOC100039175	4.30	ILMN_1225825	PREDICTED: similar to Placenta specific 9 (LOC100039175), mRNA.
Trpc7	4.27	ILMN_1242557	transient receptor potential cation channel, subfamily C, member 7 (Trpc7),
Agxt2l1	4.15	ILMN_1229990	alanine-glyoxylate aminotransferase 2-like 1 (Agxt2l1), mRNA.
Gpr37l1	4.12	ILMN_1228699	G protein-coupled receptor 37-like 1 (Gpr37l1), mRNA.
Traf3ip2	4.08	ILMN_1232123	Traf3 interacting protein 2 (Traf3ip2), mRNA.
Slc35a3	3.95	ILMN_1231551	
Hey1	3.85	ILMN_2690596	hairy/enhancer-of-split related with YRPW motif 1 (Hey1), mRNA.
Gstm1	3.78	ILMN_1228233	glutathione S-transferase, mu 1 (Gstm1), mRNA.
LOC100048169	3.53	ILMN_2430359	PREDICTED: hypothetical protein LOC100048169 (LOC100048169), mRNA.
Stard3nl	3.23	ILMN_2598775	STARD3 N-terminal like (Stard3nl), mRNA.
Anxa1	3.21	ILMN_1259252	annexin A1 (Anxa1), mRNA.
EG665033	3.20	ILMN_2533531	PREDICTED: predicted gene, EG665033 (EG665033), misc RNA.
Mmrn2	3.17	ILMN_2494159	multimerin 2 (Mmrn2), mRNA.
Lrrc34	3.03	ILMN_2519746	leucine rich repeat containing 34 (Lrrc34), mRNA.
Aqp4	2.90	ILMN_1237969	
Foxg1	2.86	ILMN_2599125	forkhead box G1 (Foxg1), mRNA.
Ifit3	2.84	ILMN_2699233	interferon-induced protein with tetratricopeptide repeats 3 (Ifit3), mRNA.
Meig1	2.79	ILMN_2588789	meiosis expressed gene 1 (Meig1), mRNA.
E430002G05Rik	2.77	ILMN_1227947	
Id2	2.69	ILMN_1228557	inhibitor of DNA binding 2 (Id2), mRNA.
Coro2b	2.62	ILMN_1216552	coronin, actin binding protein, 2B (Coro2b), mRNA.
Phactr1	2.55	ILMN_2596560	phosphatase and actin regulator 1 (Phactr1), transcript variant 2, mRNA.
5730494M16Rik	2.53	ILMN_3163221	RIKEN cDNA 5730494M16 gene (5730494M16Rik), mRNA.

Table 9B … continued

SYMBOL	Fold change	PROBE_ID	DEFINITION
Odf3l1	2.38	ILMN_1226833	outer dense fiber of sperm tails 3-like 1 (Odf3l1), mRNA.
Tlcd1	2.30	ILMN_2624326	TLC domain containing 1 (Tlcd1), mRNA.
LOC664837	2.30	ILMN_2537209	PREDICTED: hypothetical LOC664837, transcript variant 2 (LOC664837), mRNA.
Tnnt2	2.19	ILMN_2466462	troponin T2, cardiac (Tnnt2), mRNA.
6330549D23Rik	2.15	ILMN_1229583	RIKEN cDNA 6330549D23 gene (6330549D23Rik) on chromosome 3.
Plscr2	2.12	ILMN_2635895	phospholipid scramblase 2 (Plscr2), mRNA.
Got1l1	2.07	ILMN_1246289	glutamic-oxaloacetic transaminase 1-like 1 (Got1l1), mRNA.
Carhsp1	1.99	ILMN_1225035	calcium regulated heat stable protein 1 (Carhsp1), mRNA.
Acsbg1	1.97	ILMN_2686611	acyl-CoA synthetase bubblegum family member 1 (Acsbg1), mRNA.
LOC381146	1.97	ILMN_1251693	
Phtf1	1.96	ILMN_2615864	
Wwtr1	1.95	ILMN_1219016	WW domain containing transcription regulator 1 (Wwtr1), mRNA.
Mtus1	1.78	ILMN_1253492	mitochondrial tumor suppressor 1 (Mtus1), transcript variant 1, mRNA.
LOC193533	1.75	ILMN_1229008	
2700094F01Rik	1.72	ILMN_2751396	RIKEN cDNA 2700094F01 gene (2700094F01Rik), mRNA.
Cideb	1.69	ILMN_3160626	cell death-inducing DNA fragmentation factor, alpha subunit-like effector B (Cideb).
mtDNA_CytB	1.60	ILMN_1239040	
Olfr448	1.57	ILMN_2645100	olfactory receptor 448 (Olfr448), mRNA.
Ttll10	1.56	ILMN_2701211	tubulin tyrosine ligase-like family, member 10 (Ttll10), mRNA. XM_922509 XM_990853
2010007H06Rik	1.38	ILMN_1252288	
Adprhl2	1.26	ILMN_2639063	ADP-ribosylhydrolase like 2 (Adprhl2), mRNA.
LOC100044538	1.18	ILMN_1254241	PREDICTED: similar to immunity-associated nucleotide 4 (LOC100044538), misc RNA.
Iws1	1.17	ILMN_2674060	IWS1 homolog (S. cerevisiae) (Iws1), mRNA.

Table 9: Genes differentially expressed ($p < 0.05$) between $CD133^+/CD24^+/CD45^-/CD34^-$ spinal cord and LVW ependymal cells. Fold changes indicate the average microarray gene expression differences between three biological LVW and spinal cord ependymal cell samples. SYMBOL, PROBE_ID and DEFINITION are Illumina annotations (MouseWG-6 v1.1). SYMBOL and DEFINITION indicate the gene name. The PROBE_ID represents a unique Illumina identifier for every probe. (A) Genes higher expressed in $CD133^+/CD24^+/CD45^-/CD34^-$ spinal cord ependymal cells. (B) Genes higher expressed in $CD133^+/CD24^+/CD45^-/CD34^-$ LVW ependymal cells.

First, the expression of genes, encoding the proteins that were used to isolate LVW and spinal cord ependymal cells, CD133, CD24, CD34 and CD45, was verified. In accordance with sorting criteria, both ependymal populations highly expressed *Prom1* (encoding CD133), whereas the transcript levels of *Ptprc* (encoding CD45) and *Cd34* were low to absent (Table 10). Only low mRNA levels of *CD24a* were found by array analysis, but rtPCR from independently sorted $CD133^+/CD24^+/CD34^-/CD45^-$ LVW and spinal cord cells confirmed robust expression of *Cd24a* in both populations (Fig.22, Fig.24). *Cd24a* was represented with only one probe set on the array and weak binding affinity between sample cRNA and probe set might explain the low Cd24a expression levels of the array analysis. Elevated transcript levels of *Foxj1*, a gene specifically expressed in ciliated cells (Blatt et al., 1999; Meletis et al., 2008; Carlen et al., 2009), were found in ependymal cells from both regions (Table 10). Importantly, *Foxj1* expression is limited to cells with motile cilia and absent in cells with a primary/sensory cilium, as for example in ventricle-contacting type B cells.

Gene	Avg LVW	Avg SC
Cd24a	8.56	7.05
Cd34	6.78	6.80
Ptprc	6.67	6.65
	6.58	6.58
	6.64	6.61
Prom1	13.19	11.58
	6.78	6.79
Foxj1	8.81	9.21

Table 10: Microarray gene expression values of *Cd24a*, *Cd34*, *Ptprc*, *Prom1* and *Foxj1*. Average (Avg) logarithmic gene expression values of three biological $CD133^+/CD24^+/CD45^-/CD34^-$ spinal cord (SC) and LVW ependymal cell samples are shown. Logarithmic gene expression values ranged from 6.46 to 14.51. Note that *Ptprc* and *Prom1* genes are represented with more than one probe on the array.

A literature survey was performed to obtain biological information about the genes differentially expressed between adult LVW and spinal cord ependymal cells. Relevant publications were used to extract data about pathways, target genes and involvement in biological processes associated with the genes of interest. This information provided the framework to establish categories of genes, which are associated with the same function or regulatory mechanism and will be described in the following chapters.

4.2.2.1 Gene expression pattern specific for spinal cord ependymal cells

A substantial number of genes, involved in apoptosis, telomere stability/maintenance and cell cycle related processes, such as progression through cell cycle stages and cell division, were identified among the genes with higher transcript levels in spinal cord ependymal cells (Table 11A). Notably, several of these genes are associated with proto-oncogenic or tumor-suppressive activity.

Gene	A	B	FC	Ref. A	Ref. B
Bhlhb2		x	3.47		(Boudjelal et al., 1997)
Brd2	x		1.93	(Sinha et al., 2005) (Denis et al., 2000)	
Dbc1	x		15.93	(Nishiyama et al., 2001; Wright et al., 2004)	
D0H4S114		x	2.79		(Leung et al., 2008)
Efnb1	x	x	3.62	(Qiu et al., 2008)	(Bouillet et al., 1995)
Ei24	x		1.78	(Gu et al., 2000)	
Fen1	x		3.56	(Sampathi et al., 2009)	
Hoxa5	x	x	59.49	(Raman et al., 2000; Chen et al., 2004; Mishra et al., 2009)	(Chen et al., 2007)
Hoxa7	x	x	108.01 56.54	(Mishra et al., 2009)	(Kessel and Gruss, 1991)
Hoxb2		x	19.22		(Simeone et al., 1990)
Hoxb5		x	23.63		(Oosterveen et al., 2003)
Hoxb7	x	x	41.13	(Care et al., 1996) (Care et al., 1999)	(Simeone et al., 1990)
Hoxc6	x	x	66.73	(Ramachandran et al., 2005)	(Manohar et al., 1996)
Hoxc8	x	x	16.37	(Kamel et al., 2009)	(Kessel and Gruss, 1991)
Hoxd4		x	26.04		(Zhang et al., 2000)
Hoxd8		x	11.88		(Manohar et al., 1996)
Hoxd10		x	5.01		(Merrill et al., 2004)
Nf2	x		2.26	(Curto and McClatchey, 2008)	
Ovca2		x	5.96		(Prowse et al., 2002)
Ret	x	x	5.01	(Arighi et al., 2005)	(Cerchia et al., 2006)
Rtel1	x		3.12 2.03	(Ding et al., 2004)	
Rxrg		x	4.17		(Barger and Kelly, 1997; McDermott et al., 2002)
Tmem55b	x		2.31	(Zou et al., 2007)	

Table 11: Selection of genes higher expressed by adult spinal cord ependymal cells, which are involved in cell cycle regulation, apoptosis, telomere stability/maintenance (A) and/or RA-signaling (B). Respective references (Ref) are shown. Fold changes (FC) indicate the average microarray gene expression differences between three biological $CD133^+/CD24^+/CD45^-/CD34^-$ spinal cord and LVW ependymal cell samples. Note that some genes are represented by more than one array probe.

To verify results of the microarray analysis with an independent method, semi-quantitative rtPCR was used to analyze the expression of *Nf2*, *Rtel1*, *Fen1* and *Rxrg* genes in $CD133^+/CD24^+/CD45^-/CD34^-$ sorted spinal cord cells. The expression of *Prom1*, *Cd24a* and *Foxj1* genes was included as positive control. As illustrated in Figure 22, the rtPCR results confirmed the microarray gene expression data. The tested genes *Nf2*, *Rtel1*, *Fen1* and *Rxrg* are part of identified functional or regulatory spinal cord categories summarized in Table 11. Furthermore, selected genes associated with cell cycle regulation, retinoic acid-responsiveness and telomere stability/maintenance, *Efnb1* and *Fen1* (Table 11), were investigated on the protein level. Virtually all ependymal cells were immunoreactive to an anti-Ephrin-B1

antibody and CD133 co-localized with Ephrin-B1 at the apical cell membrane (Fig.23A). The FEN-1 nuclear protein was present in a subpopulation of spinal cord ependymal cells, but also in white and grey matter cells outside the ependymal layer (Fig.23B).

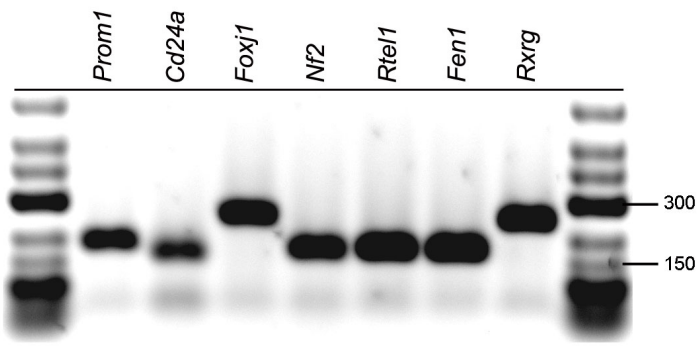

Figure 22: Validation of spinal cord ependymal cell transcriptional profile by multiplex rtPCR. rtPCR products of $CD133^{+}/CD24^{+}/CD45^{-}/CD34^{-}$ spinal cord ependymal cells visualized by gel electrophoresis. Investigated genes are indicated on top. First and last lanes contain a molecular weight marker (Gene ruler DNA ladder, low range; Fermentas; 150bp and 300bp bands are indicated). The faint, fast-running bands below 100 bp are derived from residual primers.

20.8% of the genes higher expressed in spinal cord ependymal cells were shown to be direct or indirect retinoic acid (RA) target genes (Table 11B). This raised the question whether spinal cord ependymal cells can be influenced by RA. $CD133^{+}/CD24^{+}/CD45^{-}/CD34^{-}$ spinal cord cells were cultivated as adherent cells directly after sorting. Within 60 hours sorted cells attached and started to acquire a flat morphology. At this point, medium containing RA or vehicle (DMSO) was added and the cells were cultivated under these conditions for six additional days. Immunostainings after cultivation revealed that most RA- and vehicle-treated cells were positive for Nestin, a protein found in spinal cord ependymal cells (Meletis et al., 2008), and some of these cells expressed the proliferation marker Ki-67 (Fig.23C). Single cells or small cell clusters were found in RA- and DMSO-treated cultures. Interestingly, only in RA-supplemented cultures, large cobblestone-like cell sheets were observed. These cells had a squamous appearance and were connected through adherens junctions, displayed by Catenin beta-1 staining (Fig.23C). Both, RA and vehicle-treated cells were negative for GFAP, Tubulin beta-III and O4, which suggests that these cells proliferate, but that they do not differentiate into cells from the neural lineage. Cell number determination before and after nine days in culture confirmed a general cell number increase in RA-treated and untreated cultures (8.1±1.7 fold for RA; 3.7±0.7 fold for DMSO; mean±S.E.M.; n=3; Fig.23D), however RA-exposure increased the cell number on average two times more compared to the vehicle-treated control (2.3±0.5; mean±S.E.M.; n=3). *P*-values of the comparison RA versus DMSO from two experiments with four technical replicates were: 0.0286 and 0.0571 (Mann Whitney test). The *p*-value from one experiment with only two technical replicates for RA and DMSO could not be determined.

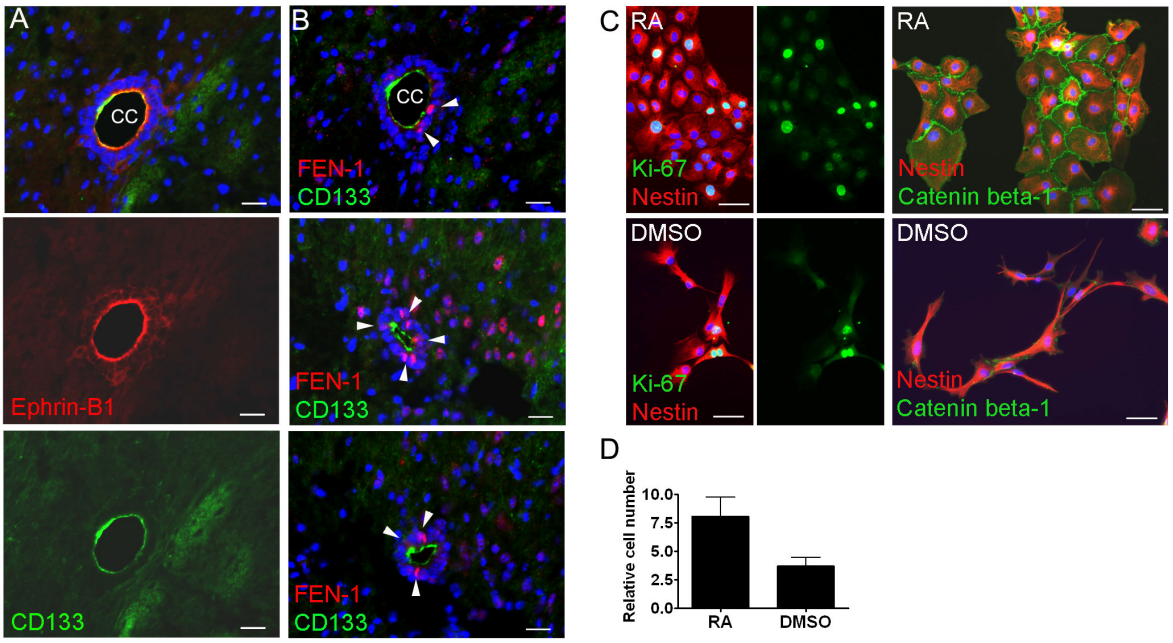

Figure 23: Immunostainings and *in vitro* assays with retinoic acid to confirm spinal cord ependymal cell gene expression data. Adult CD133-positive spinal cord central canal (CC) ependymal cells co-stained with (A) anti-Ephrin-B1 and (B) anti-3220 (FEN-1, arrowheads) antibodies. Scale bars: 20µm. Cell nuclei are visualized with DAPI (blue). (C) Nestin- and Ki-67-positive adherent $CD133^+/CD24^+/CD45^-/CD34^-$ spinal cord ependymal cells after cultivation in the presence of retinoic acid (RA) or vehicle (DMSO). Adherens junctions between cells are illustrated by Catenin beta-1 staining. Scale bars: 50µm. Cell nuclei are visualized with DAPI (blue). (D) Relative cell numbers of RA- and vehicle (DMSO)-treated spinal cord ependymal cells, indicating the average number of cells counted after cultivation per initially plated cells. Bars represent standard errors of three independent experiments.

4.2.2.2 Gene expression pattern specific for LVW ependymal cells

Several genes, involved in the regulation of neural stem cell maintenance and neurogenesis, were found to be higher expressed in LVW ependymal cells (Table 12): *Dlx2*, *Foxg1*, *Hey1* and *Id2*. Semi-quantitative single cell rtPCR was used to verify the expression of *Dlx2*, *Foxg1*, *Hey1* and *Id2* genes in LVW ependymal cells. To exclude potential contamination by non-ependymal cells, $CD133^+/CD24^+/CD45^-/CD34^-$ sorted LVW cells were evaluated and documented by light microscopy for the presence of long motile cilia. rtPCR of cells with approved morphology confirmed the presence of *Dlx2*, *Foxg1*, *Hey1* and *Id2* transcripts in single *Prom1*- and *Cd24a*-expressing cells (Fig.24).

Gene	Fold change
Dlx2	13.61
Foxg1	2.86
Hey1	3.85
Id2	2.69

Table 12: Selection of genes higher expressed by adult LVW ependymal cells, which are involved in neural stem cell maintenance and neurogenesis. Fold changes indicate the average microarray gene expression differences between three biological $CD133^+/CD24^+/CD45^-/CD34^-$ spinal cord and LVW ependymal cell samples.

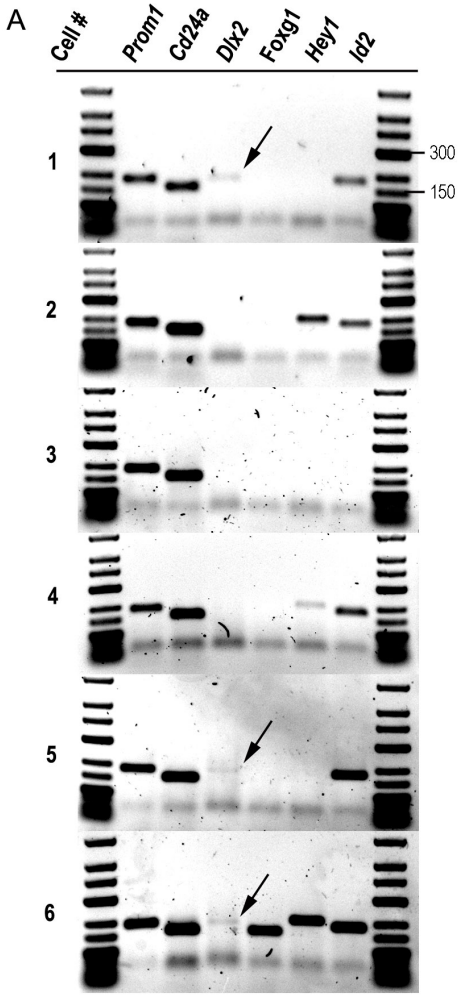

B

Cell #	Prom1	Cd24a	Dlx2	Foxg1	Hey1	Id2
1	+	+	+	-	-	+
2	+	+	-	-	+	+
3	+	+	-	-	-	-
4	+	+	-	-	+	+
5	+	+	+	-	-	+
6	+	+	+	+	+	+

Figure 24: Validation of LVW ependymal cell transcriptional profile by multiplex single cell rtPCR. $CD133^+/CD24^+/CD45^-/CD34^-$ sorted adult LVW cells were manually selected by their morphology (multiple long cilia), documented, utilized for semi-quantitative rtPCR and analysed by gel electrophoresis. (A) rtPCR products visualized by agarose gel electrophoresis. The number of the cell used for rtPCR is depicted to the left and investigated genes are indicated on top. First and last lanes contain a molecular weight marker (Gene ruler DNA ladder, low range; Fermentas; 150bp and 300bp bands are indicated). Arrows indicate rtPCR products for *Dlx2*. The fast-running bands below 100 bp are derived from residual primers. (B) Summary of data shown in (A). Documented cells, corresponding to the individual rtPCR reactions described in (A), are illustrated to the left. Presence and absence of PCR products are indicated by plus (+) and minus (-) symbols.

4.2.2.3 Comparison of gene expression data from LVW and spinal cord ependymal cells, RGC and spinal cord-derived NSPs

To compare the transcriptional profile of a known neural stem/progenitor cell population, which also expresses CD133, to that of LVW and spinal cord ependymal cells, $CD133^+/CD24^-/CD45^-/CD34^-$ RGC were isolated from the embryonic forebrain (Fig.25A,B). $CD133^+/CD24^-/CD45^-/CD34^-$ cells gave rise to primary NSPs, which could be maintained in culture for more than ten passages and differentiated into all three cell types of the neural lineage (n=3; Fig.25C,D,E). A population with a similar marker combination as adult ependymal cells, $CD133^+/CD24^{hi}/CD45^-/CD34^-$ embryonic cells, was evaluated as well. Isolated cells from this population formed primary NSPs in culture, but could not be kept in culture for 11 passages in all experiments (n=3; Fig.25C,D). Thus, only $CD133^+/CD24^-/CD45^-/CD34^-$ cells fulfilled all requirements for neural stem cells (long-term self-renewal and multipotency), and were used for the microarray analysis. In addition, the transcriptional profile of NSPs (passage 2-3), derived from $CD133^+/CD24^+/CD45^-/CD34^-$ spinal cord

ependymal cells was included into the analysis. NSP culture conditions induce spinal cord ependymal cells to proliferate and enrich for proliferating stem/progenitor cells.

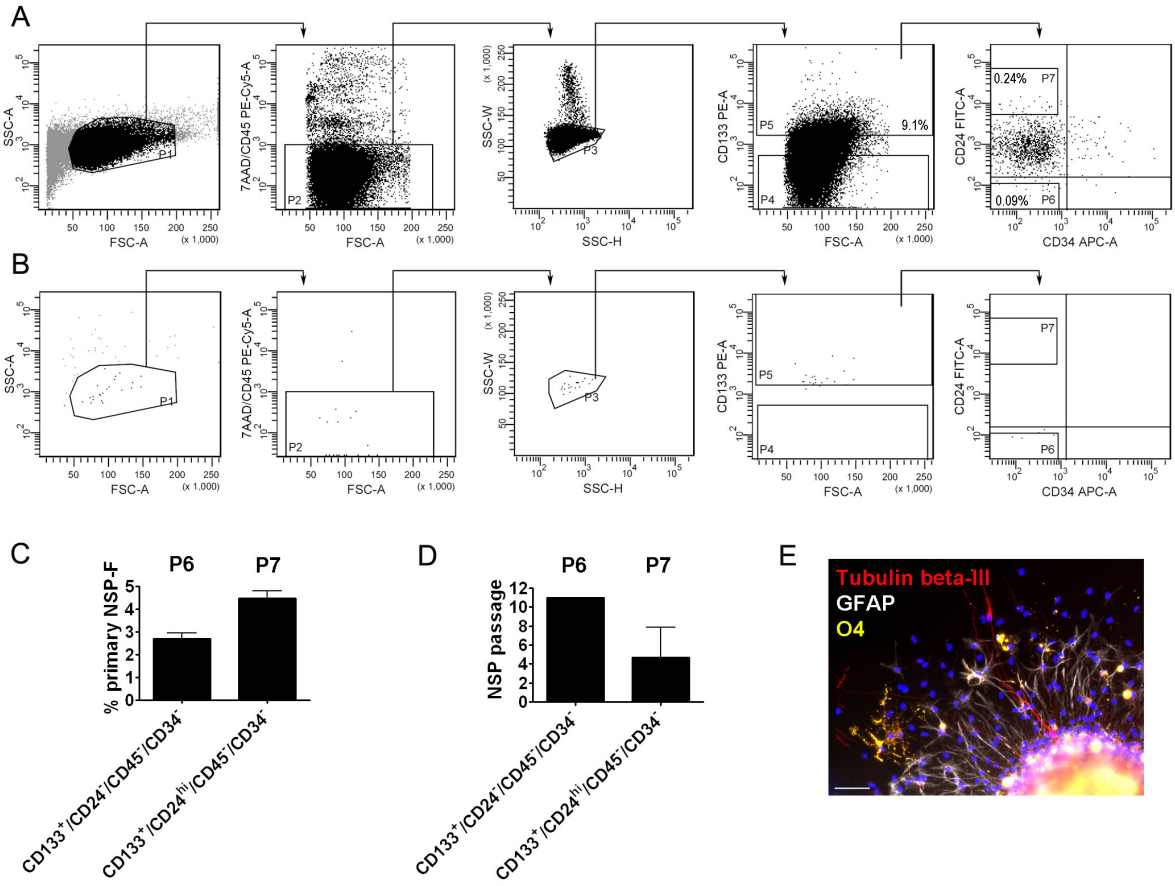

Figure 25: Isolation, *in vitro* self-renewal and differentiation assay of embryonic forebrain stem/progenitor cells. (A) Representative FACS plots illustrate the sorting strategy to purify stem/progenitor cells from embryonic day 14.5 forebrain preparations. Forward and Side Scatter (FSC-A and SSC-A) were used to separate cells (gate P1) from debris (light grey). 7-AAD-positive dead cells and CD45-positive white blood cells were excluded and SSC-Width (SSC-W) versus SSC-Height (SSC-H) gating was used to select single cells (P3). From CD133-positive cells (P5), two populations were isolated: P6 ($CD133^+/CD24^-/CD45^-/CD34^-$) and P7 ($CD133^+/CD24^{hi}/CD45^-/CD34^-$). Isotype matched control antibodies were used as negative controls. Arrows display the gating sequence. Percentages of gated cells with respect to P1 are indicated within the gated regions. (B) Reanalysis of the sorted $CD133^+/CD24^-/CD45^-/CD34^-$ cell population (P6) shown in (A). (C) Primary NSP frequency (NSP-F) and (D) long-term self-renewal of $CD133^+/CD24^-/CD45^-/CD34^-$ (P6) and $CD133^+/CD24^{hi}/CD45^-/CD34^-$ (P7) sorted cells. The primary NSP frequency indicates the percentage of primary NSPs related to the number of plated cells. Long-term self-renewal was measured by the number of cell passages (P6: until passage 11 (n=3), P7: until passage 1, 2, 11 (each n=1)). Note that the long-term self-renewal assay was discontinued after 11 passages. Bars indicate standard errors from three independent experiments. (E) Neurospheres derived from $CD133^+/CD24^-/CD45^-/CD34^-$ (P6) sorted cells give rise to GFAP-positive astrocytes, Tubulin beta-III–positive neuronal cells and O4-positive oligodendrocytes. Cell nuclei are visualized with DAPI (blue). Scale bar: 50 µm.

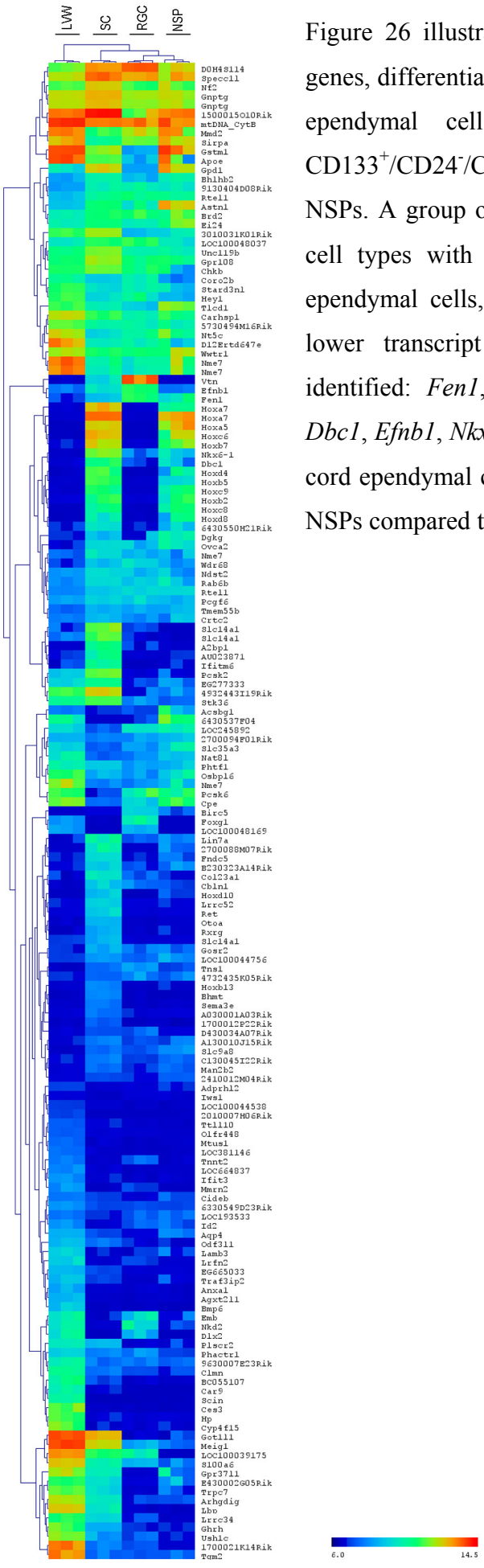

Figure 26 illustrates a hierarchical biclustering of the 156 genes, differentially expressed between LVW and spinal cord ependymal cells, together with expression data of $CD133^{+}/CD24^{-}/CD45^{-}/CD34^{-}$ RGC and spinal cord-derived NSPs. A group of genes with higher expression in the three cell types with stem/progenitor cell features (spinal cord ependymal cells, RGC and spinal cord-derived NSPs), but lower transcript levels in LVW ependymal cells, was identified: *Fen1*, *Ovca2* and *Rtel1*. Furthermore, *Bhlhb2*, *Dbc1*, *Efnb1*, *Nkx6-1* and *Vtn* were higher expressed in spinal cord ependymal cells and either RGC or spinal cord–derived NSPs compared to LVW ependymal cells.

Figure 26: Biclustering of gene expression profiles. The figure displays a hierarchical biclustering of normalized absolute logarithmic expression values of genes differentially expressed between adult LVW and spinal cord (SC) ependymal cells together with corresponding expression data of radial glial cells (RGC) and spinal cord-derived NSPs (NSP). Microarray data from three independent samples per cell type are shown. Logarithmic expression values ranged from 6.0 to 14.5 and are color-coded according to the color bar next to the figure. Here, low expression is encoded by blue and high expression by red coloring. Intermediate expression values are depicted in light blue, green and yellow. On the y-axis gene symbols are shown and on the x-axis experiments are given.

5. Discussion

5.1 Identification and functional characterization of CD133-positive cells in stem cell regions of the murine central nervous system

The surface protein CD133 is synthesized by early human and murine neural stem cells during development and was used to enrich tumor stem cells of several human central nervous system (CNS) tumor (Weigmann et al., 1997; Uchida et al., 2000; Singh et al., 2004; Taylor et al., 2005). In this study, the cellular localization of CD133 in neurogenic regions around the lateral ventricles of the developing and adult brain as well as in the stem cell region of the adult spinal cord was investigated. Furthermore, CD133-presenting cells were investigated for their stem/progenitor cell properties *in vitro*. A potential lineage relationship between CD133-positive CNS tumor stem cells and normal CD133-positive CNS cells will be discussed.

5.1.1 CD133-positive cells in the developing forebrain and adult CNS

Neuroepithelial cells, which give rise to RGC at the onset of neurogenesis, were shown previously to carry CD133-positive microvilli at their apical cell membrane (Weigmann et al., 1997). In immunostainings presented here, CD133 was found at the apical surface of ventricle-contacting RGC in the embryonic forebrain midway through neurogenesis (embryonic day 14.5; E14.5). No CD133-positivity was observed outside the ventricular zone, where further restricted intermediate progenitor cells (IPC) or neuronal cells are located. Both, neuroepithelial and RGC function as stem cells in the developing telencephalon (Mori et al., 2005; Malatesta et al., 2008) and proteins of the apical membrane, such as CD133, were suggested to play an important role to maintain the immature status of a cell (Kosodo et al., 2004; Dubreuil et al., 2007). The presence of CD133 at the apical membrane of RGC, but not at IPC or further differentiated cells supports this hypothesis.

RGC give rise to ependymal cells in the LVW and this transition occurs via an intermediate radial glial/ependymal cell state (Merkle et al., 2004; Spassky et al., 2005). In the postnatal day 4 (P4) LVW investigated here, CD133-positive cells had Tubulin beta-IV-positive cilia and synthesized a mixture of glial (GLAST) and ependymal (S100) cell proteins, similar to the intermediate radial glial/ependymal cell type described by Spassky et al. (Spassky et al., 2005). The location of CD133-positive intermediate radial glial/ependymal cells mainly at the ventral, but not the dorsal LVW probably reflects local developmental differences in

ependymal cell maturation, which is in agreement with the previous observation that ependymal cells mature along a ventrodorsal and caudorostral gradient in the LVW (Spassky et al., 2005).

In the adult LVW investigated here, the majority of CD133-positive cells corresponded to ependymal cells, lining the ventricular surface. These cells had long CD133- and Tubulin beta-IV-positive cilia, synthesized ependymal cell proteins, such as S100 and CD24, but were negative for GFAP. In a recent study, whole mounts of lateral ventricles (three-dimensional tissue sections) were used to investigate the cytoarchitecture of the adult LVW and two types of CD133-positive ependymal cells, E1 and E2, were identified. E1 and E2 cells can be discriminated by the number of cilia (E1:multiciliated; E2: biciliated) (Mirzadeh et al., 2008). The immunostaining technique used in this thesis (two-dimensional tissue sections) did not allow the distinction between both subtypes.

GFAP is expressed by type B cells in the ventricular and subventricular zone of the adult LVW region and a subpopulation of ventricle-contacting type B cells was reported to be CD133-positive (Doetsch et al., 1997; Mirzadeh et al., 2008). In LVW immunostainings presented here, most GFAP-expressing cells were negative for CD133, however some of them, close to or intercalated between ependymal cells were immunoreactive to this protein. Thus, the $GFAP^{+}/CD133^{+}$ cells found in this thesis probably correspond to CD133-positive ventricle-contacting type B cells (CD133-positive type B1 cells) described by Mirzadeh *et al*. (2008).

Immunostainings of the adult spinal cord showed that CD133 is present at lumen-contacting ependymal cells around the central canal and similar observations were made in other studies (Meletis et al., 2008; Sabourin et al., 2009). The spinal cord ependyma is morphologically and antigenically heterogeneous (Meletis et al., 2008; Hamilton et al., 2009; Sabourin et al., 2009) and functional differences among ependymal cells were postulated (Hamilton et al., 2009). Furthermore, a subpopulation of ependymal and subependymal cells, which expresses GFAP, was suggested to represent the most immature population within the central canal region (Sabourin et al., 2009). Immunostainings of this thesis showed that CD133 is expressed uniformly among ependymal cells and all CD133-positive cells appeared negative for GFAP. However, the distinction between GFAP-expressing subependymal and ependymal cells is technically challenging and was not investigated in detail in this thesis. The GFAP-positivity

of ependymal cells also seems to vary between different anti-GFAP antibodies (Sabourin et al., 2009).

Taken together, the CD133-positive cells identified in this thesis, a subpopulation of RGC, intermediate radial glial/ependymal cells, LVW and spinal cord ependymal cells, and a subpopulation of ventricle-contacting LVW type B cells, most probably belong to the same lineage: Neuroepithelial cells were shown to give rise to RGC, which in turn transform into ependymal cells via an intermediate radial glial/ependymal cell type and type B cells in the adult LVW (Fig.2) (Kriegstein and Alvarez-Buylla, 2009). In addition, ependymal cells of the adult spinal cord were suggested to be derived from the ventral neuroepithelium (Fu et al., 2003).

5.1.2 Stem/progenitor cell properties of CD133-positive cells

Due to its presence on several cell types associated with stem cell properties (Weigmann et al., 1997; Yin et al., 1997; Uchida et al., 2000; Lee et al., 2005), CD133 is frequently referred to as a ´stem cell marker` in the literature. Thus, self-renewal and multipotency of CD133-positive and as control CD133-negative FACS/MACS-isolated LVW cell populations from different developmental stages were investigated by means of the neurosphere (NSP) assay. As described in the introductory section 1.2, not only neural stem cells, but also neural progenitor cells are able to give rise to NSPs and both can be multipotent in culture (Doetsch et al., 2002). To distinguish these two cell types, NSPs should be cultivated for more than five passages, which is supposed to eliminate progenitor cells with a limited self-renewal capacity (Reynolds and Rietze, 2005). NSPs in this work were passaged for at least eight times to demonstrate their long-term self-renewal capacity. This, together with their ability to generate neuronal and glial cells defines them as *bona fide* stem cells. However, since the cells were studied on the population level and not as single cells, a mix of stem and progenitor cells might be present in the investigated cell populations. Thus, even though cells with stem cell properties were contained in the investigated populations, the term ´stem/progenitor cell` was used.

In the embryonic brain around E9.5, a time point shortly before the onset of neurogenesis, NSP formation and the ability to generate neural and glial progeny resided exclusively in the CD133-positive sorted cell population. This is in agreement with previously published findings, that neuroepithelial cells are the only cells with neural stem cell properties at this

developmental stage and that they are CD133-positive (Weigmann et al., 1997; Kriegstein and Alvarez-Buylla, 2009).

At E14.5, CD133-positive RGC gave rise to long-term passageable NSPs and differentiated into neuronal cells, astrocytes and oligodendrocytes, indicative of their neural stem/progenitor cell nature. Long-term self-renewing and multipotent cells were also found among CD133-negative cells. As ventricle-contacting RGC are divided into regional and functional subpopulations (Mori et al., 2005; Kriegstein and Alvarez-Buylla, 2009) and not all RGC are positive for CD133, CD133-negative RGC could be the origin of NSPs in the CD133-negative fraction. An alternative source would be IPC, even though it is unlikely that these cells can self-renew for such a long time in culture. Similar results were obtained with CD133-positive and CD133-negative isolated cells from the immature LVW at P4. Interestingly, even though these CD133-positive cells are in transition from RGC to ependymal cells, they possess the ability to self-renew long-term and give rise to progeny in culture.

In the adult LVW, the majority of neural stem/progenitor cells were found in the CD133-negative cell population. The few, small NSPs derived from CD133-positive cells could not be passaged more than twice and CD133-positive cells gave rise to astrocytes only. These results were consistent under different culture conditions and upon co-cultivation of CD133-positive and CD133-negative cells to rule out a lack of extracellular factors. Most CD133-positive cells in the LVW were ependymal cells. Live-cell microscopy directly after sorting confirmed the presence of cells with multiple beating cilia in the CD133-positive fraction. Recent publications provided evidence that adult LVW ependymal cells are quiescent under physiological conditions (Spassky et al., 2005; Mirzadeh et al., 2008; Carlen et al., 2009). Under pathological conditions, they can give rise to progeny but are not able to self-renew (Carlen et al., 2009). The inability of CD133-positive adult LVW cells to self-renew for a longer time in culture or to form NSPs at all, together with their restricted differentiation potential, is in accordance with the above described findings. Notably, ependymal cells mechanically isolated from the adult LVW in a previous study, gave rise to NSPs with very similar characteristics to the ones derived from CD133-positive LVW cells (Chiasson et al., 1999).

A small number of ventricle-contacting CD133-positive type B cells was found in the adult LVW in this thesis. Type B cells with contact to the ventricle were shown to be

neurogenic *in vivo* and *in vitro* and a subfraction of them expresses CD133 (Mirzadeh et al., 2008). Chojnacki *et al*. raised the question whether ventricle-contacting type B cells can be subdivided into functionally different populations according to the absence or presence of CD133 (Chojnacki et al., 2009). Hence, it might be possible that the neurogenic activity shown for ventricle-contacting type B cells, resides only within the CD133-negative population. This could provide an explanation for the lack of long-term passageable NSPs in the sorted CD133-positive LVW population containing CD133-positive type B cells. It would be interesting to investigate if CD133-positivity can be observed on mitotic ventricle-contacting type B cells *in situ*. Alternatively, as the CD133 staining of type B cells was shown to be relatively weak (Mirzadeh et al., 2008), the CD133 levels of type B cells investigated in this thesis could have been too low to isolate them as CD133-positive cells.

To summarize, CD133-positive cells in the developing brain - neuroepithelial cells, RGC and intermediate radial glial/ependymal cells - had neural stem/progenitor cell properties in culture. Spinal cord ependymal cells were positive for CD133 and were shown by others to posses certain stem/progenitor cell properties *in vivo* (Meletis et al., 2008). *In vitro* experiments performed in other parts of this work, confirmed that CD133-positive spinal cord ependymal cells can self-renew long-term and are multipotent (see 4.2.1.3). However, cells which belong to the same ´lineage`, CD133-positive ependymal cells and CD133-positive type B cells in the adult LVW, lacked stem/progenitor cell properties *in vitro*. As discussed above, in case of CD133-positive type B cells, it is not clear if the absence of stem cell features is due to technical or biological reasons. Notably, cells with stem/progenitor properties were found among CD133-negative cells from the E14.5 forebrain, P4 and adult LVW. These results indicate that in stem cell regions investigated in this thesis, CD133-positive cells do not always correspond to cells with stem/progenitor properties and furthermore not all neural stem cells are CD133-positive.

5.1.3 Lineage relationship between CD133-positive tumor stem cells and CD133-positive CNS cells?

Great effort has been invested to establish the cellular origin of CNS tumors. Stem and progenitor cells are discussed as possible candidates. As they already possess pathways that promote proliferation and survival, they are thought to be predisposed to neoplastic transformation (Sanai et al., 2005). In stem/progenitor cells, it may take fewer mutations to aberrantly activate these pathways compared to postmitotic cells, in which these processes are

not active any more. It is not clear yet whether mature cells, such as astrocytes or ependymal cells, are able to become tumorigenic. They would need to acquire mutations to be able to self-renew and give rise to progeny, abilities neural stem and progenitor cells already possess (Shih and Holland, 2004). A recent study, addressing this question in the adult murine brain, showed that upon tumor suppressor inactivation, cells within the LVW stem cell niche, but not further differentiated cortical or striatal cells, were able to give rise to astrocytomas (Alcantara Llaguno et al., 2009).

Tumor stem cells are cells within the tumor, which are able to self-renew and maintain the whole tumor, whereas the remaining tumor cells lack those properties (Clarke et al., 2006). Due to certain similarities, a derivation of CNS tumor stem cells from normal neural stem cells was postulated. Both can self-renew and give rise to further committed cells and the location of premalignant or malignant lesions is often found at or close to stem cell niches (Sanai et al., 2005; Quinones-Hinojosa and Chaichana, 2007). Furthermore, the presence of CD133 on early neural stem cells and the use of this marker to enrich tumor stem cells in certain CNS tumors was taken as support of this idea (Uchida et al., 2000; Singh et al., 2004; Taylor et al., 2005; Quinones-Hinojosa and Chaichana, 2007).

CD133 was found to enrich tumor stem cells in glioblastomas, medulloblastomas and ependymomas. In case, that phenotypic and functional properties of tumor stem cells allow to determine the cell type they are derived from, CD133-positive stem/progenitor cells in the developing and adult CNS might be the most probable candidates as origin of CD133-positive CNS tumor stem cells. Several CD133-positive cell types were identified in this study: RGC and intermediate radial glial/ependymal cells from the immature forebrain as well as CD133-positive LVW and spinal cord ependymal cells and a subpopulation of LVW type B cells in the adult CNS (Fig.27). Neuroepithelial cells, the primary neural stem cells in the CNS, were shown earlier to express CD133 (Weigmann et al., 1997). As discussed above, mature cells probably need to acquire more hits to become tumorigenic compared to stem/progenitor cells. Hence, LVW ependymal cells are considered to be an unlikely source of CD133-positive tumor stem cells, even though they share the expression of CD133 with the latter. Similarly poor candidates are neuroepithelial cells, as they only exist for a short period of time during development and disappear long before birth. RGC and intermediate radial glial/ependymal cells on the other hand, are present in the early postnatal CNS. This, together with their stem/progenitor cell properties, makes them a possible source of CD133-positive tumor stem

cells in pediatric tumors, such as intracranial ependymomas. Consistent with this, RGC were previously suggested as cells of origin for ependymomas (Taylor et al., 2005). However, RGC or intermediate radial glial/ependymal cells are not present in the adult CNS and therefore an implausible origin for tumors arising during adulthood, such as glioblastomas and spinal cord ependymomas. A possible origin of adult spinal cord ependymoma stem cells are CD133-positive spinal cord ependymal cells (Fig.27), which are present at the time and location where these tumors arise and possess certain stem/progenitor cell properties.

Experimental findings indicate that GFAP-positive cells are capable of brain tumor initiation (Shih and Holland, 2004). In addition, Alcantara Llaguno *et al.* suggested LVW stem/progenitor cells as cells of origin for adult forebrain astrocytoma in a somatic tumor suppressor mouse model (Alcantara Llaguno et al., 2009). Thus, LVW type B cells are in principle a source for adult brain tumor stem cells. A small number of CD133-positive adult LVW type B cells was found in this study. However, results from *in vitro* experiments performed with CD133-positive adult LVW cells in this thesis do not allow to draw any conclusions concerning a linage relationship between CD133-positive type B cells and CD133-positive adult brain tumor stem cells. As discussed in section 5.1.2, the CD133 staining of CD133-positive type B cells could have been too weak to identify them as CD133-positive cells according to the FACS settings used in this thesis. Thus, this population might have been isolated as CD133-negative cells, and cells with stem/progenitor properties were found within the CD133-negative sorted fraction. In this case, it is possible that CD133-positive type B cells could be the origin for certain tumors in the adult forebrain. On the other hand, if neurogenic ventricle-contacting type B cells can be subdivided into functionally different populations according to the presence or absence of CD133 (see 5.1.2), it might be possible that the CD133-positive type B cells identified in this study do not possess the self-renewing and multipotent properties of the CD133-negative ventricle-contacting type B cells. According to that scenario, CD133-positive type B cells would be an unlikely source for CD133-positive adult brain tumor stem cells.

In this context, is it important to point out, that more recently also CD133-negative glioblastoma stem cells were identified (Beier et al., 2007; Ogden et al., 2008; Wang et al., 2008), thereby implying that a tumor stem cell derivation from CD133-negative CNS cells is possible as well. Another alternative is that CD133-positive tumor stem cells are derived from CD133-negative CNS cells, such as neurogenic CD133-negative type B cells, and start to produce CD133 themselves. In this case, phenotypic similarities between tumor stem cells

and their origin would be absent and a functional importance of CD133 for the tumor stem cell might be possible.

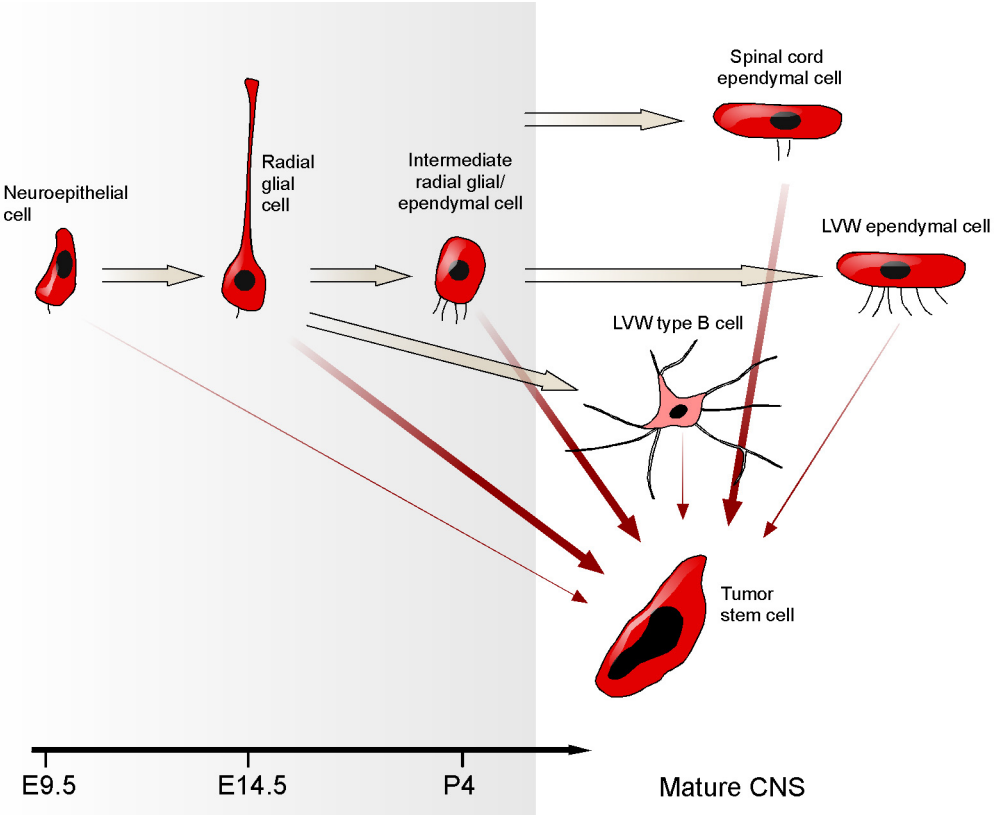

Figure 27: Illustration of investigated CD133-positive cell types in the developing and adult CNS and their potential lineage relationship to CD133-positive CNS tumor stem cells. CD133-negative LVW type B cells and RGC are not depicted. The neuroepithelial, radial glial, intermediate radial glial/ependymal, spinal cord ependymal and LVW ependymal cell are illustrated with their ventricular surface oriented downwards. Developmental relationships between normal CNS cells based on published findings are indicated by thick, grey arrows. The origin of CD133-positive spinal cord ependymal cells requires further experimental investigation. Red arrows illustrate possible cells of origin for CD133-positive tumor stem cells. Thickness of the red arrows indicates stronger (thick) and weaker (thin) candidates according to functional properties and presence at the time and location of tumor formation. Red color, CD133-positivity; Pink color, weak CD133-positivity.

The role of CD133 as tumor stem cell marker was questioned by the identification of CD133-negative tumor stem cells. However, an explanation might be the existence of distinct tumor subclasses and heterogeneity among cells within a tumor (Fomchenko and Holland, 2005; Taylor et al., 2005; Phillips et al., 2006), which could be reflected by different tumor stem cell populations. In addition, experimental differences in cell isolation and culture conditions might influence the expression of CD133. This is especially important for the determination of CD133-negative cells (Cheng et al., 2009). On the other hand, CD133-positive tumor stem cell populations were identified by xenograft transplantations, adding an unknown factor, the influence of the host environment, to the equation. It was suggested that xenotransplantion assays rather select for cells that survive in the foreign host, than for *bona fide* tumor stem cells (Clarke et al., 2006; Sakariassen et al., 2007). A recent study, performing species-

matched transplantation studies, showed that tumor stem cells of murine medulloblastomas are not contained in the CD133-positive, but a $Math1^{+}/CD15^{+}$ cell population (Read et al., 2009). This challenges results obtained by the transplantation of human medulloblastoma cells in NOD-SCID mouse brains, where tumor stem cells were enriched with CD133 (Singh et al., 2004).

In summary, several CD133-positive cell types of the developing and adult CNS were discussed as origin of CD133-positive tumor stem cells. Phenotypic and functional similarities, together with the presence at the time and location where the tumor arises, identified RGC and intermediate radial glial/ependymal cells as most probable candidates for pediatric tumors and adult spinal cord ependymal cells for ependymomas in the adult spinal cord. Experiments performed in this thesis, do not allow to draw any conclusions about a potential lineage relationship between CD133-positive LVW type B cells and CD133-positive tumor stem cells in the adult brain, however a derivation of adult forebrain tumors from LVW type B cells was suggested elsewhere (Alcantara Llaguno et al., 2009). To clarify the role of CD133 as a CNS tumor stem cell marker and even more to pinpoint the cellular origin of CD133-positive tumor stem cells, further studies are necessary. It will be important to target the CD133-expressing cell populations, described in this thesis and investigate their susceptibility to neoplastic transformation. In addition, the identification of tumor stem cells in species-matched settings and in this context, further investigations of tumor mouse models for the presence of CD133-positive tumor stem cell populations might help to elucidate the role of CD133 in tumor formation.

5.2 Comparison of CD133-positive ependymal cells from the adult murine LVW and spinal cord

Adult LVW ependymal cells were shown to be quiescent under physiological conditions *in vivo* (Spassky et al., 2005; Carlen et al., 2009). This is supported by NSP assay results from the previous part of this work, which indicate that CD133-positive adult LVW ependymal cells lack self-renewal and multipotency in culture. On the other hand, ependymal cells from the adult spinal cord possess certain stem cell properties, as they can self-renew *in vivo* and *in vitro* and give rise to progeny upon activation by injury or in culture (Meletis et al., 2008). Little is known about the molecular basis underlying these functional differences.

In this work, a combination of four surface markers was applied to purify ependymal cells from the adult LVW and spinal cord by flow cytometry. Isolated LVW and spinal cord ependymal cells were used to cultivate both populations under identical conditions to investigate their functional properties and to determine and compare their molecular profiles.

5.2.1 Stem/progenitor cell properties of ependymal cells in the adult LVW and spinal cord

CD133 is not an exclusive marker for ependymal cells. This protein is also found on a variety of other cells, such as hematopoietic progenitor cells, endothelial progenitor cells, oligodendrocytes and a subpopulation of type B cells (Corbeil et al., 2000; Balasubramaniam et al., 2007; Nolan et al., 2007; Mirzadeh et al., 2008; Corbeil et al., 2009; Rosell et al., 2009). Hence, an antibody combination, $CD133^+/CD24^+/CD45^-/CD34^-$, was used to isolate pure ependymal cell populations. This combination was chosen due to the following reasons: The vast majority of ependymal cells in the adult LVW or spinal cord could be co-stained with CD133 and CD24. Thus, the combination of CD133 and CD24 antibodies provides the possibility to select CD133-positive ependymal cells, but exclude potential CD133-positive oligodendrocytes and CD133-positive LVW type B cells. Ventricle-contacting type B cells were shown to be negative for CD24 (Mirzadeh et al., 2008). The use of CD45 and CD34 antibodies allows the elimination of CD133-positive hematopoietic and endothelial progenitor cells. In addition, CD34 might also prevent a contamination with potential CD133-positive endothelial cells. CD34 is a well-known marker for endothelial cells and $CD133^+/CD34^+$ cells were detected in vessel-like structures in immunostainings of the adult spinal cord in this thesis. Considering the sparsity of circulating endothelial progenitor cells under homeostatic conditions (Ingram et al., 2005), and the fact that blood cells, including CD34-positive hematopoietic progenitor cells, are mainly washed out of the tissue section during the staining procedure, these cells could represent CD133-positive endothelial cells. However co-stainings with other antibodies are necessary to determine the exact identity of these cells.

The NSP assay was used to investigate *in vitro* self-renewal and multipotency of different cell populations from the adult spinal cord. $CD133^+/CD24^+/CD45^-/CD34^-$ ependymal cells formed long-term passageable NSPs and gave rise to all three neural lineages in culture, indicative of their stem/progenitor cell nature. These results support previous published data that ependymal cells function as stem cells in the adult spinal cord (Meletis et al., 2008). In this thesis, only a subpopulation of isolated adult spinal cord ependymal cells gave rise to NSPs in

culture. It was shown that ependymal cells need to be activated by extrinsic factors, provided for example upon injury or infusion of growth factors, to leave their dormancy (Martens et al., 2002; Meletis et al., 2008). Thus, it might be possible that the applied *in vitro* conditions did not provide enough stimuli to activate all ependymal cells to form NSPs. This idea is supported by studies, in which increased spinal cord NSP-formation was observed after trauma (Moreno-Manzano et al., 2009). It should also be noted, that the isolation procedure can influence the features of spinal cord ependymal cells in culture. Compared to direct cultivation, cell isolation by flow cytometry was shown to diminish the NSP frequency of adult spinal cord ependymal cells (Meletis et al., 2008). Thus, *in vitro* NSP-formation might not reflect the true number of spinal cord ependymal cells with stem/progenitor cell properties.

Low numbers of NSPs were formed by $CD133^-/CD45^-$ spinal cord cells and these cells could not be kept in culture for more than four passages. Besides CD133-positive ependymal stem cells in the central canal region, progenitor cells are present in the parenchyma of the spinal cord, which could be the source of $CD133^-/CD45^-$ derived NSPs. This is supported by the findings, that parenchymal progenitor cells can give rise to NSPs, that can be passaged for a certain period of time in culture (Yamamoto et al., 2001). CD133 was found to be expressed by oligodendrocytes in the CNS (Corbeil et al., 2009). Given that these cells are present in the spinal cord, the fraction which could contain CD133-positive oligodendrocytes would be $CD133^+/CD24^-/CD45^-$ cells. These cells never gave rise to NSPs, suggesting that, at least *in vitro*, $CD133^+/CD24^-/CD45^-$ cells and among them potential CD133-positive oligodendrocytes, can not self-renew.

$CD133^+/CD24^+/CD45^-/CD34^-$ ependymal cells from the LVW lacked stem/progenitor cell properties, as indicated by the absence of primary NSPs. This is in agreement with the finding that ependymal cells are quiescent *in vivo* under physiological conditions (Carlen et al., 2009). Neural stem/progenitor cells were found in the $CD133^-/CD45^-$ negative fraction, which is similar to results obtained with CD133 as a single marker (section 5.1.2). Results from a previous study by Coskun *et al.* suggested that neural stem cells in the adult LVW correspond to an ependymal subpopulation with a $CD133^+/CD24^-$ phenotype. In this context, NSP-formation from CD133-positive LVW was demonstrated (Coskun et al., 2008). However, different results were obtained by experiments performed in this thesis. Isolated $CD133^+/CD24^-/CD45^-$ LVW cells were not able to form NSPs in culture, indicating that these cells, at least *in vitro*, lack neural stem/progenitor cell properties. Due to the absence of FACS plots, which could illustrate the sort settings and a purity analysis of the sorted fractions in the

publication of Coskun et al. (2008), it is not possible to explain the discrepant findings of the latter study and results presented in this thesis. It can only be speculated that contaminating CD133-negative cells within the CD133-positive sorted cell fraction could have been the origin of the observed ´CD133-positive-derived NSPs`. Alternatively, it was suggested elsewhere that $CD133^+/CD24^-$ cells are not ependymal cells, but type B1 cells, which have a relatively weak CD133-positivity (Mirzadeh et al., 2008). In this case, as discussed in previous chapters, it might be possible that the CD133 levels of these cells have been too low to select them as CD133-positive cells according to the sort settings used in this thesis.

Taken together, the comparison of $CD133^+/CD24^+/CD45^-/CD34^-$ adult LVW and spinal cord ependymal cells under similar culture conditions revealed that they have different functional properties *in vitro*. $CD133^+/CD24^+/CD45^-/CD34^-$ ependymal cells from the LVW lacked stem/progenitor properties, whereas $CD133^+/CD24^+/CD45^-/CD34^-$ ependymal cells from the spinal cord could long-term self-renew and gave rise to neural progeny in culture.

5.2.2 Transcriptional profiling of adult LVW and spinal cord ependymal cells

As shown by the above discussed *in vitro* experiments and findings by others (Spassky et al., 2005; Meletis et al., 2008; Carlen et al., 2009), ependymal cells in the adult LVW and spinal cord have distinct functional properties. Spinal cord ependymal cells possess certain neural stem/progenitor cell features, whereas ependymal cells of the LVW are not able to self-renew *in vitro* and *in vivo*. This provided the unique possibility to investigate the molecular profile of ´stem cells` versus ´non-stem cells` in the same cellular background. As the microarray experiments were performed with cells directly isolated from the tissue, the obtained molecular profiles reflect *in vivo* gene expression levels of $CD133^+/CD24^+/CD45^-/CD34^-$ LVW and spinal cord ependymal cells (hereafter termed LVW and spinal cord ependymal cells).

Of the 156 genes differentially expressed between LVW and spinal cord ependymal cells, 49% were higher expressed in spinal cord ependymal cells and 51% in LVW ependymal cells. Several of the genes, with higher transcript levels in spinal cord ependymal cells (Table 9A), were previously shown to be present in the spinal cord ependyma, providing an independent confirmation of the obtained array results: The transcription factor NKX6-1 was found in human and mouse spinal cord ependymal cells (Fu et al., 2003; Dromard et al., 2008) and *Hoxb5* expression was observed in the adult spinal cord by Krumlauf et al. (Krumlauf et al.,

1987). A comparative gene expression analysis of embryonic cortical- and spinal cord-derived neurospheres identified a large number of *Hox* genes higher expressed in the latter (Kelly et al., 2009). In line with the last two reports, 12 *Hox* genes (16% of all higher expressed spinal cord genes), among them *Hoxb5*, were found to have elevated transcript levels in spinal cord ependymal cells.

Seventy-nine genes were higher expressed in LVW ependymal cells compared to their spinal cord counterpart (Table 9B). Among them are *Aqp4*, *Anxa1*, *Clmn*, *Cpe*, which were shown to be present on the mRNA or protein level in adult rodent brain ependymal cells in earlier reports (MacCumber et al., 1990; Nielsen et al., 1997; Takaishi et al., 2003; Solito et al., 2008).

Transcriptional analysis of LVW ependymal cells was performed earlier by Lim et al. (2006). In this study ependymal cells were isolated with only one surface marker, CD24, which is not exclusive for these cells, and compared to GFAP-positive type B cells. Among the 1,282 genes, differentially expressed between these two cell types, ependymal cells were found to have increased transcript levels of genes promoting cell cycle arrest, which is in agreement with their quiescent nature under physiological conditions.

Literature research, conducted for all differentially expressed genes between LVW and spinal cord ependymal cells, identified a variety of functional and regulatory categories they are associated with. Since it was not feasible to follow all the information retrieved, this study focussed on genes that could provide a molecular basis for the different functional properties of LVW and spinal cord ependymal cells. In addition, a potential regulatory mechanism for spinal cord ependymal cells was investigated in greater detail. Genes that, based on previous published data, might be associated with the same function or mechanism were grouped into ´categories` and are discussed in the following chapters.

5.2.3 Genes associated with stem cell properties of adult spinal cord ependymal cells

One important feature of adult spinal cord ependymal cells is their ability to self-renew *in vitro* and *in vivo* (Johansson et al., 1999; Meletis et al., 2008; Hamilton et al., 2009). Furthermore, spinal cord ependymal cells start to proliferate extensively upon activation by injury (Johansson et al., 1999; Mothe and Tator, 2005; Meletis et al., 2008). A substantial number of genes which play a role in the regulation of cell cycle-related processes, such as cell division or progression through the cell cycle, apoptosis, as well as telomere stability and

maintenance, were found to have higher expression levels in spinal cord ependymal cells (Table 11). Among them is *Efnb1* (Ephrin-B1), which encodes a ligand for Eph receptors. The presence of Ephrin-B1 on cells of the adult spinal cord ependyma was confirmed by immunostainings. In the developing cortex, Ephrin-B1 was shown to have a role in neural stem/progenitor cell maintenance by preventing differentiation (Qiu et al., 2008). In accordance with this, high levels of *Efnb1* were also expressed by $CD133^{+}/CD24^{-}/CD45^{-}/CD34^{-}$ RGC, but low transcript levels were found in LVW ependymal cells. The *Hoxb7* protein was shown to mediate cell proliferation in normal and neoplastic cells (Care et al., 1996; Care et al., 1999) and NF2 was suggested to play a role in contact-dependant inhibition of cell proliferation (Curto and McClatchey, 2008). Genes, whose products are associated with the regulation of cell cycle progression, are *Dbc1* (Deleted in bladder cancer 1) (Nishiyama et al., 2001) and *Brd2*, encoding Bromodomain-containing protein 2 (Denis et al., 2000; Sinha et al., 2005), as well as several *Hox* genes, *Hoxa5*, *Hoxa7* (Mishra et al., 2009) and *Hoxc8* (Kamel et al., 2009).

Apoptosis contributes to preserve the genomic integrity of stem cells (Morrison, 2009) and it may also serve to retain the overall tissue homeostasis in stem cell niches (Potten, 1992). Several genes higher expressed by spinal cord ependymal cells play a role in this process. Gene products of *Dbc1* (Wright et al., 2004), *Ei24* (Gu et al., 2000), *Hoxa5* (Raman et al., 2000; Chen et al., 2004), *Tmem55b* (Transmembrane protein 55B) (Zou et al., 2007) and the loss of the *Hoxc6* encoded protein (Ramachandran et al., 2005), were shown to be involved in apoptosis induction.

Telomere length is one mechanism to define the replicative life span of stem cells (Pardal et al., 2005; Morrison, 2009). Telomeres can shorten through cell division or the loss of telomeric DNA, e.g. due to the dysfunction of proteins involved in telomere protection. At a certain critical length, cellular senescence or apoptosis will be induced. In some cells, the loss of telomeric sequences can be balanced by telomerase-mediated addition of new DNA repeats (Denchi, 2009). In the adult murine brain, telomerase was shown to be active in LVW cells (Caporaso et al., 2003). It was suggested that telomere shortening due to cell divisions only plays a role in human, but not murine cells, since laboratory inbred mice have significantly longer telomeres (Kipling and Cooke, 1990). However, this seems to apply to long-term inbred strains only, as more recent established mouse strains were shown to have a significantly shorter telomere length, which is in some strains similar to the one from humans

(Hemann and Greider, 2000). Thus, telomere maintenance and stability are of vital importance to maintain the proliferative capacity of stem cells and preserve the genomic integrity. Two genes, *Fen1* and *Rtel1*, are critical for these processes and were found to be higher expressed in spinal cord ependymal cells (Ding et al., 2004; Sampathi et al., 2009). The presence of the FEN-1 protein on adult spinal cord ependyma was confirmed by immunostainings. FEN-1 was also detected on cells in the spinal cord parenchyma, which might be explained by additional functions of this protein, such as its involvement in DNA replication (Shen et al., 2005). Alternatively, it is also possible that other cells, like parenchymal progenitors, produce FEN-1 for telomere maintenance.

5.2.4 Genes associated with tumorigenesis in adult spinal cord ependymal cells

A hallmark of stem cells is their ability to long-term self-renew. Involved in this process are proto-oncogenic and tumor-suppressor pathways. Proto-oncogenic pathways promote the regenerative capacity of stem cells, but include the risk of neoplastic transformation. Tumor-suppressor activity is necessary to counteract these processes. Since a disturbance of the balance between tumor promoting and tumor suppressing gene products can lead to an oncogenic transformation, self-renewing cells need to tightly control respective gene activities (Pardal et al., 2005). Several established or putative proto-oncogenes and tumor suppressor genes were found to be higher expressed in spinal cord ependymal cells, such as *Dbc1* (Nishiyama et al., 2001; Wright et al., 2004), *Ei24* (Gu et al., 2000), *Hoxa5*, *Hoxb7* (Abate-Shen, 2002) *Hoxc6* (Ramachandran et al., 2005), *Nf2* (Curto and McClatchey, 2008) and *Ret* (Arighi et al., 2005) (Table 11).

Ependymomas are tumors that commonly arise along the wall of the ventricular system and the central canal of the spinal cord (Hamilton and Pollack, 1997). Due to phenotypic and molecular similarities, RGC were postulated as origin of ependymomas (Taylor et al., 2005). While this may hold true for pediatric ependymomas, it is less likely for spinal cord ependymomas, which develop mainly in adulthood (Hamilton and Pollack, 1997), when RGC are not present any more. The spatiotemporal correlation of adult spinal cord ependymal cells and spinal cord ependymomas together with the proto-oncogene-driven self-renewal of spinal cord ependymal cells, suggests the latter as potential origin for spinal cord ependymomas. This is supported by the higher expression of *Hoxa7*, *Hoxb5*, *Hoxb7*, *Hoxc6*, *Vtn* and *Rxrg* genes in adult spinal cord ependymal cells (Table 9A), which were previously identified as ´signature genes` for ependymomas from the spinal cord region (Korshunov et al., 2003;

Taylor et al., 2005). In addition, the tumor suppressor gene *Nf2*, which is frequently mutated in spinal cord ependymomas (Ebert et al., 1999), was found to be higher expressed in spinal cord ependymal cells compared to LVW ependymal cells. Aberrant expression of the latter genes could play a role in neoplastic transformation of spinal cord ependymal cells. Additionally, as discussed in 5.1.3, the CD133-positivity of adult spinal cord ependymal cells and the identification of CD133-positive tumor stem cells in ependymomas might provide a further hint regarding spinal cord ependymal cells as origin of spinal cord ependymomas.

5.2.5 Retinoic acid-signaling in adult spinal cord ependymal cells

Retinoic acid (RA), a metabolite of vitamin A, is involved in a variety of cellular processes during development and in the adult CNS (Maden, 2001; Mey, 2006). RA-signaling regulates the expression of a large number of genes and their identification is crucial to elucidate the effect of RA in specific tissues. More than 20% of the genes higher expressed in spinal cord ependymal cells are known to be RA-responsive. For example the genes *Bhlhb2* (also known as *Bhlhe40* / *Dec1), D0H4S114*, *Efnb1*, *Ovca2* and *Ret* were shown to change their expression upon RA-exposure (Bouillet et al., 1995; Boudjelal et al., 1997; Prowse et al., 2002; Cerchia et al., 2006; Leung et al., 2008). Well-known target genes of RA signaling are *Hox* genes (Maden, 2001) and the majority of *Hox* genes highly expressed in spinal cord ependymal cells is regulated by RA (Simeone et al., 1990; Kessel and Gruss, 1991; Manohar et al., 1996; Merrill et al., 2004). The expression of *Hoxd4*, *Hoxa5* and *Hoxb5* is directly controlled by RA via retinoic acid response elements (RAREs) in their genomic region, which can be bound by nuclear retinoid receptors (Zhang et al., 2000, Oosterveen et al., 2003; Chen et al., 2007). In addition, a higher expression of *Rxrg* was found in spinal cord ependymal cells. This gene encodes a 9-cis-RA activated nuclear transcription factor, which can be regulated by RA through a retinoid X response element in its promoter region (Barger and Kelly, 1997; McDermott et al., 2002).

Dorsal spinal cord ependymal cells in the adult CNS were previously suggested to be regulated by RA (Thompson Haskell et al., 2002). Thus, the effect of RA on $CD133^+/CD24^+/CD45^-/CD34^-$ spinal cord ependymal cells *in vitro* was tested in this thesis. In the presence of RA, the proliferation rate of spinal cord ependymal cells increased more than twice compared to the vehicle control, indicating responsiveness to RA. Notably, differentiation of ependymal cells into neural cells was not observed. These results are somewhat unexpected, considering the well-known role of RA as inhibitor of cell

proliferation. The inhibition of cell growth can be caused by differentiation, apoptosis or cell cycle arrest and is mediated by the ´classical RA pathway`, where RA is transported by cytosolic CRABP-II (Cellular retinoic acid-binding protein-II) into the nucleus to activate retinoic acid receptors (RAR), which in turn bind to regulatory regions of target genes and modulate their transcription (Maden, 2001; Schug et al., 2007). However, it was reported, that RA can also bind to the nuclear receptor PPARbeta/delta (Peroxisome proliferator-activated receptor beta/delta), which is mediated by FABP5 (Fatty acid-binding protein 5) (Fig.28). This pathway triggers a different response, as cell growth is stimulated and apoptosis inhibited. Since both pathways co-exist within one cell, RA-binding to RAR or PPAR beta/delta seems to depend on the ratio of CRABP-II and FABP5 (Schug et al., 2007).

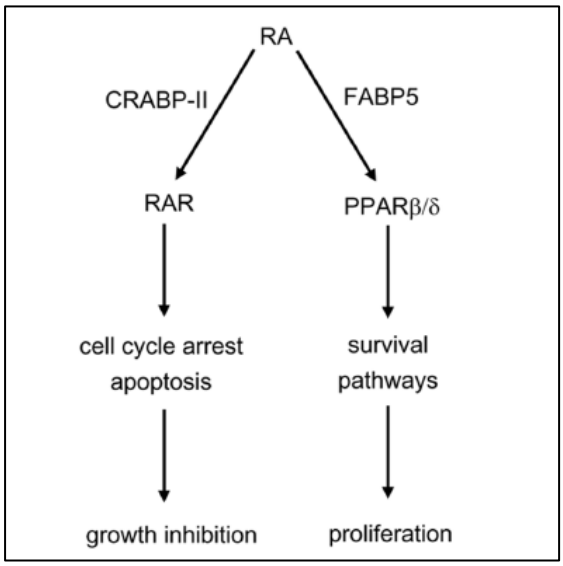

Figure 28: Model illustrating the two opposing RA pathways. CRABP-II mediates RA binding to RAR, whereas FABP5 directs RA to PPARbeta/delta. Presence of higher levels of CRABP-II results in growth inhibition through RAR-mediated gene transcription, whereas higher levels of FABP5 induce proliferation via PPARbeta/delta. Figure taken from Schug et al. (2007).

In case, that RA-signaling is mediated by these two pathways in ependymal cells, the observed RA-induced proliferative response of cultivated spinal cord ependymal cells could be explained by a high cellular FABP5/CRABP-II ratio, which suppressed differentiation and promoted increased proliferation.

The enrichment of RA-responsive genes, among the genes higher expressed in spinal cord ependymal cells, together with the RA-induced proliferative response in isolated spinal cord ependymal cells *in vitro*, suggests that RA-signaling could be a regulatory mechanism for spinal cord ependymal cells in the adult CNS. Notably, increased levels of Retinaldehyde dehydrogenase 2, an enzyme involved in the production of RA, were observed in the spinal cord after injury (van Neerven and Mey, 2007). The levels of FABP5 or CRABP-II in spinal cord ependymal cells after injury have not been addressed so far. It will be interesting to

investigate the effect of RA on spinal cord ependymal cells *in vivo* and moreover their response in the injured spinal cord in future experiments.

5.2.6 Genes associated with functional properties of adult LVW ependymal cells

Ependymal cells from the LVW do not self-renew, proliferate or give rise to progeny under physiological conditions (Carlen et al., 2009). However they were suggested to represent a ´reservoir population`, since they are able to give rise to further differentiated cells, such as neuronal cells upon stroke or inhibition of Notch-signaling. The higher expression of *Dlx2*, *Hey1*, *Foxg1*, and *Id2* genes in LVW ependymal cells in this thesis, provides a possible mechanism to explain these features. *Dlx2* encodes a transcription factor with a key role in neurogenesis during development and in the adult forebrain (Petryniak et al., 2007; Brill et al., 2008). DLX2 immunoreactivity was reported for type C and type A cells, but not for ependymal cells in the adult LVW (Doetsch et al., 2002). The presence of *Dlx2* transcripts, but not the protein, could indicate that LVW ependymal cells are ´prepared` to differentiate into neuronal cells upon environmental changes, but this potential is restricted under physiological conditions. This hypothesis is supported by the higher expression of *Foxg1*, *Id2* and *Hey1* in LVW ependymal cells. All three genes encode transcriptional regulators, which promote the undifferentiated status of neural stem cells by inhibiting neuronal differentiation (Sakamoto et al., 2003; Martynoga et al., 2005; Bai et al., 2007). Furthermore, *Hey1* is a target gene of Notch (Iso et al., 2001), supporting its role as repressor of neuronal differentiation. Thus, HEY1, FOXG1 and ID2 might mediate the quiescence of LVW ependymal cells and inhibit DLX2-instructed production of neuronal cells under physiological conditions.

The expression of these four transcriptional regulators was confirmed in single *Prom1*- and *Cd24*-expressing LVW ependymal cells by rtPCR. The presence of multiple long cilia, a hallmark of forebrain ependymal cells, was confirmed for every cell used for rtPCR to exclude a contamination with other cells. In one of the investigated LVW ependymal cells, the expression of all six tested genes was observed, whereas different gene expression patterns were found among the remaining cells. This might be explained by the technical variability of single cell multiplex rtPCR in connection with low transcript levels of some of the tested genes. Alternatively, it could indicate the presence of different LVW ependymal subpopulations with distinct gene expression patterns.

5.2.7 Transcriptional profiling of adult LVW and spinal cord ependymal cells, RGC and spinal cord neurospheres

The gene expression profile of $CD133^+/CD24^-/CD45^-/CD34^-$ RGC was included in the analysis, to be able to compare the transcriptional profile of well-known neural stem cells, which are also CD133-positive, to the one of LVW and spinal cord ependymal cells. *In vitro* experiments confirmed that these cells are able to self-renew long-term and give rise to cells of all three neural lineages. The same antibody-combination was used previously to isolate human fetal neural stem cells (Uchida et al., 2000).

The fourth group included into the array analysis were NSPs derived from $CD133^+/CD24^+/CD45^-/CD34^-$ spinal cord ependymal cells. The transcriptional profile of spinal cord NSPs served to identify genes with similar or changed expression upon cultivation of ependymal stem cells. As discussed previously, spinal cord ependymal cells divide rarely *in vivo*, but they increase their proliferative rate and give rise to neural progeny under NSP-culture conditions. Here it is important to note, that besides stem cells, NSPs also contain progenitor cells and some further differentiated cells. This has to be considered when interpreting the obtained results, as the transcriptional profile might reflect the gene expression pattern of a heterogeneous mix of cells.

The combination of adult LVW and spinal cord ependymal cells, RGC and spinal cord-derived NSPs allowed to compare the molecular profile of different stem cell populations to a ´non-stem cell` population, the LVW ependymal cells. The three stem cell types are distinct, as spinal cord ependymal cells constitute a rather dormant stem cell population, RGC are active cycling stem cells and NSPs are formed by spinal cord stem cells under non-physiological conditions. Their combination might prevent a biased selection of genes, which rather reflect the proliferative status or the environmental influence, than functions associated with the immature state of the cell. Several genes, with higher transcript levels in spinal cord ependymal cells, RGC and/or NSPs, but lower gene expression in LVW ependymal cells were identified. Among them are *Fen1*, *Rtel1* and *Efnb1*, encoding proteins that are involved in processes crucial for stem cells, like telomere maintenance or the perpetuation of an immature cell state (see 5.2.3). Genes similarly expressed between spinal cord ependymal cells and RGC, might also be expressed by other stem cells of the same lineage, such as LVW type B cells. However, these results have to be interpreted with caution, as it was suggested that the stem cell state of a cell is not strictly associated with the expression of specific genes, but an

open chromatin status and interaction with the stem cell niche (Mikkers and Frisen, 2005). Furthermore, it was shown that the existence of general "stemness" genes, common between stem cells from different tissues, embryonic, hematopoietic and neural stem cells, is questionable (Fortunel et al., 2003). However, it is not known if this applies to stem cells from the same tissue as well.

5.2.8 Concluding remarks

It is clear that a complex network of genes and their products regulates LVW and spinal cord ependymal cells. The presented gene expression profiles of LVW and spinal cord ependymal cells provide a molecular basis that allows to propose certain regulatory mechanisms, however detailed studies evaluating the different suggested mechanisms need to follow. Many of the genes differentially expressed between LVW and spinal cord ependymal cells, have not been evaluated further in this study, thus providing a catalogue of candidate genes for future investigations.

6. Summary

The surface protein CD133, often referred to as ´stem cell marker` in the literature, was found on early human and murine neural stem cells during development and certain human tumor stem cells in the central nervous system (CNS). Whether CD133 is a general marker for neural stem cell populations in the CNS remained to be determined. The first part of this thesis focussed on the identification of CD133-positive cells in stem cell regions of the developing and adult murine CNS and the evaluation of their stem/progenitor cell properties *in vitro*.

Several CD133-positive cell types were identified: A subpopulation of radial glial cells (RGC) and intermediate radial glial/ependymal cells in the embryonic and postnatal lateral ventricle region, as well as ependymal cells from the lateral ventricle wall (LVW) and the spinal cord central canal in the adult CNS. In addition, CD133-positive ventricle-contacting type B cells were found in the adult LVW.

CD133-positive cells in the developing lateral ventricle region, RGC and intermediate radial glia/ependymal cells, could self-renew long-term and gave rise to different neural cell types *in vitro*, which are characteristics of neural stem/progenitor cells. In contrast, CD133-positive cells from the adult LVW, ependymal cells and a subpopulation of type B cells, lacked stem/progenitor cell properties in culture. However, *in vitro* long-term self-renewing and multipotent cells were found among CD133-negative adult LVW cells. Stem/progenitor cells were also present among CD133-negative cells from the embryonic forebrain and the postnatal lateral ventricle region.

Thus, in the stem cell regions investigated in this thesis, not all CD133-positive cells corresponded to cells with stem/progenitor cell properties *in vitro* and furthermore, not all neural stem/progenitor cells were CD133-positive. A potential lineage relationship between CD133-positive tumor stem cells and the in this thesis investigated CD133-positive cells in the CNS was discussed.

In the second part of this thesis, CD133-positive ependymal cells from two adult murine stem cell niches, the LVW and the central canal of the spinal cord were compared. The surface marker combination $CD133^+/CD24^+/CD45^-/CD34^-$ was used to purify ependymal cells from both regions by flow cytometry. Direct comparison of their functional properties under identical culture conditions revealed that spinal cord ependymal cells can self-renew long-

term and are multipotent, whereas ependymal cells from the LVW lack those stem/progenitor cell features.

Microarray experiments were performed to determine the underlying molecular basis of these functional differences. Several genes, which were higher expressed in spinal cord ependymal cells, possibly contribute to their stem cell properties, as they encode proteins associated with cell cycle regulation, telomere maintenance and induction of apoptosis. Furthermore, a potential regulation of adult spinal cord ependymal cells by retinoic acid (RA) was identified based on a) the enrichment of RA-responsive genes among the genes higher expressed by spinal cord ependymal cells and b) a responsiveness of spinal cord ependymal cells to RA-signaling *in vitro*.

It was shown by others, that ependymal cells from the adult LVW are quiescent under physiological conditions *in vivo*. However, under certain conditions, such as stroke, they can get activated to differentiate into neuronal cells. Array data obtained in this thesis revealed higher expression levels of the transcriptional regulator genes *Dlx2*, *Foxg1*, *Hey1* and *Id2* in LVW ependymal cells, which could provide a molecular basis for these functional properties.

Finally, differentially expressed genes between LVW and spinal cord ependymal cells were compared with corresponding gene expression data from RGC and spinal cord ependymal cell-derived neurospheres (NSPs). A group of genes with higher expression in cells with stem cell features (spinal cord ependymal cells, RGC and / or NSPs), but lower transcript levels in LVW ependymal cells, was identified. These genes could be of functional importance for the immature state of neural stem cells and might be expressed by other neural stem cell populations as well.

The transcriptional profiles of CD133-positive LVW and spinal cord ependymal cells presented in this thesis contribute to an increased understanding of their different functional properties and provide a launching point for future studies.

7. Zusammenfassung

Das Oberflächenprotein CD133 wurde auf frühen humanen und murinen neuralen Stammzellen und bestimmten humanen Tumorstammzellen des Zentralnervensystems (ZNS) detektiert und wird in diesem Zusammenhang in der Literatur häufig als ´Stammzellmarker` zitiert. Ob CD133 ein genereller Marker für neurale Stammzellpopulationen des ZNS ist, blieb noch zu zeigen. Der erste Teil dieser Doktorarbeit befasst sich mit der Identifizierung von CD133-positiven Zellen in Stammzellregionen des embryonalen, postnatalen und adulten murinen ZNS, sowie der anschliessenden Evaluierung der *in vitro* Stamm/Vorläuferzelleigenschaften dieser CD133-positiven Zellen.

Mehrere CD133-positive Zelltypen wurden gefunden: Eine Subpopulation von Radialen Gliazellen (RGZ) und intermediäre Radiale Glia/Ependymale Zellen in der embryonalen und postnatalen Seitenventrikelregion, sowie Ependymzellen der Seitenventrikelwand (SVW) und des Zentralkanals im Rückenmark im adulten ZNS. Des Weiteren wurden CD133-positive Ventrikellumen-kontaktierende Typ B Zellen in der adulten SVW entdeckt. Die CD133-positiven Zellen der embryonalen und postnatalen Seitenventrikelregion, RGZ und intermediäre Radiale Glia/Ependymale Zellen, konnten sich *in vitro* langfristig selbst erneuern und in verschiedene neurale Zelltypen differenzieren. Diese Merkmale werden als charakteristisch für neurale Stamm/Vorläuferzellen betrachtet. Im Gegensatz dazu wiesen die CD133-positiven Zellen der adulten SVW, Ependymzellen und die Subpopulation von Typ B Zellen, in Kultur keine Stamm/Vorläuferzelleigenschaften auf. Zellen, die sich *in vitro* langfristig selbst erneuern konnten und multipotent waren, wurden jedoch innerhalb der CD133-negativen adulten SVW Zellpopulation gefunden. Stamm/Vorläuferzellen gab es auch unter den CD133-negativen Zellen des embryonalen Vorderhirns und der postnatalen Seitenventrikelregion.
Das zeigt fuer die in dieser Doktorarbeit untersuchten Stammzellregionen, dass nicht alle CD133-positive Zellen *in vitro* Stamm/Vorläuferzelleigenschaften aufwiesen, und darüber hinaus, dass nicht alle neuralen Stammzellen CD133-positiv waren. Eine mögliche Abstammung CD133-positiver Tumorstammzellen von den in dieser Arbeit untersuchten CD133-positiven Zellen des ZNS wurde diskutiert.

Im zweiten Teil dieser Arbeit wurden CD133-positive Ependymzellen zweier adulter muriner Stammzellnischen, nämlich der SVW und dem Zentralkanal des Rückenmarks vergleichend analysiert. Eine Kombination von vier verschiedenen Antikörpern ($CD133^{+}/CD24^{+}/CD45^{-}$

/CD34$^-$) wurde benutzt um Ependymzellen von beiden Regionen mittels Durchflusszytometrie zu isolieren. Der direkte Vergleich der isolierten Ependymzellen unter identischen Kulturbedingungen zeigte, dass sich Ependymzellen des Rückenmarks langfristig selbst erneuern können und multipotent sind, während Ependymzellen der Seitenventrikelwand keine Stamm/Vorläuferzelleigenschaften aufweisen.

Mit Hilfe von Microarray Analysen wurde die molekulare Basis dieser funktionellen Unterschiede untersucht. Einige Gene, die in den Rückenmarks-Ependymzellen stärker exprimiert wurden, könnten von potentieller Relevanz für ihre Stammzelleigenschaften sein, da sie Proteine kodieren, die an der Regulierung des Zellzyklus, dem Erhalt von Telomeren sowie an der Apoptoseinduktion beteiligt sind. Des Weiteren wurde bei adulten Rückenmarks-Ependymzellen eine potentielle Regulation über Retinsäure (RA) identifiziert, basierend zum einen auf der Anreicherung von RA-regulierten Genen innerhalb der von Rückenmarks-Ependymzellen stärker exprimierten Gene, zum anderen auf Grund eines RA-induzierten proliferativen Effekts auf Rückenmarks-Ependymzellen *in vitro*.

Es wurde in anderen Studien gezeigt, dass sich Ependymzellen der adulten SVW unter physiologischen Bedingungen in einem Ruhezustand befinden. Unter bestimmten Bedingungen, wie z.B. nach einem Schlaganfall, können sie jedoch dazu angeregt werden in neuronale Zellen zu differenzieren. Die Genexpressionsdaten, die in dieser Doktorarbeit erstellt wurden, zeigten eine stärkere Expression der Transkriptionsregulatorgene *Dlx2*, *Foxg1*, *Hey1* und *Id2* in SVW Ependymzellen, was eine mögliche molekulare Basis für diese Eigenschaften darstellen könnte.

Abschließend wurden die unterschiedlich exprimierten Gene von SVW und Rückenmarks-Ependymzellen mit den entsprechenden Expressionswerten von RGZ und Neurosphären (NSPs), die von Rückenmarks-Ependymzellen abstammen, vergleichend analysiert. Eine Gruppe von Genen mit höheren Expressionswerten in den Stammzellpopulationen (Rückenmarks-Ependymzellen, RGZ und/oder NSPs) aber niedrigeren Transkriptionswerten in SVW Ependymzellen, wurde identifiziert. Diesen Genen könnte eine funktionale Rolle in der Erhaltung des undifferenzierten Status von neuralen Stammzellen zukommen und sie könnten möglicherweise auch in anderen neuralen Stammzellpopulationen exprimiert werden.

Die in dieser Doktorarbeit erstellten Genexpressionsprofile von CD133-positiven SVW und Rückenmarks-Ependymzellen tragen zu einem verbesserten Verständnis ihrer unterschiedlichen funktionellen Eigenschaften bei und stellen eine Ausgangsbasis für weitere Studien dar.

8. References

Abate-Shen C (2002) Deregulated homeobox gene expression in cancer: cause or consequence? Nat Rev Cancer 2:777-785.

Alcantara Llaguno S, Chen J, Kwon CH, Jackson EL, Li Y, Burns DK, Alvarez-Buylla A, Parada LF (2009) Malignant astrocytomas originate from neural stem/progenitor cells in a somatic tumor suppressor mouse model. Cancer Cell 15:45-56.

Alvarez-Buylla A, Garcia-Verdugo JM (2002) Neurogenesis in adult subventricular zone. J Neurosci 22:629-634.

Alvarez JI, Teale JM (2007) Differential changes in junctional complex proteins suggest the ependymal lining as the main source of leukocyte infiltration into ventricles in murine neurocysticercosis. J Neuroimmunol 187:102-113.

Arighi E, Borrello MG, Sariola H (2005) RET tyrosine kinase signaling in development and cancer. Cytokine Growth Factor Rev 16:441-467.

Bai G, Sheng N, Xie Z, Bian W, Yokota Y, Benezra R, Kageyama R, Guillemot F, Jing N (2007) Id sustains Hes1 expression to inhibit precocious neurogenesis by releasing negative autoregulation of Hes1. Dev Cell 13:283-297.

Balasubramaniam V, Mervis CF, Maxey AM, Markham NE, Abman SH (2007) Hyperoxia reduces bone marrow, circulating, and lung endothelial progenitor cells in the developing lung: implications for the pathogenesis of bronchopulmonary dysplasia. Am J Physiol Lung Cell Mol Physiol 292:L1073-1084.

Barger PM, Kelly DP (1997) Identification of a retinoid/chicken ovalbumin upstream promoter transcription factor response element in the human retinoid X receptor gamma2 gene promoter. J Biol Chem 272:2722-2728.

Barnabe-Heider F, Frisen J (2008) Stem cells for spinal cord repair. Cell Stem Cell 3:16-24.

Beier D, Hau P, Proescholdt M, Lohmeier A, Wischhusen J, Oefner PJ, Aigner L, Brawanski A, Bogdahn U, Beier CP (2007) CD133(+) and CD133(-) glioblastoma-derived cancer stem cells show differential growth characteristics and molecular profiles. Cancer Res 67:4010-4015.

Blatt EN, Yan XH, Wuerffel MK, Hamilos DL, Brody SL (1999) Forkhead transcription factor HFH-4 expression is temporally related to ciliogenesis. Am J Respir Cell Mol Biol 21:168-176.

Boudjelal M, Taneja R, Matsubara S, Bouillet P, Dolle P, Chambon P (1997) Overexpression of Stra13, a novel retinoic acid-inducible gene of the basic helix-loop-helix family, inhibits mesodermal and promotes neuronal differentiation of P19 cells. Genes Dev 11:2052-2065.

Bouillet P, Oulad-Abdelghani M, Vicaire S, Garnier JM, Schuhbaur B, Dolle P, Chambon P (1995) Efficient cloning of cDNAs of retinoic acid-responsive genes in P19 embryonal carcinoma cells and characterization of a novel mouse gene, Stra1 (mouse LERK-2/Eplg2). Dev Biol 170:420-433.

Brill MS, Snapyan M, Wohlfrom H, Ninkovic J, Jawerka M, Mastick GS, Ashery-Padan R, Saghatelyan A, Berninger B, Gotz M (2008) A dlx2- and pax6-dependent transcriptional code for periglomerular neuron specification in the adult olfactory bulb. J Neurosci 28:6439-6452.

Bruni JE (1998) Ependymal development, proliferation, and functions: a review. Microsc Res Tech 41:2-13.

Calaora V, Chazal G, Nielsen PJ, Rougon G, Moreau H (1996) mCD24 expression in the developing mouse brain and in zones of secondary neurogenesis in the adult. Neuroscience 73:581-594.

Caporaso GL, Lim DA, Alvarez-Buylla A, Chao MV (2003) Telomerase activity in the subventricular zone of adult mice. Mol Cell Neurosci 23:693-702.

Care A, Silvani A, Meccia E, Mattia G, Stoppacciaro A, Parmiani G, Peschle C, Colombo MP (1996) HOXB7 constitutively activates basic fibroblast growth factor in melanomas. Mol Cell Biol 16:4842-4851.

Care A, Valtieri M, Mattia G, Meccia E, Masella B, Luchetti L, Felicetti F, Colombo MP, Peschle C (1999) Enforced expression of HOXB7 promotes hematopoietic stem cell proliferation and myeloid-restricted progenitor differentiation. Oncogene 18:1993-2001.

Carlen M, Meletis K, Goritz C, Darsalia V, Evergren E, Tanigaki K, Amendola M, Barnabe-Heider F, Yeung MS, Naldini L, Honjo T, Kokaia Z, Shupliakov O, Cassidy RM, Lindvall O, Frisen J (2009) Forebrain ependymal cells are Notch-dependent and generate neuroblasts and astrocytes after stroke. Nat Neurosci 12:259-267.

Cerchia L, D'Alessio A, Amabile G, Duconge F, Pestourie C, Tavitian B, Libri D, de Franciscis V (2006) An autocrine loop involving ret and glial cell-derived neurotrophic factor mediates retinoic acid-induced neuroblastoma cell differentiation. Mol Cancer Res 4:481-488.

Chaichana K, Zamora-Berridi G, Camara-Quintana J, Quinones-Hinojosa A (2006) Neurosphere assays: growth factors and hormone differences in tumor and nontumor studies. Stem Cells 24:2851-2857.

Chen H, Chung S, Sukumar S (2004) HOXA5-induced apoptosis in breast cancer cells is mediated by caspases 2 and 8. Mol Cell Biol 24:924-935.

Chen H, Zhang H, Lee J, Liang X, Wu X, Zhu T, Lo PK, Zhang X, Sukumar S (2007) HOXA5 acts directly downstream of retinoic acid receptor beta and contributes to retinoic acid-induced apoptosis and growth inhibition. Cancer Res 67:8007-8013.

Cheng JX, Liu BL, Zhang X (2009) How powerful is CD133 as a cancer stem cell marker in brain tumors? Cancer Treat Rev 35:403-408.

Chiasson BJ, Tropepe V, Morshead CM, van der Kooy D (1999) Adult mammalian forebrain ependymal and subependymal cells demonstrate proliferative potential, but only subependymal cells have neural stem cell characteristics. J Neurosci 19:4462-4471.

Chojnacki AK, Mak GK, Weiss S (2009) Identity crisis for adult periventricular neural stem cells: subventricular zone astrocytes, ependymal cells or both? Nat Rev Neurosci 10:153-163.

Clarke MF, Dick JE, Dirks PB, Eaves CJ, Jamieson CH, Jones DL, Visvader J, Weissman IL, Wahl GM (2006) Cancer stem cells--perspectives on current status and future directions: AACR Workshop on cancer stem cells. Cancer Res 66:9339-9344.

Corbeil D, Roper K, Fargeas CA, Joester A, Huttner WB (2001) Prominin: a story of cholesterol, plasma membrane protrusions and human pathology. Traffic 2:82-91.

Corbeil D, Joester A, Fargeas CA, Jaszai J, Garwood J, Hellwig A, Werner HB, Huttner WB (2009) Expression of distinct splice variants of the stem cell marker prominin-1 (CD133) in glial cells. Glia 57:860-874.

Corbeil D, Roper K, Hellwig A, Tavian M, Miraglia S, Watt SM, Simmons PJ, Peault B, Buck DW, Huttner WB (2000) The human AC133 hematopoietic stem cell antigen is also expressed in epithelial cells and targeted to plasma membrane protrusions. J Biol Chem 275:5512-5520.

Coskun V, Wu H, Blanchi B, Tsao S, Kim K, Zhao J, Biancotti JC, Hutnick L, Krueger RC, Jr., Fan G, de Vellis J, Sun YE (2008) CD133+ neural stem cells in the ependyma of mammalian postnatal forebrain. Proc Natl Acad Sci U S A 105:1026-1031.

Curto M, McClatchey AI (2008) Nf2/Merlin: a coordinator of receptor signalling and intercellular contact. Br J Cancer 98:256-262.

Denchi EL (2009) Give me a break: How telomeres suppress the DNA damage response. DNA Repair (Amst) 8:1118-1126.

Denis GV, Vaziri C, Guo N, Faller DV (2000) RING3 kinase transactivates promoters of cell cycle regulatory genes through E2F. Cell Growth Differ 11:417-424.

Ding H, Schertzer M, Wu X, Gertsenstein M, Selig S, Kammori M, Pourvali R, Poon S, Vulto I, Chavez E, Tam PP, Nagy A, Lansdorp PM (2004) Regulation of murine telomere length by Rtel: an essential gene encoding a helicase-like protein. Cell 117:873-886.

Doetsch F, Garcia-Verdugo JM, Alvarez-Buylla A (1997) Cellular composition and three-dimensional organization of the subventricular germinal zone in the adult mammalian brain. J Neurosci 17:5046-5061.

Doetsch F, Garcia-Verdugo JM, Alvarez-Buylla A (1999a) Regeneration of a germinal layer in the adult mammalian brain. Proc Natl Acad Sci U S A 96:11619-11624.

Doetsch F, Caille I, Lim DA, Garcia-Verdugo JM, Alvarez-Buylla A (1999b) Subventricular zone astrocytes are neural stem cells in the adult mammalian brain. Cell 97:703-716.

Doetsch F, Petreanu L, Caille I, Garcia-Verdugo JM, Alvarez-Buylla A (2002) EGF converts transit-amplifying neurogenic precursors in the adult brain into multipotent stem cells. Neuron 36:1021-1034.

Dromard C, Guillon H, Rigau V, Ripoll C, Sabourin JC, Perrin FE, Scamps F, Bozza S, Sabatier P, Lonjon N, Duffau H, Vachiery-Lahaye F, Prieto M, Tran Van Ba C, Deleyrolle L, Boularan A, Langley K, Gaviria M, Privat A, Hugnot JP, Bauchet L (2008) Adult human spinal cord harbors neural precursor cells that generate neurons and glial cells in vitro. J Neurosci Res 86:1916-1926.

Du P, Kibbe WA, Lin SM (2008) lumi: a pipeline for processing Illumina microarray. Bioinformatics 24:1547-1548.

Dubreuil V, Marzesco AM, Corbeil D, Huttner WB, Wilsch-Brauninger M (2007) Midbody and primary cilium of neural progenitors release extracellular membrane particles enriched in the stem cell marker prominin-1. J Cell Biol 176:483-495.

Ebert C, von Haken M, Meyer-Puttlitz B, Wiestler OD, Reifenberger G, Pietsch T, von Deimling A (1999) Molecular genetic analysis of ependymal tumors. NF2 mutations and chromosome 22q loss occur preferentially in intramedullary spinal ependymomas. Am J Pathol 155:627-632.

Fargeas CA, Corbeil D, Huttner WB (2003) AC133 antigen, CD133, prominin-1, prominin-2, etc.: prominin family gene products in need of a rational nomenclature. Stem Cells 21:506-508.

Fargeas CA, Huttner WB, Corbeil D (2007) Nomenclature of prominin-1 (CD133) splice variants - an update. Tissue Antigens 69:602-606.

Ferri AL, Cavallaro M, Braida D, Di Cristofano A, Canta A, Vezzani A, Ottolenghi S, Pandolfi PP, Sala M, DeBiasi S, Nicolis SK (2004) Sox2 deficiency causes neurodegeneration and impaired neurogenesis in the adult mouse brain. Development 131:3805-3819.

Fomchenko EI, Holland EC (2005) Stem cells and brain cancer. Exp Cell Res 306:323-329.

Fortunel NO, Otu HH, Ng HH, Chen J, Mu X, Chevassut T, Li X, Joseph M, Bailey C, Hatzfeld JA, Hatzfeld A, Usta F, Vega VB, Long PM, Libermann TA, Lim B (2003) Comment on " 'Stemness': transcriptional profiling of embryonic and adult stem cells" and "a stem cell molecular signature". Science 302:393; author reply 393.

Fu H, Qi Y, Tan M, Cai J, Hu X, Liu Z, Jensen J, Qiu M (2003) Molecular mapping of the origin of postnatal spinal cord ependymal cells: evidence that adult ependymal cells are derived from Nkx6.1+ ventral neural progenitor cells. J Comp Neurol 456:237-244.

Gabrion JB, Herbute S, Bouille C, Maurel D, Kuchler-Bopp S, Laabich A, Delaunoy JP (1998) Ependymal and choroidal cells in culture: characterization and functional differentiation. Microsc Res Tech 41:124-157.

Gentleman RC, Carey VJ, Bates DM, Bolstad B, Dettling M, Dudoit S, Ellis B, Gautier L, Ge Y, Gentry J, Hornik K, Hothorn T, Huber W, Iacus S, Irizarry R, Leisch F, Li C, Maechler M, Rossini AJ, Sawitzki G, Smith C, Smyth G, Tierney L, Yang JY, Zhang J (2004) Bioconductor: open software development for computational biology and bioinformatics. Genome Biol 5:R80.

Gotz M, Huttner WB (2005) The cell biology of neurogenesis. Nat Rev Mol Cell Biol 6:777-788.

Gu Z, Flemington C, Chittenden T, Zambetti GP (2000) ei24, a p53 response gene involved in growth suppression and apoptosis. Mol Cell Biol 20:233-241.

Hamilton LK, Truong MK, Bednarczyk MR, Aumont A, Fernandes KJ (2009) Cellular organization of the central canal ependymal zone, a niche of latent neural stem cells in the adult mammalian spinal cord. Neuroscience.

Hamilton RL, Pollack IF (1997) The molecular biology of ependymomas. Brain Pathol 7:807-822.

Hemann MT, Greider CW (2000) Wild-derived inbred mouse strains have short telomeres. Nucleic Acids Res 28:4474-4478.

Hochberg Y, Benjamini Y (1990) More powerful procedures for multiple significance testing. Stat Med 9:811-818.

Horner PJ, Power AE, Kempermann G, Kuhn HG, Palmer TD, Winkler J, Thal LJ, Gage FH (2000) Proliferation and differentiation of progenitor cells throughout the intact adult rat spinal cord. J Neurosci 20:2218-2228.

Ingram DA, Caplice NM, Yoder MC (2005) Unresolved questions, changing definitions, and novel paradigms for defining endothelial progenitor cells. Blood 106:1525-1531.

Iso T, Sartorelli V, Chung G, Shichinohe T, Kedes L, Hamamori Y (2001) HERP, a new primary target of Notch regulated by ligand binding. Mol Cell Biol 21:6071-6079.

Johansson CB, Momma S, Clarke DL, Risling M, Lendahl U, Frisen J (1999) Identification of a neural stem cell in the adult mammalian central nervous system. Cell 96:25-34.

Kamel S, Kruger C, Salbaum JM, Kappen C (2009) Morpholino-mediated knockdown in primary chondrocytes implicates Hoxc8 in regulation of cell cycle progression. Bone 44:708-716.

Kelly TK, Karsten SL, Geschwind DH, Kornblum HI (2009) Cell lineage and regional identity of cultured spinal cord neural stem cells and comparison to brain-derived neural stem cells. PLoS One 4:e4213.

Kessel M, Gruss P (1991) Homeotic transformations of murine vertebrae and concomitant alteration of Hox codes induced by retinoic acid. Cell 67:89-104.

Kipling D, Cooke HJ (1990) Hypervariable ultra-long telomeres in mice. Nature 347:400-402.

Korshunov A, Neben K, Wrobel G, Tews B, Benner A, Hahn M, Golanov A, Lichter P (2003) Gene expression patterns in ependymomas correlate with tumor location, grade, and patient age. Am J Pathol 163:1721-1727.

Kosodo Y, Roper K, Haubensak W, Marzesco AM, Corbeil D, Huttner WB (2004) Asymmetric distribution of the apical plasma membrane during neurogenic divisions of mammalian neuroepithelial cells. Embo J 23:2314-2324.

Kriegstein A, Alvarez-Buylla A (2009) The glial nature of embryonic and adult neural stem cells. Annu Rev Neurosci 32:149-184.

Krumlauf R, Holland PW, McVey JH, Hogan BL (1987) Developmental and spatial patterns of expression of the mouse homeobox gene, Hox 2.1. Development 99:603-617.

Lee A, Kessler JD, Read TA, Kaiser C, Corbeil D, Huttner WB, Johnson JE, Wechsler-Reya RJ (2005) Isolation of neural stem cells from the postnatal cerebellum. Nat Neurosci 8:723-729.

Leung JK, Cases S, Vu TH (2008) P311 functions in an alternative pathway of lipid accumulation that is induced by retinoic acid. J Cell Sci 121:2751-2758.

Lim DA, Suarez-Farinas M, Naef F, Hacker CR, Menn B, Takebayashi H, Magnasco M, Patil N, Alvarez-Buylla A (2006) In vivo transcriptional profile analysis reveals RNA splicing and chromatin remodeling as prominent processes for adult neurogenesis. Mol Cell Neurosci 31:131-148.

Lippoldt A, Jansson A, Kniesel U, Andbjer B, Andersson A, Wolburg H, Fuxe K, Haller H (2000) Phorbol ester induced changes in tight and adherens junctions in the choroid plexus epithelium and in the ependyma. Brain Res 854:197-206.

MacCumber MW, Snyder SH, Ross CA (1990) Carboxypeptidase E (enkephalin convertase): mRNA distribution in rat brain by in situ hybridization. J Neurosci 10:2850-2860.

Maden M (2001) Role and distribution of retinoic acid during CNS development. Int Rev Cytol 209:1-77.

Malatesta P, Appolloni I, Calzolari F (2008) Radial glia and neural stem cells. Cell Tissue Res 331:165-178.

Manohar CF, Salwen HR, Furtado MR, Cohn SL (1996) Up-regulation of HOXC6, HOXD1, and HOXD8 homeobox gene expression in human neuroblastoma cells following chemical induction of differentiation. Tumour Biol 17:34-47.

Martens DJ, Seaberg RM, van der Kooy D (2002) In vivo infusions of exogenous growth factors into the fourth ventricle of the adult mouse brain increase the proliferation of neural progenitors around the fourth ventricle and the central canal of the spinal cord. Eur J Neurosci 16:1045-1057.

Martynoga B, Morrison H, Price DJ, Mason JO (2005) Foxg1 is required for specification of ventral telencephalon and region-specific regulation of dorsal telencephalic precursor proliferation and apoptosis. Dev Biol 283:113-127.

Marzesco AM, Janich P, Wilsch-Brauninger M, Dubreuil V, Langenfeld K, Corbeil D, Huttner WB (2005) Release of extracellular membrane particles carrying the stem cell marker prominin-1 (CD133) from neural progenitors and other epithelial cells. J Cell Sci 118:2849-2858.

Maw MA, Corbeil D, Koch J, Hellwig A, Wilson-Wheeler JC, Bridges RJ, Kumaramanickavel G, John S, Nancarrow D, Roper K, Weigmann A, Huttner WB, Denton MJ (2000) A frameshift mutation in prominin (mouse)-like 1 causes human retinal degeneration. Hum Mol Genet 9:27-34.

McDermott NB, Gordon DF, Kramer CA, Liu Q, Linney E, Wood WM, Haugen BR (2002) Isolation and functional analysis of the mouse RXRgamma1 gene promoter in anterior pituitary cells. J Biol Chem 277:36839-36844.

Meletis K, Barnabe-Heider F, Carlen M, Evergren E, Tomilin N, Shupliakov O, Frisen J (2008) Spinal cord injury reveals multilineage differentiation of ependymal cells. PLoS Biol 6:e182.

Merkle FT, Alvarez-Buylla A (2006) Neural stem cells in mammalian development. Curr Opin Cell Biol 18:704-709.

Merkle FT, Tramontin AD, Garcia-Verdugo JM, Alvarez-Buylla A (2004) Radial glia give rise to adult neural stem cells in the subventricular zone. Proc Natl Acad Sci U S A 101:17528-17532.

Merrill RA, Ahrens JM, Kaiser ME, Federhart KS, Poon VY, Clagett-Dame M (2004) All-trans retinoic acid-responsive genes identified in the human SH-SY5Y neuroblastoma cell line and their regulated expression in the nervous system of early embryos. Biol Chem 385:605-614.

Mey J (2006) New therapeutic target for CNS injury? The role of retinoic acid signaling after nerve lesions. J Neurobiol 66:757-779.

Mikkers H, Frisen J (2005) Deconstructing stemness. Embo J 24:2715-2719.

Mirzadeh Z, Merkle FT, Soriano-Navarro M, Garcia-Verdugo JM, Alvarez-Buylla A (2008) Neural stem cells confer unique pinwheel architecture to the ventricular surface in neurogenic regions of the adult brain. Cell Stem Cell 3:265-278.

Mishra BP, Ansari KI, Mandal SS (2009) Dynamic association of MLL1, H3K4 trimethylation with chromatin and Hox gene expression during the cell cycle. FEBS J 276:1629-1640.

Moreno-Manzano V, Rodriguez-Jimenez FJ, Garcia-Rosello M, Lainez S, Erceg S, Calvo MT, Ronaghi M, Lloret M, Planells-Cases R, Sanchez-Puelles JM, Stojkovic M (2009) Activated spinal cord ependymal stem cells rescue neurological function. Stem Cells 27:733-743.

Mori T, Buffo A, Gotz M (2005) The novel roles of glial cells revisited: the contribution of radial glia and astrocytes to neurogenesis. Curr Top Dev Biol 69:67-99.

Morrison SJ (2009) Mechanisms of Stem Cell Self-Renewal. Annu Rev Cell Dev Biol.

Mothe AJ, Tator CH (2005) Proliferation, migration, and differentiation of endogenous ependymal region stem/progenitor cells following minimal spinal cord injury in the adult rat. Neuroscience 131:177-187.

Nielsen S, Nagelhus EA, Amiry-Moghaddam M, Bourque C, Agre P, Ottersen OP (1997) Specialized membrane domains for water transport in glial cells: high-resolution immunogold cytochemistry of aquaporin-4 in rat brain. J Neurosci 17:171-180.

Nishiyama H, Gill JH, Pitt E, Kennedy W, Knowles MA (2001) Negative regulation of G(1)/S transition by the candidate bladder tumour suppressor gene DBCCR1. Oncogene 20:2956-2964.

Nolan DJ, Ciarrocchi A, Mellick AS, Jaggi JS, Bambino K, Gupta S, Heikamp E, McDevitt MR, Scheinberg DA, Benezra R, Mittal V (2007) Bone marrow-derived endothelial progenitor cells are a major determinant of nascent tumor neovascularization. Genes Dev 21:1546-1558.

Obermair FJ, Schroter A, Thallmair M (2008) Endogenous neural progenitor cells as therapeutic target after spinal cord injury. Physiology (Bethesda) 23:296-304.

Ogden AT, Waziri AE, Lochhead RA, Fusco D, Lopez K, Ellis JA, Kang J, Assanah M, McKhann GM, Sisti MB, McCormick PC, Canoll P, Bruce JN (2008) Identification of A2B5+CD133- tumor-initiating cells in adult human gliomas. Neurosurgery 62:505-514; discussion 514-505.

Okabe M, Ikawa M, Kominami K, Nakanishi T, Nishimune Y (1997) 'Green mice' as a source of ubiquitous green cells. FEBS Lett 407:313-319.

Oosterveen T, Niederreither K, Dolle P, Chambon P, Meijlink F, Deschamps J (2003) Retinoids regulate the anterior expression boundaries of 5' Hoxb genes in posterior hindbrain. EMBO J 22:262-269.

Otegui MS, Verbrugghe KJ, Skop AR (2005) Midbodies and phragmoplasts: analogous structures involved in cytokinesis. Trends Cell Biol 15:404-413.

Panchision DM, Chen HL, Pistollato F, Papini D, Ni HT, Hawley TS (2007) Optimized flow cytometric analysis of central nervous system tissue reveals novel functional relationships among cells expressing CD133, CD15, and CD24. Stem Cells 25:1560-1570.

Pardal R, Molofsky AV, He S, Morrison SJ (2005) Stem cell self-renewal and cancer cell proliferation are regulated by common networks that balance the activation of proto-oncogenes and tumor suppressors. Cold Spring Harb Symp Quant Biol 70:177-185.

Petryniak MA, Potter GB, Rowitch DH, Rubenstein JL (2007) Dlx1 and Dlx2 control neuronal versus oligodendroglial cell fate acquisition in the developing forebrain. Neuron 55:417-433.

Phillips HS, Kharbanda S, Chen R, Forrest WF, Soriano RH, Wu TD, Misra A, Nigro JM, Colman H, Soroceanu L, Williams PM, Modrusan Z, Feuerstein BG, Aldape K (2006)

Molecular subclasses of high-grade glioma predict prognosis, delineate a pattern of disease progression, and resemble stages in neurogenesis. Cancer Cell 9:157-173.

Potten CS (1992) The significance of spontaneous and induced apoptosis in the gastrointestinal tract of mice. Cancer Metastasis Rev 11:179-195.

Potten CS, Loeffler M (1990) Stem cells: attributes, cycles, spirals, pitfalls and uncertainties. Lessons for and from the crypt. Development 110:1001-1020.

Prowse AH, Vanderveer L, Milling SW, Pan ZZ, Dunbrack RL, Xu XX, Godwin AK (2002) OVCA2 is downregulated and degraded during retinoid-induced apoptosis. Int J Cancer 99:185-192.

Qiu R, Wang X, Davy A, Wu C, Murai K, Zhang H, Flanagan JG, Soriano P, Lu Q (2008) Regulation of neural progenitor cell state by ephrin-B. J Cell Biol 181:973-983.

Quinones-Hinojosa A, Chaichana K (2007) The human subventricular zone: a source of new cells and a potential source of brain tumors. Exp Neurol 205:313-324.

Ramachandran S, Liu P, Young AN, Yin-Goen Q, Lim SD, Laycock N, Amin MB, Carney JK, Marshall FF, Petros JA, Moreno CS (2005) Loss of HOXC6 expression induces apoptosis in prostate cancer cells. Oncogene 24:188-198.

Raman V, Martensen SA, Reisman D, Evron E, Odenwald WF, Jaffee E, Marks J, Sukumar S (2000) Compromised HOXA5 function can limit p53 expression in human breast tumours. Nature 405:974-978.

Read TA, Fogarty MP, Markant SL, McLendon RE, Wei Z, Ellison DW, Febbo PG, Wechsler-Reya RJ (2009) Identification of CD15 as a marker for tumor-propagating cells in a mouse model of medulloblastoma. Cancer Cell 15:135-147.

Renthal R, Schneider BG, Miller MM, Luduena RF (1993) Beta IV is the major beta-tubulin isotype in bovine cilia. Cell Motil Cytoskeleton 25:19-29.

Reynolds BA, Weiss S (1992) Generation of neurons and astrocytes from isolated cells of the adult mammalian central nervous system. Science 255:1707-1710.

Reynolds BA, Rietze RL (2005) Neural stem cells and neurospheres--re-evaluating the relationship. Nat Methods 2:333-336.

Rosell A, Arai K, Lok J, He T, Guo S, Navarro M, Montaner J, Katusic ZS, Lo EH (2009) Interleukin-1beta augments angiogenic responses of murine endothelial progenitor cells in vitro. J Cereb Blood Flow Metab.

Sabourin J, Ackema K, Ohayon D, Guichet P, Perrin F, Garces A, Ripoll C, Charite J, Simonneau L, Kettenmann H, Zine A, Privat A, Valmier J, Pattyn A, Hugnot J (2009) A Mesenchymal-Like Zeb1(+) Niche Harbors Dorsal Radial GFAP(+) Stem Cells in the Spinal Cord. Stem Cells.

Saeed AI, Sharov V, White J, Li J, Liang W, Bhagabati N, Braisted J, Klapa M, Currier T, Thiagarajan M, Sturn A, Snuffin M, Rezantsev A, Popov D, Ryltsov A, Kostukovich E, Borisovsky I, Liu Z, Vinsavich A, Trush V, Quackenbush J (2003) TM4: a free, open-source system for microarray data management and analysis. Biotechniques 34:374-378.

Sakamoto M, Hirata H, Ohtsuka T, Bessho Y, Kageyama R (2003) The basic helix-loop-helix genes Hesr1/Hey1 and Hesr2/Hey2 regulate maintenance of neural precursor cells in the brain. J Biol Chem 278:44808-44815.

Sakariassen PO, Immervoll H, Chekenya M (2007) Cancer stem cells as mediators of treatment resistance in brain tumors: status and controversies. Neoplasia 9:882-892.

Sampathi S, Bhusari A, Shen B, Chai W (2009) Human flap endonuclease I is in complex with telomerase and is required for telomerase-mediated telomere maintenance. J Biol Chem 284:3682-3690.

Sanai N, Alvarez-Buylla A, Berger MS (2005) Neural stem cells and the origin of gliomas. N Engl J Med 353:811-822.

Sawamoto K, Wichterle H, Gonzalez-Perez O, Cholfin JA, Yamada M, Spassky N, Murcia NS, Garcia-Verdugo JM, Marin O, Rubenstein JL, Tessier-Lavigne M, Okano H, Alvarez-Buylla A (2006) New neurons follow the flow of cerebrospinal fluid in the adult brain. Science 311:629-632.

Schug TT, Berry DC, Shaw NS, Travis SN, Noy N (2007) Opposing effects of retinoic acid on cell growth result from alternate activation of two different nuclear receptors. Cell 129:723-733.

Shen B, Singh P, Liu R, Qiu J, Zheng L, Finger LD, Alas S (2005) Multiple but dissectible functions of FEN-1 nucleases in nucleic acid processing, genome stability and diseases. Bioessays 27:717-729.

Shen Q, Wang Y, Kokovay E, Lin G, Chuang SM, Goderie SK, Roysam B, Temple S (2008) Adult SVZ stem cells lie in a vascular niche: a quantitative analysis of niche cell-cell interactions. Cell Stem Cell 3:289-300.

Shih AH, Holland EC (2004) Developmental neurobiology and the origin of brain tumors. J Neurooncol 70:125-136.

Shihabuddin LS (2002) Adult rodent spinal cord derived neural stem cells. Isolation and characterization. Methods Mol Biol 198:67-77.

Simeone A, Acampora D, Arcioni L, Andrews PW, Boncinelli E, Mavilio F (1990) Sequential activation of HOX2 homeobox genes by retinoic acid in human embryonal carcinoma cells. Nature 346:763-766.

Singec I, Knoth R, Meyer RP, Maciaczyk J, Volk B, Nikkhah G, Frotscher M, Snyder EY (2006) Defining the actual sensitivity and specificity of the neurosphere assay in stem cell biology. Nat Methods 3:801-806.

Singh SK, Hawkins C, Clarke ID, Squire JA, Bayani J, Hide T, Henkelman RM, Cusimano MD, Dirks PB (2004) Identification of human brain tumour initiating cells. Nature 432:396-401.

Sinha A, Faller DV, Denis GV (2005) Bromodomain analysis of Brd2-dependent transcriptional activation of cyclin A. Biochem J 387:257-269.

Solito E, McArthur S, Christian H, Gavins F, Buckingham JC, Gillies GE (2008) Annexin A1 in the brain--undiscovered roles? Trends Pharmacol Sci 29:135-142.

Spassky N, Merkle FT, Flames N, Tramontin AD, Garcia-Verdugo JM, Alvarez-Buylla A (2005) Adult ependymal cells are postmitotic and are derived from radial glial cells during embryogenesis. J Neurosci 25:10-18.

Sturrock RR (1981) An electron microscopic study of the development of the ependyma of the central canal of the mouse spinal cord. J Anat 132:119-136.

Takaishi M, Ishisaki Z, Yoshida T, Takata Y, Huh NH (2003) Expression of calmin, a novel developmentally regulated brain protein with calponin-homology domains. Brain Res Mol Brain Res 112:146-152.

Taylor MD, Poppleton H, Fuller C, Su X, Liu Y, Jensen P, Magdaleno S, Dalton J, Calabrese C, Board J, Macdonald T, Rutka J, Guha A, Gajjar A, Curran T, Gilbertson RJ (2005) Radial glia cells are candidate stem cells of ependymoma. Cancer Cell 8:323-335.

Thompson Haskell G, Maynard TM, Shatzmiller RA, Lamantia AS (2002) Retinoic acid signaling at sites of plasticity in the mature central nervous system. J Comp Neurol 452:228-241.

Tropepe V, Sibilia M, Ciruna BG, Rossant J, Wagner EF, van der Kooy D (1999) Distinct neural stem cells proliferate in response to EGF and FGF in the developing mouse telencephalon. Dev Biol 208:166-188.

Uchida N, Buck DW, He D, Reitsma MJ, Masek M, Phan TV, Tsukamoto AS, Gage FH, Weissman IL (2000) Direct isolation of human central nervous system stem cells. Proc Natl Acad Sci U S A 97:14720-14725.

van Neerven S, Mey J (2007) RAR/RXR and PPAR/RXR Signaling in Spinal Cord Injury. PPAR Res 2007:29275.

Wang J, Sakariassen PO, Tsinkalovsky O, Immervoll H, Boe SO, Svendsen A, Prestegarden L, Rosland G, Thorsen F, Stuhr L, Molven A, Bjerkvig R, Enger PO (2008) CD133 negative glioma cells form tumors in nude rats and give rise to CD133 positive cells. Int J Cancer 122:761-768.

Weigmann A, Corbeil D, Hellwig A, Huttner WB (1997) Prominin, a novel microvilli-specific polytopic membrane protein of the apical surface of epithelial cells, is targeted to plasmalemmal protrusions of non-epithelial cells. Proc Natl Acad Sci U S A 94:12425-12430.

Weiss S, Dunne C, Hewson J, Wohl C, Wheatley M, Peterson AC, Reynolds BA (1996) Multipotent CNS stem cells are present in the adult mammalian spinal cord and ventricular neuroaxis. J Neurosci 16:7599-7609.

Wright KO, Messing EM, Reeder JE (2004) DBCCR1 mediates death in cultured bladder tumor cells. Oncogene 23:82-90.

Yamamoto S, Yamamoto N, Kitamura T, Nakamura K, Nakafuku M (2001) Proliferation of parenchymal neural progenitors in response to injury in the adult rat spinal cord. Exp Neurol 172:115-127.

Yang Z, Chen Y, Lillo C, Chien J, Yu Z, Michaelides M, Klein M, Howes KA, Li Y, Kaminoh Y, Chen H, Zhao C, Chen Y, Al-Sheikh YT, Karan G, Corbeil D, Escher P, Kamaya S, Li C, Johnson S, Frederick JM, Zhao Y, Wang C, Cameron DJ, Huttner WB, Schorderet DF, Munier FL, Moore AT, Birch DG, Baehr W, Hunt DM, Williams DS, Zhang K (2008) Mutant prominin 1 found in patients with macular degeneration disrupts photoreceptor disk morphogenesis in mice. J Clin Invest 118:2908-2916.

Yin AH, Miraglia S, Zanjani ED, Almeida-Porada G, Ogawa M, Leary AG, Olweus J, Kearney J, Buck DW (1997) AC133, a novel marker for human hematopoietic stem and progenitor cells. Blood 90:5002-5012.

Yoo S, Wrathall JR (2007) Mixed primary culture and clonal analysis provide evidence that NG2 proteoglycan-expressing cells after spinal cord injury are glial progenitors. Dev Neurobiol 67:860-874.

Zacchigna S, Oh H, Wilsch-Brauninger M, Missol-Kolka E, Jaszai J, Jansen S, Tanimoto N, Tonagel F, Seeliger M, Huttner WB, Corbeil D, Dewerchin M, Vinckier S, Moons L, Carmeliet P (2009) Loss of the cholesterol-binding protein prominin-1/CD133 causes disk dysmorphogenesis and photoreceptor degeneration. J Neurosci 29:2297-2308.

Zhang F, Nagy Kovacs E, Featherstone MS (2000) Murine hoxd4 expression in the CNS requires multiple elements including a retinoic acid response element. Mech Dev 96:79-89.

Zou J, Marjanovic J, Kisseleva MV, Wilson M, Majerus PW (2007) Type I phosphatidylinositol-4,5-bisphosphate 4-phosphatase regulates stress-induced apoptosis. Proc Natl Acad Sci U S A 104:16834-16839.

9. Acknowledgements

First, I want to thank Prof. Ulrike Nuber for providing the possibility to write my PhD thesis under her supervision. I want to thank her for the interesting scientific projects she provided, for her continuous support during my PhD time and that she was always available for dicussions and to solve problems.

I thank Prof. Roland Lauster for the external supervision of my PhD thesis, his ´unconventional way` to deal with formalities, and his support in critical times.

I am grateful to Zhi Ma, who made it possible to use the FACS machine whenever necessary, Christine Steinhoff for the fast and professional microarray analysis, Prof. Sten Eirik Jacobsen for the single cell rtPCR protocol and Anne Hultquist who helped to establish it.

Special thanks to the members of the ´Nuber group`, the best colleagues one could wish for. Everyone, in its own way, contributed to a supportive, stimulating and fun environment. Thank you Ralph, for your excellent technical help and the homelike atmosphere you created during the first time in Sweden, thanks Denise for your practical support in emergency situations and thank you Kristen for your encouragement during the final thesis writing periode. Sebastian, thanks for dragging me to Govindas every day and for your idealistic philosophy of life.

I am indebted to all members of the BMC, and especially my colleagues from B10, for their scientific and personal support and, of course, the evenings outside the lab. Teia, I want to thank you for being my friend and roommate, for your emotional support and for your own special way to cheer me up.

I want to thank my family for providing a loving environment for me.

Lastly, and most importantly, I want to thank Falk, who supported me in every possible way during my time in Sweden. Without him, this thesis wouldn’t have been possible.

10. Publications

Data presented in this thesis are in part based on the following publications:

I. Pfenninger CV, Roschupkina T, Hertwig F, Kottwitz D, Englund E, Bengzon J, Jacobsen SE, Nuber UA (2007) CD133 is not present on neurogenic astrocytes in the adult subventricular zone, but on embryonic neural stem cells, ependymal cells, and glioblastoma cells. Cancer Res 67:5727-5736.

Modified figures from article I: Fig.9, 10, 12, 14, 27

II. Pfenninger CV, Steinhoff C, Hertwig F, Nuber UA (2011) Prospectively isolated CD133/CD24-positive ependymal cells from the adult spinal cord and lateral ventricle wall differ in their long-term in vitro self-renewal and in vivo gene expression. Glia 59:68-81.

Modified figures and tables from article II: Fig.10, 11, 21, 22, 23, 24, 26; Table 9A/B, 11, 12